RELATIVE Lg AND P-CODA MAGNITUDE ANALYSIS OF THE LARGEST SHAGAN RIVER EXPLOSIONS

Douglas R. Baumgardt

SAS-TR-84-03

RELATIVE Lg AND P-CODA MAGNITUDE ANALYSIS OF THE LARGEST SHAGAN RIVER EXPLOSIONS

Douglas R. Baumgardt

Final Report
28 December 1984

Sponsored By:
Advanced Research Projects Agency (DOD)
ARPA Order No. 4691
Monitored by AFOSR
Under Contract No. F49620-84-C-0046

ENSCO, Inc.
Signal Analysis and Systems Division
5400 Port Royal Road
Springfield, Virginia 22151

SECURITY CLASSIFICATION OF THIS PAGE

REPORT DOCUMENTATION PAGE

1a. REPORT SECURITY CLASSIFICATION UNCLASSIFIED	1b. RESTRICTIVE MARKINGS
2a. SECURITY CLASSIFICATION AUTHORITY	3. DISTRIBUTION/AVAILABILITY OF REPORT Approved for public release; distribution unlimited.
2b. DECLASSIFICATION/DOWNGRADING SCHEDULE	
4. PERFORMING ORGANIZATION REPORT NUMBER(S) SAS-TR-84-03	5. MONITORING ORGANIZATION REPORT NUMBER(S) AFOSR-TR- 85-0235
6a. NAME OF PERFORMING ORGANIZATION ENSCO, Inc. — 6b. OFFICE SYMBOL (If applicable)	7a. NAME OF MONITORING ORGANIZATION Air Force Office of Scientific Research
6c. ADDRESS (City, State and ZIP Code) 5400 Port Royal Road Springfield, VA 22151-2388	7b. ADDRESS (City, State and ZIP Code) Bolling Air Force Base Washington, DC 20332
8a. NAME OF FUNDING/SPONSORING ORGANIZATION Defense Advanced Research Projects Agency — 8b. OFFICE SYMBOL (If applicable)	9. PROCUREMENT INSTRUMENT IDENTIFICATION NUMBER F49620-84-C-0046
8c. ADDRESS (City, State and ZIP Code) 1400 Wilson Blvd. Arlington, VA 22209	10. SOURCE OF FUNDING NOS. PROGRAM ELEMENT NO. 62714E — PROJECT NO. 4691 — TASK NO. 02 — WORK UNIT NO.
11. TITLE (Include Security Classification) RELATIVE Lg AND P-CODA MAGNITUDE ANALYSIS OF THE LARGEST SHAGAN RIVER EXPLOSIONS	
12. PERSONAL AUTHOR(S) Douglas R. Baumgardt	
13a. TYPE OF REPORT Final Technical — 13b. TIME COVERED FROM 4-2-84 TO 10-31-84 — 14. DATE OF REPORT (Yr., Mo., Day) 1984 Dec 28 — 15. PAGE COUNT	
16. SUPPLEMENTARY NOTATION	
17. COSATI CODES FIELD / GROUP / SUB. GR.	18. SUBJECT TERMS (Continue on reverse if necessary and identify by block number) P-coda, Lg, magnitudes, scattering, Eurasia, Graefenburg, NORSAR, Yield Estimation, Shagan River

19. ABSTRACT. (Continue on reverse if necessary and identify by block number)

We have investigated the characteristics of P-coda and Lg measurements at the NORSAR and Graefenburg arrays for presumed underground nuclear explosions in the Semipalatinsk region of the Soviet Union. Our main objectives in this study were to investigate the effects of the propagation paths in western Russia on the narrowband and broadband recordings of Lg at teleseismic distances and to study the relative P-coda and Lg amplitudes recorded at these two arrays for the largest (m_b > 6.0) Shagan River Explosions.

Comparison of broadband recordings of teleseismic Lg at Graefenburg (Δ=42°) with narrowband NORSAR (Δ=38°) and filtered Graefenburg recordings of Lg from Shagan River events reveals that Lg is more obvious, relative to the preceding P-coda, on broadband seismograms than on

20. DISTRIBUTION/AVAILABILITY OF ABSTRACT UNCLASSIFIED/UNLIMITED ☒ SAME AS RPT. ☐ DTIC USERS ☐	21. ABSTRACT SECURITY CLASSIFICATION UNCLASSIFIED
22a. NAME OF RESPONSIBLE INDIVIDUAL Dr. Howard R. Radoski	22b. TELEPHONE NUMBER (Include Area Code) (202) 767-4904 — 22c. OFFICE SYMBOL AFOSR

DD FORM 1473, 83 APR — EDITION OF 1 JAN 73 IS OBSOLETE.

UNCLASSIFIED

SECURITY CLASSIFICATION OF THIS PAGE

BLOCK 11: TITLE

ANALYSIS OF THE LARGEST SHAGAN RIVER EXPLOSIONS (UNCLASSIFIED)

BLOCK 19: ABSTRACT

high-frequency seismograms. Broadband recordings of Lg and Graefenburg are about 0.5 log units stronger in the 0.2 - 1.0 Hz band than in the 0.6 - 3.0 Hz range although noise is also correspondingly higher.

The early P-coda at NORSAR is stronger, relative to Lg, than that at Graefenburg. Also, the coda-envelope shapes are quite different for the two arrays; the NORSAR coda flattens between about 200 to 340 seconds after P, whereas the Graefenburg coda decays monitonically from the P-wave out to the S_n and Lg arrival times. The standard deviations of Lg and S-coda phases at NORSAR are higher by about 0.05 to 0.06 log-rms amplitude units than those of P-coda phases, which is probably related to differential site and propagation effects on P, S and Lg waves. The most stable part of the P-coda before Lg is the flat part of the coda, where the spatial standard deviation in log-rms amplitude in 5 second windows drops to a minimum of less than 0.1 units. The flat coda envelopes from about 200 to 340 seconds after P, recorded at NORSAR for Semipalatinsk explosions, are consistent, on the basis of timing, to Lg - P forward scattering from lateral heterogeneities in the Ural Mountains.

Measurements on Graefenburg data of vertical and transverse log-rms amplitudes in the P-coda and Lg phase in two frequency bands correlate well with network m_b. These measurements indicate that Lg and P-coda amplitudes do not appear to be strongly affected by the tectonic component as revealed by surface-wave studies. However, the slopes of the regression of Lg amplitude versus m_b were small ranging from 0.6 to 0.8. The slopes of the P-coda regressions were higher, ranging from 0.9 to over 1.0. This supports the idea that early P-coda waves are generated by P scattering. The principal cause of the small slopes is that the variance of the Lg and P-coda amplitudes for the largest Shagan River events are significantly smaller than that of the corresponding network-averaged m_bs. We argue that P-coda and Lg amplitudes are more robust estimators of relative yield than m_b, and that the yield range for these events, based on Lg and P-coda measurements at NORSAR and Graefenburg, is smaller by approximately a factor of 2 than the yield range indicated by m_b. This is consistent with the conjecture of Sykes and Cifuentes (1983), based on surface-wave studies, that the largest Shagan explosions, with m_b greater than 6.0, have nearly the same yield.

ARPA Order No. 4691

Program Code 3A10

Effective Date of Contract: 1 April 1983

Original Contract Expiration Date: 31 January 1985

Amount of Contract: $102,362

Contract No. F49620-84-C-0046

Principal Investigator:
Dr. Douglas Baumgardt
703/321-9000, Ext. 406

Program Manager:
Dr. Howard R. Radoski
202/767-4904

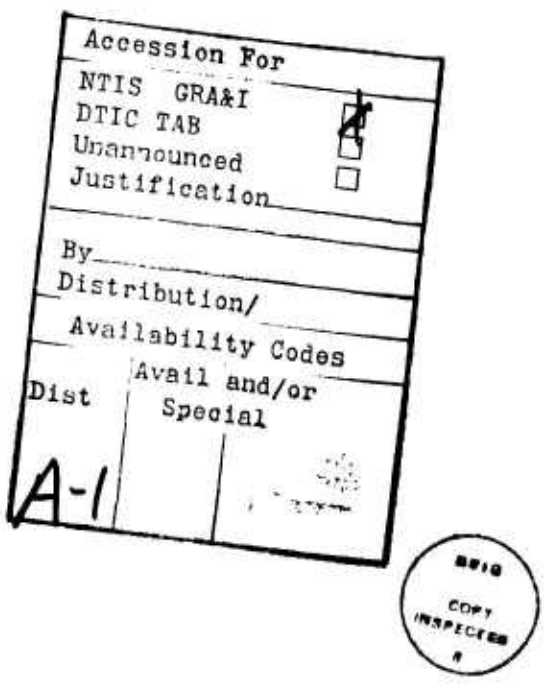

TABLE OF CONTENTS

SECTION			Page
LIST OF FIGURES			ii
LIST OF TABLES			v
ABSTRACT			vi
1.0	INTRODUCTION		1-1
2.0	TELESEISMIC P-CODA AND Lg-WAVES IN EURASIA		2-1
	2.1	Introduction	2-1
	2.2	Data and Analysis Procedures	2-2
	2.3	Comparison of P-coda and Lg Recordings at NORSAR and Graefenburg	2-11
	2.4	Spatial Variation Across NORSAR of P-coda and Lg-wave Amplitude	2-19
	2.5	Lg-to-P Forward Scattering	2-29
3.0	RELATIVE Lg AND P-CODA MAGNITUDE ANALYSIS		3-1
	3.1	Introduction	3-1
	3.2	Graefenburg Lg and P-coda Measurements	3-2
	3.3	Relative Magnitudes and Yields of the Largest Shagan River Explosions	3-25
4.0	CONCLUSIONS AND RECOMMENDATIONS		4-1
ACKNOWLEDGEMENTS			
REFERENCES			

LIST OF FIGURES

Figure No.		Page
1	Map of Western Russia	2-3
2	Deployment of the Original 22 NORSAR Subarrays	2-5
3	Location of Graefenburg Array Stations	2-6
4	Time Windows used for Noise and P-coda Magnitude Measurements	2-8
5	3 Semipalatinsk Explosions Recorded at NORSAR	2-12
6	Broadband and Filtered Traces	2-13
7	NORSAR, Graefenburg Broadband & Filtered Traces	2-15
8	NORSAR and Graefenburg Coda Envelopes	2-16
9	Mid-band and High-band Filtered coda Envelopes	2-18
10	Log-rms P and Coda Envelopes	2-20
11	Array-averaged Log-rms P and Coda Envelopes	2-21
12	Standard Deviations of Log-rms P and Coda Envelopes	2-22
13	NORSAR Array-average rms Amplitudes and Standard Deviations for 3 Shagan River Events	2-23
14	Travel-time Curve for Western Russia from King and Calcagnile (1976)	2-25
15	Log-rms Coda Amplitude Standard Deviation for NORSAR Recordings of the March 25, 1971 Degelen Mountain Event for Traces Beamed to P (top) and Lg (bottom)	2-27
16	Regional Reduced Travel-time Curves for Western Russia	2-31
17	Lg Propagation Paths from Semipalatinsk to NORSAR and Graefenburg	2-32
18	Schematic Illustration of P and Lg Scattering Mechanism	2-33
19	Log-rms Amplitudes of Transverse and Vertical Component Lg at Graefenburg A1 Site	3-3

LIST OF FIGURES (CONT)

Figure No.		Page
20	Scatter Plot of Vertical, High-Frequency Lg Log-rms Amplitudes Recorded at Graefenburg Al Versus m_b	3-6
21	Scatter Plot of Vertical, Mid-Frequency Lg Log-rms Amplitudes Recorded at Graefenburg Al Versus m_b	3-7
22	Scatter Plot of Transverse High-Frequency Lg Log-rms Amplitudes Recorded at Graefenburg Al Versus m_b	3-8
23	Scatter Plot of Mid-Frequency, Transverse Lg Log-rms Amplitudes Recorded at Graefenburg Al Versus m_b	3-9
24	Scatter Plot of High-Frequency, Vertical P-coda Log-rms Amplitudes Recorded at Graefenburg Al Versus m_b	3-10
25	Scatter Plot of Mid-Frequency, Vertical P-coda Log-rms Amplitudes Recorded at Graefenburg Al Versus m_b	3-11
26	Scatter Plot of High-Frequency, Transverse P-coda Log-rms Amplitudes Recorded at Graefenburg Al Versus m_b	3-12
27	Scatter Plot of Mid-Frequency, Transverse P-coda Log-rms Amplitudes Recorded at Graefenburg Al Versus m_b	3-13
28	Histograms of Vertical, High-Frequency Lg Log-rms Amplitudes Recorded at Graefenburg and m_b for Shagan River Events	3-18
29	Histograms of Vertical, Mid-Frequency Lg Log-rms Amplitudes Recorded at Graefenburg and m_b for Shagan River Events	3-19

LIST OF FIGURES (CONT.)

Figure No.		Page
30	Histograms of Transverse, High-Frequency Lg Log-rms Amplitudes Recorded at Graefenburg and m_b for Shagan River Events	3-20
31	Histograms of Transverse, Mid-Frequency Lg Log-rms Amplitudes Recorded at Graefenburg and m_b for Shagan River Events	3-21
32	Histograms of Vertical, High-Frequency P-coda Log-rms Amplitudes Recorded at Graefenburg and m_b for Shagan River Events	3-22
33	Histograms of Vertical, Mid-Frequency P-coda Log-rms Amplitudes Recorded at Graefenburg and m_b for Shagan River Events	3-23
34	Histograms of Transverse, High-Frequency P-coda Log-rms Amplitudes Recorded at Graefenburg and m_b for Shagan River Events	3-24
35	Histograms of Transverse, Mid-Frequency P-coda Log-rms Amplitudes Recorded at Graefenburg and m_b for Shagan River Events	3-25

LIST OF TABLES

Table No.		Page
1	Shagan River Data Used in This Study	1-5
2	Log-rms Amplitude Measurements of Lg and P-coda at the Graefenburg A1 Site for the Largest Shagan River Explosions	3-5
3	Source Parameters for the Largest Shagan River Explosions	3-15
4	Means and Standard Deviations for Magnitude Measurements of Largest Soviet Explosions, 1976-1982	3-27
5	Surface Wave Results for the Largest Shagan River Events (Sykes and Cifuentes, 1983)	3-30

ABSTRACT

We have investigated the characteristics of P-coda and Lg measurements at the NORSAR and Graefenburg arrays for presumed underground nuclear explosions in the Semipalatinsk region of the Soviet Union. Our main objectives in this study were to investigate the effects of the propagation paths in western Russia on the narrowband and broadband recordings of Lg at teleseismic distances and to study the relative P-coda and Lg amplitudes recorded at these two arrays for the largest (m_b > 6.0) Shagan River explosions.

Comparison of broadband recordings of teleseismic Lg at Graefenburg (Δ=42°) with narrowband NORSAR (Δ=38°) and filtered Graefenburg recordings of Lg from Shagan River events reveals that Lg is more obvious, relative to the preceding P-coda, on broadband seismograms than on high-frequency seismograms. Broadband recordings of Lg at Graefenburg are about 0.5 log units stronger in the 0.2 - 1.0 Hz band than in the 0.6 - 3.0 Hz range although noise is also correspondingly higher.

The early P-coda at NORSAR is stronger, relative to Lg, than that at Graefenburg. Also, the coda-envelope shapes are quite different for the two arrays; the NORSAR coda flattens between about 200 to 340 seconds after P, whereas the Graefenburg coda decays monitonically from the P-wave out to the S_n and Lg arrival times. The standard deviations of Lg and S-coda phases at NORSAR are higher by about 0.05 to 0.06 log-rms amplitude units than those of P-coda phases, which is probably related to differential site and propagation effects on P, S and Lg waves. The most stable part of the P-coda before Lg is the flat part of the coda,

where the spatial standard deviation in log-rms amplitude in 5 second windows drops to a minimum of less than 0.1 units. The flat coda envelopes from about 200 to 340 seconds after P, recorded at NORSAR for Semipalatinsk explosions, are consistent, on the basis of timing, to Lg - P forward scattering from lateral heterogeneities in the Ural Mountains.

Measurements on Graefenburg data of vertical and transverse log-rms amplitudes in the P-coda and Lg phase in two frequency bands correlate well with network m_b. These measurements indicate that Lg and P-coda amplitudes do not appear to be strongly affected by the tectonic component as revealed by surface-wave studies. However, the slopes of the regression of Lg amplitude versus m_b were small ranging from 0.6 to 0.8. The slopes of the P-coda regressions were higher, ranging from 0.9 to over 1.0. This supports the idea that early P-coda waves are generated by P scattering. The principal cause of the small slopes is that the variance of the Lg and P-coda amplitudes for the largest Shagan River events are significantly smaller than that of the corresponding network-averaged m_bs. We argue that P-coda and Lg amplitudes are more robust estimators of relative yield than m_b, and that the yield range for these events, based on Lg and P-coda measurements at NORSAR and Graefenburg, is smaller by approximately a factor of 2 than the yield range indicated by m_b. This is consistent with the conjecture of Sykes and Cifuentes (1983), based on surface-wave studies, that the largest Shagan explosions, with m_b greater than 6.0, have nearly the same yield.

1.0 INTRODUCTION

Since mid-1978, the body-wave and surface-wave magnitudes of the largest Soviet nuclear-weapons tests at the Shagan River test site have increased by nearly a factor of two (Alewine and Bache, 1983). Typically, the body-wave magnitudes, m_b, for Shagan River explosions fired since 1978 have been in the range of 5.8 to 6.2. Because explosions with these magnitudes detonated at the Nevada Test Site (NTS) have yields well in excess of 150 kt, the large m_bs of the recent Shagan River explosions have raised concerns about possible violations of the Threshold Test Ban Treaty (TTBT).

The accuracy of absolute yield estimates of underground nuclear explosions, using seismic methods, is reduced by a number of factors, the most important one being the uncertainty in the attenuation bias between NTS and the Shagan River test site. Several direct and indirect methods have been applied to determine the m_b bias so that the m_b-yield calibration, determined for NTS, can be directly used to estimate yields of explosions at Shagan River. However, the large range of bias estimates (0.2 to 0.4 m_b) makes it difficult to determine with m_b the yields of the largest Shagan explosion with a large degree of certainty.

An alternative approach is to utilize measurements which are not as much affected by attenuation bias as m_b. One such measurement is the surface-wave magnitude, or M_s. Sykes and Cifuentes (1984) estimated the yields of the largest Shagan River explosions with low tectonic release with M_s measurements and concluded that the explosions with m_bs ranging from 6.0 to 6.2 had essentially the same yield but less than 150 kt. They argued

that the large variance in m_b results from geologic variations in the source region and measurement uncertainties.

The problem with M_s yield estimation is that surface waves can be affected by non-isotropic, tectonic component. Sykes and Cifuentes (1984) avoided this problem by selecting events for calibration and yield estimation which had low tectonic component. Given et al (1983) and Given and Mellman (1984) have applied source inversion techniques to the Shagan River explosions in order to obtain a magnitude correction for the tectonic component. However, this method is still being tested.

The Lg phase has proven to be useful for yield estimation because it combines the advantages of surface waves along with the fact that Lg magnitudes appear to be insensitive to tectonic component (Alexander, 1984). Nuttli (1984) has developed an absolute Lg magnitude method in which Lg magnitude attenuation corrections are determined from Lg-coda Q estimates. Although Nuttli has had great success with applying this method to events of known yield, other investigators have not been as successful (Rondout Associates, 1984). The problem seems to be large uncertainties in the estimation of Lg-coda Q from the time decay of frequencies in the coda. Nuttli (1984) has suggested that the possible causes of these uncertainties are interference of fundamental mode Rayleigh waves and noise with the coda which can cause inaccurate frequency estimates at large epoch times into the coda.

Nuttli (1984) has applied his Lg magnitude yield estimation technique to regional recordings of Shagan River explosions, including some of the largest explosions. His yield estimates for the largest explosions (m_b between 6.0 and 6.2) range from 120 to 229 kt. Also, by comparing Lg magnitudes with network-

averaged m_b for events at NTS and Shagan River and assuming absolute Lg magnitudes to be insensitive attenuated bias, Nuttli (1984) obtains a preliminary m_b bias between NTS and Shagan River of about 0.41 magnitude units.

The network bias problem could in principle be eliminated if the TTBT were ratified, because the protocol of the treaty calls for two calibration shots of known yield to be fired within each distinct geologic region at each test site in the U.S. and the USSR. Assuming that the yields of the calibration explosions are accurate, the m_b attenuation bias could be directly determined. However, there would still remain the question of the precision of m_b estimates for relative yield estimation. Sykes and Cifuentes (1984) have suggested an m_b variance as great as 0.2 magnitude units for largest Shagan River explosions of the same yield which could result in close to a factor of two uncertainty of yield estimation.

There have been a number of studies which have indicated that measurements made in the P-coda are at least as stable as network-averaged m_b estimates and significantly better than single-station m_b (Baumgardt, 1983; Bullitt and Cormier, 1984; Baumgardt, 1984; Gupta et al, 1984). Similar results have been obtained for Lg and Lg-coda wave measurements (Ringdal, 1983; Alexander, 1984). These results suggest that the yield estimation precision may be improved by using magnitudes derived from long averaging windows in the P-coda and on the Lg phase. Apparently, such measurements average out the effects of focusing and defocusing which cause the large scatter in P-wave magnitudes.

In this report, we present the results of a study of the precision of using P-coda and Lg measurements for relative yield

estimation. In particular, we focus on the P-codas and Lg-waves recorded at two seismic arrays, NORSAR and Graefenburg, from the largest underground explosions detonated at Shagan River. Table 1 gives a list of the events, their m_bs as determined by Sykes and Cifuentes (1984) and NEIS, and the NORSAR and Graefenburg data which were available for this study. In the first part of the report we discuss the broad characteristics of the long P-codas recorded at these two arrays for the largest Shagan River explosions. In this section, we suggest that Lg forward scattering from heterogeneities along the path between the source and receiver may be important for generating P-coda waves. In the second part of this report, we investigate the conjecture of Sykes and Cifuentes (1984) that the Shagan River explosions with m_bs greater than 6.0 are of approximately the same yield, by analyzing the relative P-coda and Lg amplitudes for these events. Our overall conclusions from this study are that single-site P-coda and Lg measurements are as precise as network M_s measurements for relative yield estimation and indicate that the largest Shagan River explosions are closer in yield than indicated by their network m_b estimates.

TABLE 1
SHAGAN RIVER DATA USED IN THIS STUDY

Date	m_b*	NORSAR Data	GRAEFENBURG Data
15 Sep 1978	5.963	x	x
4 Nov 1978	5.576	x	x
29 Nov 1978	5.996		x
23 Jun 1979	6.215	x	x
7 Jul 1979	5.839	x	x
4 Aug 1979	6.161	x	x
18 Aug 1979	6.170		x
28 Oct 1979	5.990		x
2 Dec 1979	5.998		x
23 Dec 1979	6.170		x
12 Jun 1980	5.6		x
29 Jun 1980	5.707		x
12 Oct 1980	5.918	x	x
14 Dec 1980	5.953		x
13 Sep 1981	6.064		x
29 Mar 1981	5.6		x
22 Apr 1981	5.954	x	
25 Apr 1982	6.1	x	
5 Dec 1982	6.1	x	
26 Dec 1982	5.7	x	
12 Jun 1983	6.1	x	
6 Oct 1983	6.0	x	
26 Oct 1983	6.1	x	
19 Feb 1984	5.9	x	
15 Apr 1984	5.7	x	
25 Apr 1984	6.0	x	
26 May 1984	6.1	x	

* Magnitude estimates to two 3-decimal places are from Sykes and Cifuentes (1983). All others are from NEIS.

2.0 TELESEISMIC P-CODA AND Lg-WAVES IN EURASIA

2.1 INTRODUCTION

In seismological studies of earthquakes and quarry blasts at local and regional distances, the short-period P and Pn coda, Lg, and Lg coda have played important roles. Theoretical and empirical attenuation studies by means of spectral analysis of P and Lg codas have provided insights into the relative importance of intrinsic and scattering attenuation of Lg and lateral variations of attenuation in the earth's crust and lithosphere. (Herrmann, 1980; Singh and Herrmann, 1983; Herrmann and Wang, 1983.) Moreover, P-coda duration magnitude and m_b (Lg) magnitudes have been routinely determined for local and regional seismic events and have long been known to provide very stable magnitude estimates. (Herrmann, 1975; Bakun and Lindh, 1977; Suteau and Whitcomb, 1979; Shapira, 1981.)

In the area of seismological monitoring of nuclear test ban treaties, yield estimation for verification of the threshold treaty is based almost entirely on m_b estimates at teleseismic distances. However, recent studies, discussed above, have revealed that m_b measures are subject to a number of biases, one of the most important being focusing and defocusing of short-period P-waves by lateral heterogeneities in the earth. Teleseismic P-coda and regional Lg magnitudes have proven to be surprisingly stable in spite of the complexity of high-frequency scattered and higher-mode waves.

In this section, we discuss the characteristics of long-term codas (P, P-coda, Lg, Lg-coda) recorded at the two arrays, Graefenburg and NORSAR, from the largest Shagan River explosions. NORSAR and Graefenburg are at distances of 38^{o} and 42^{o}, respectively, and thus, are well into the teleseismic distance range. In this section we show that Lg is well recorded at these two arrays. Further, we suggest that forward scattering of Lg-to-P from heterogeneities between the source and receiver may generate some of the pre-Lg P-coda waves. The results are important in regard to our understanding of the origin of the P-coda, the nature of scattering attenuation of Lg, and the utility of P-coda and Lg measurements for yield estimation.

2.2 DATA AND ANALYSIS PROCEDURES

Figure 1 shows the location of the Semipalatinsk test area and the two arrays, Graefenburg and NORSAR. The propagation paths from the Semipalatinsk test site to both of these arrays are very similar, although there may be some near receiver differences.

Propagation paths in western Russia are primarily shield type and Lg-wave propagation across this region has been found to be very efficient (North, 1978; Gupta et al, 1980; Nuttli, 1981). North (1978) found that the observed attenuation of Lg-waves at Scandinavian stations from sources distributed throughout western Russia was roughly consistent with that determined by Nuttli (1973) for eastern United States, or $\gamma = 0.07$ deg^{-1}. Nuttli (1981) observed a somewhat higher value of $\gamma = 0.133$ deg^{-1} for similar paths which, nevertheless, is still quite low. North (1978) also concluded that the Ural Mountains and Baltic Sea do not block or strongly attenuate Lg-waves which cross these structures from

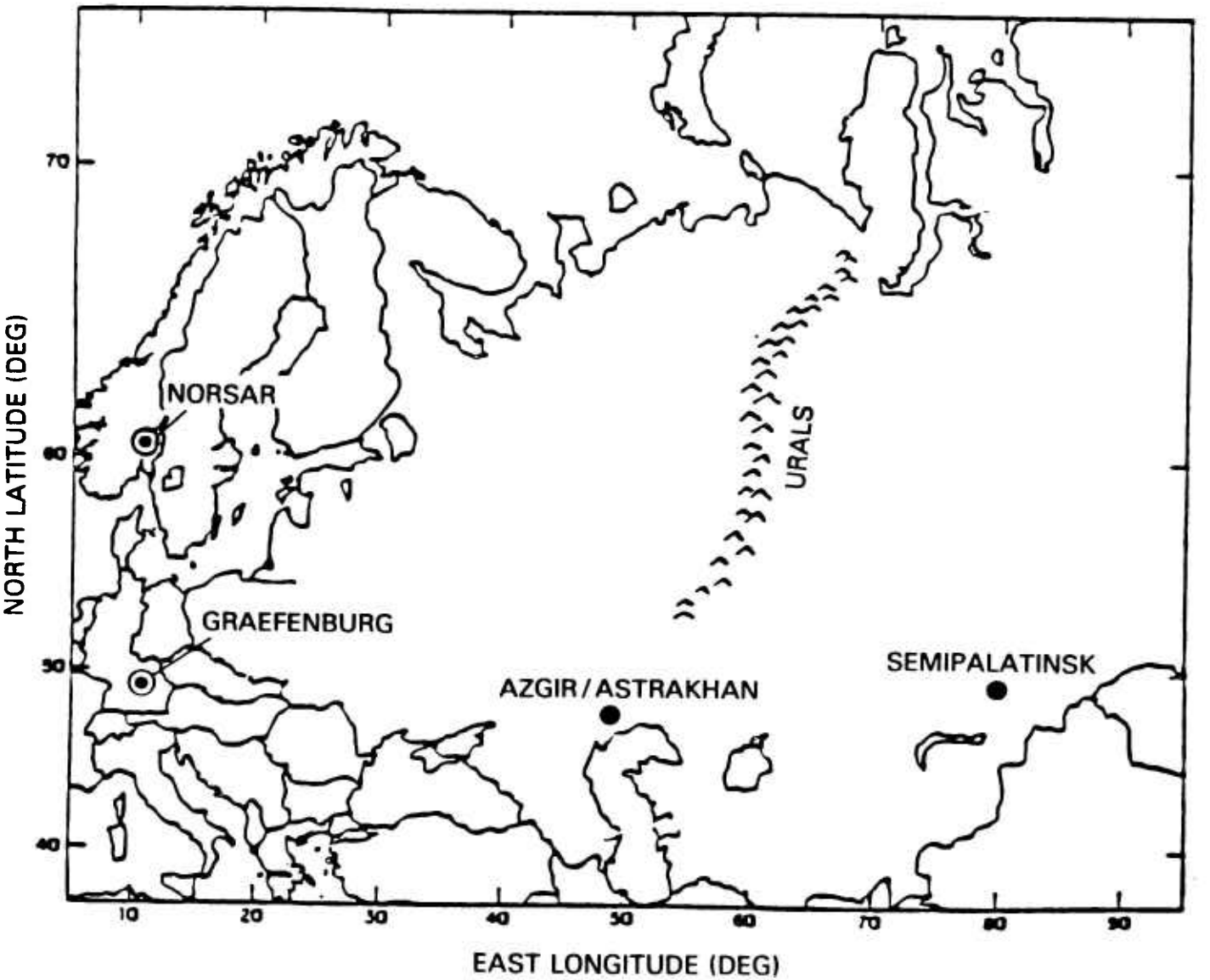

FIGURE 1 MAP OF WESTERN RUSSIA

events in western Russia to stations in Scandinavia. Thus, the low attenuation of Lg along the stable Baltic shield paths accounts for the teleseismic observation of Lg at the Scandinavian stations.

The configuration of the NORSAR array is illustrated in Figure 2. The array originally consisted of 22 subarrays, with each subarray consisting of six short-period, vertical instruments. The horizontal diameter was 100km. Since October 1, 1976, the array has consisted of seven subarrays spread over a 50 km aperture and shown in Figure 2 by the filled circles.

The Graefenburg-array instrument locations are shown in Figure 3. In the present study we have concentrated on data recorded at the A1 three-component sensor, which is also the location of the GRFO SRO station. The unique feature of the Graefenburg array data is that it is recorded broadband, with an instrument response flat to velocity from about 20 seconds period to 5 Hz (Harjes and Seidl, 1978). In contrast, the NORSAR sensors record data in the traditional short-period and long-period bands. The mid-period band, from about 1.6 to 5 seconds is not sampled at NORSAR, but is passed by the broadband instruments at Graefenburg.

Table 1 lists the events which were examined in this study, their magnitudes as determined by Sykes and Cifuentes (1983) and NEIS, and the available data from NORSAR and Graefenburg. Table 1 shows that we have data for several events that were recorded by both NORSAR and Graefenburg. Comparison of seismograms recorded at the two arrays for common events allows us to examine the effect of the bandpasses on the coda and Lg recordings and to look for subtle differences between the Shagan-NORSAR and Shagan-

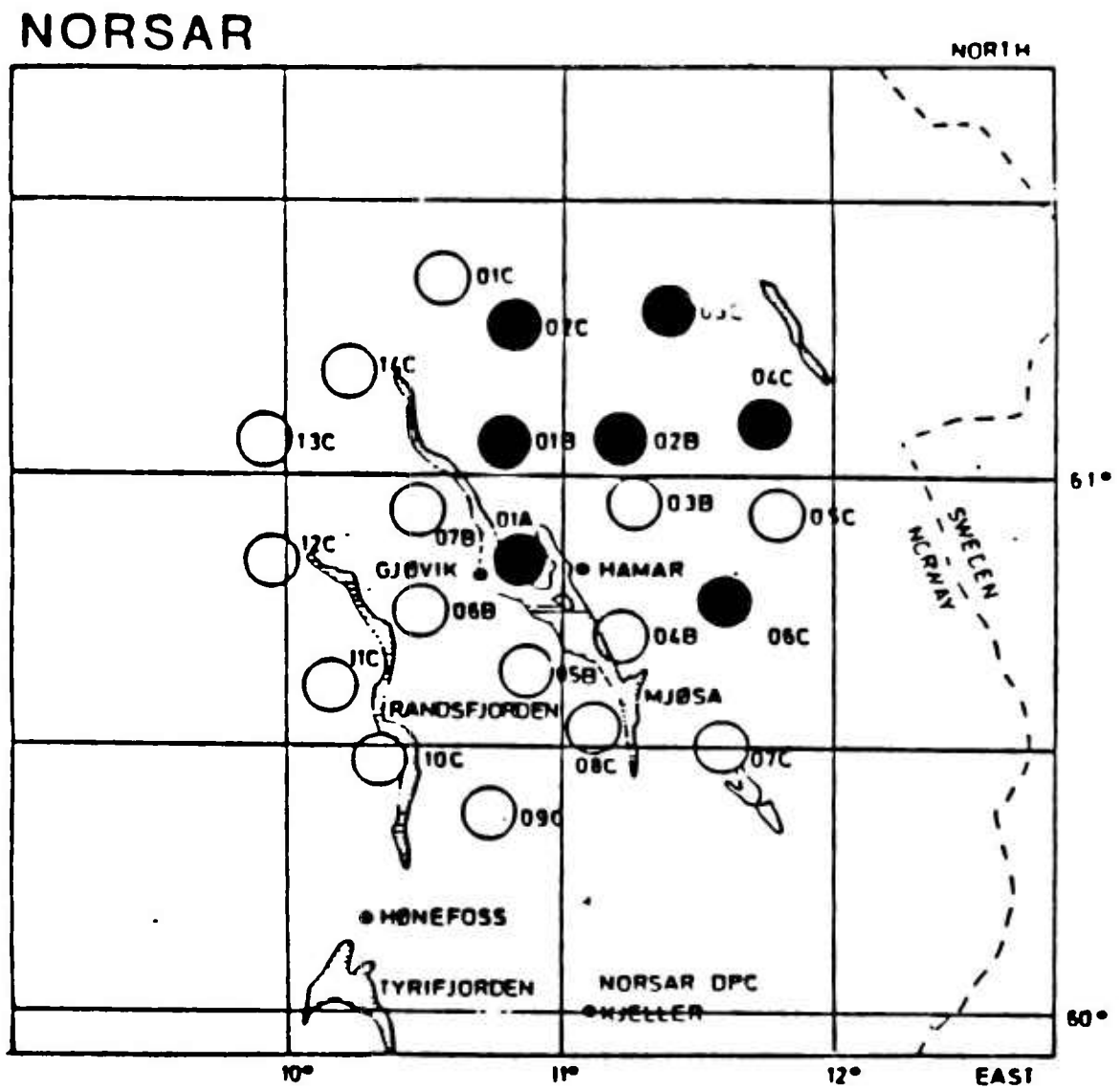

FIGURE 2 DEPLOYMENT OF THE ORIGINAL 22 NORSAR SUBARRAYS (FROM 1971 TO OCTOBER 1, 1976). THE SUBSET OF 7 SUBARRAYS IN OPERATION SINCE OCTOBER 1, 1976, ARE MARKED AS FILLED CIRCLES.

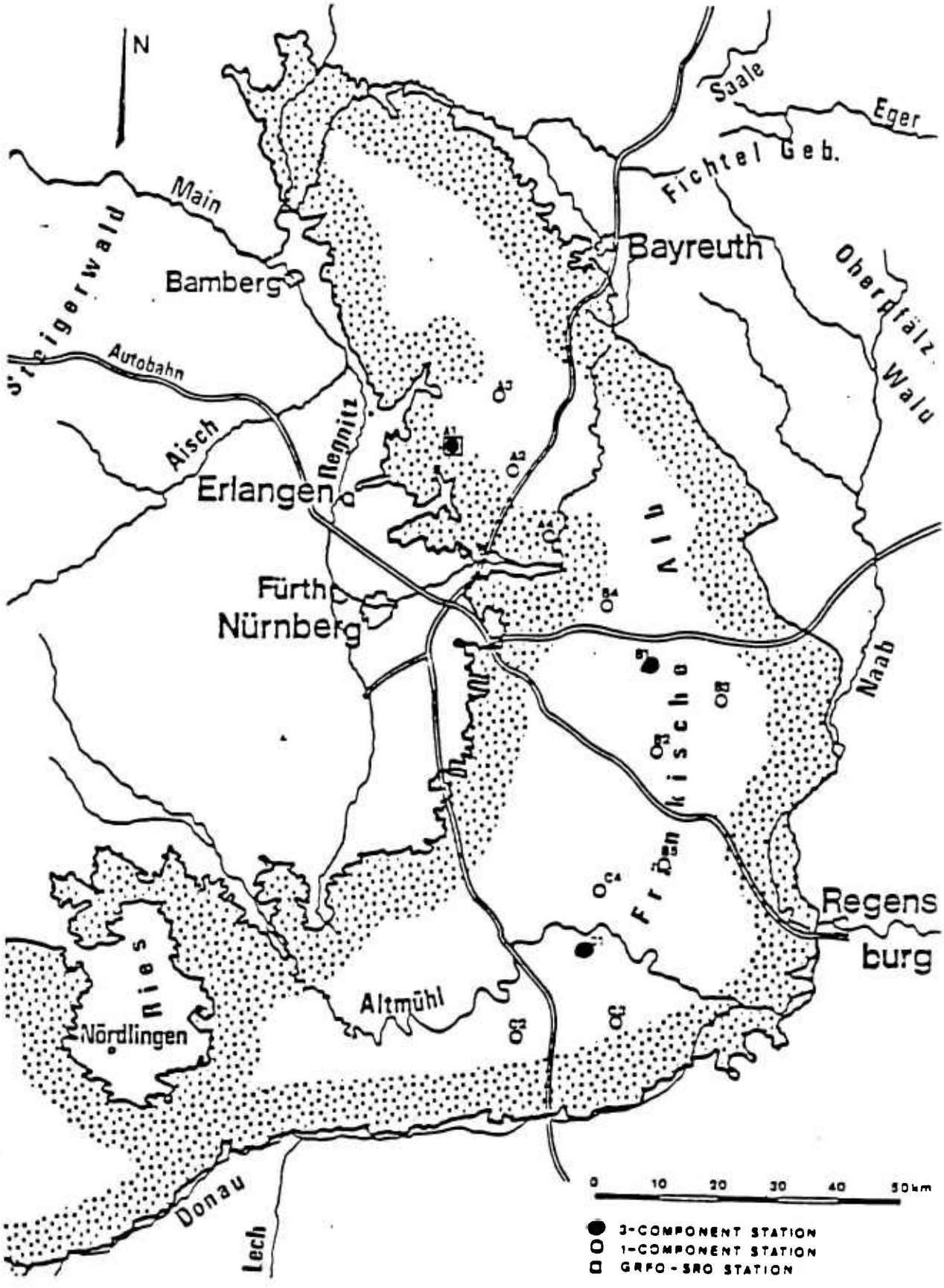

FIGURE 3 LOCATION OF GRAEFENBURG ARRAY STATIONS (FROM HARJES AND SEIDL, 1978)

Graefenburg propagation paths. We expect that the P-coda and Lg-waves, recorded in the same frequency bands, should be very similar, given the simularity of distance, if the propagation paths from Shagan to the two arrays are similar.

In addition, in examining the actual traces, we also make a number of measurements in the codas which are useful for comparison and for determining P-coda, Lg, and Lg-coda magnitudes. Each coda is first broken into a set of 5 second windows, starting 5 seconds with the first-arrival P, as shown schematically in Figure 4. The background noise ahead of the first arrival is also windowed in the same manner. The rms amplitude is then computed in each 5 second window as follows:

$$\bar{A}_{jk} = \sqrt{\frac{1}{N} \sum_{i=1}^{N} A_{ijk}^2} \qquad (1)$$

where A_{ijk} amplitude of the i'th time point, j'th window, k'th channel.

N number of time points in the window.

We compute an average noise level, $\bar{N}_k$, for the k'th channel by averaging the logarithms of the rms amplitudes in 10 adjacent 5 second windows, or 50 seconds of background noise:

$$\bar{N}_k = \frac{1}{M_n} \left[\sum_{j=1}^{M_n} \log \bar{A}_{jk}^n \right] \qquad (2)$$

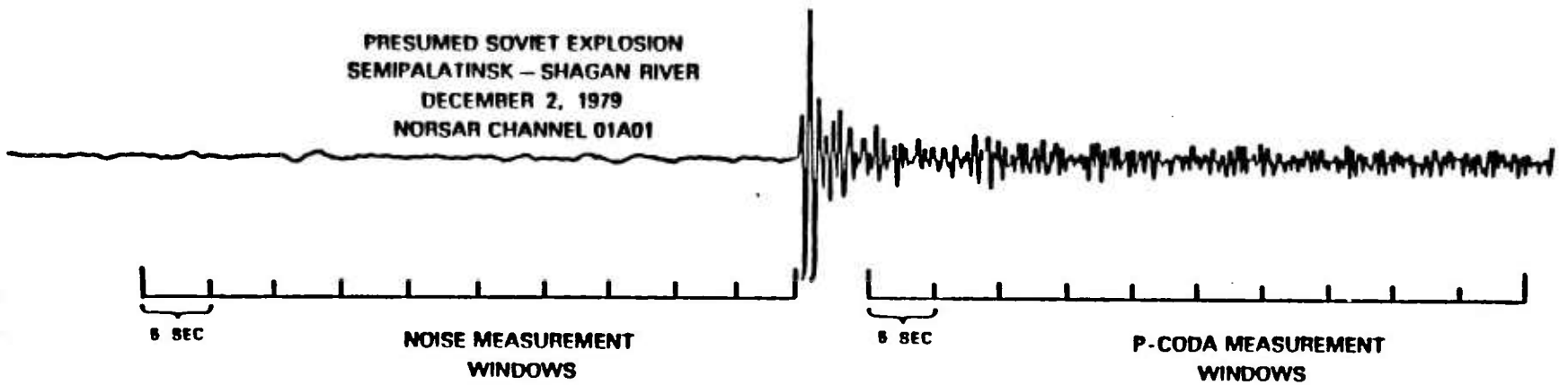

FIGURE 4 TIME WINDOWS USED FOR NOISE AND P-CODA MAGNITUDE MEASUREMENTS

where $\bar{A}_{jk}^{n}$ is rms amplitude in the $_j$'th window in the noise recorded on the $_k$'th channel and M_n is the number of windows (usually 10) in the noise.

In our analysis of long-term P-codas, we have found it very useful to plot, as coda envelopes, the log-rms amplitudes as a function of time in adjacent 5 second windows. For a single channel, the signal level in each window is:

$$S_{jk} = \log \bar{A}_{jk} \tag{3}$$

for the $_k$'th channel. The average across an array is:

$$\hat{S}_j = \frac{1}{L} \sum_{k=1}^{L} S_{jk} \tag{4}$$

and the standard deviation is

$$SD_j^S = \sqrt{\frac{1}{L-1} \sum_{k=1}^{L} (S_{jk} - S_j)^2} \tag{5}$$

where L is the number of channels in the array. For a single channel, we compare S_{jk} as a function of time, corresponding to the start of each window, with the average noise level, $\bar{N}_k$. In the multichannel case, we compare the S_j values against the noise levels averaged across the array:

$$\hat{\bar{N}} = \frac{1}{M_n} \sum_{j=1}^{M_n} \left[\frac{1}{L} \sum_{k=1}^{L} \log \bar{A}_{jk}^{n} \right] \quad (6)$$

Notice that in (6) we have taken the channel average of log-rms amplitude before taking the average over all the windows, instead of averaging the window average in (2) across all channels in the array. The corresponding noise standard deviation is

$$SD^n = \frac{1}{M_n} \sum_{j=1}^{M_n} \left[\sqrt{\frac{1}{L-1} \sum_{k=1}^{L} (\log A_{jk}^{n} - \hat{\bar{N}})^2} \right] \quad (7)$$

Thus, in comparing S_j with $\bar{N}$, SD_j^s with SD^n and S_{jk} with $\bar{N}_k$, we are comparing each 5 second windowed, log-rms P-coda amplitude as a function of time with the average of the log-rms noise amplitude, in 5 second windows, over the 50 seconds of noise ahead of P.

We determine average P-coda and Lg magnitude in the same way that we compute the average noise levels for a single channel in (2). Thus,

$$\hat{\bar{S}}_k = \frac{1}{M_s} \left[\sum_{j=1}^{M_s} \log A_{jk}^{s} \right] \quad (8)$$

where A_{jk} is an rms amplitude measurement in the $_j$'th window and the $_k$'th channel, and M_s is the number of windows.

In past studies, (Baumgardt, 1983, 1984), we have also examined array-average coda and Lg log-rms amplitudes determined in the same manner as the noise in (6). However, Ringdal (1983) and Baumgardt (1984) showed that array-average measurements were almost perfectly correlated with single-channel measurements. Thus, in this study, we have only made single-channel measurements.

2.3 COMPARISON OF P-CODA AND Lg RECORDINGS AT NORSAR AND GRAEFENBURG

Figure 5 shows traces of three large Semipalatinsk explosions recorded at one of the NORSAR sensors. The plots are highly compressed, with each plot covering a time span of 20 minutes, and the tick marks on the time scale denote 10 seconds. The plots reveal the emergent nature of the teleseismic Lg phase recorded at NORSAR. It would be very difficult to find Lg on these traces if they weren't plotted in this highly compressed form. Also, note the variability of the relative amplitude of the P and PP phases for these events, which are only 30 to 40 km apart. This is an example of the effect of ray-parameter dependent focusing and defocusing in the earth which causes significant variations of P-wave magnitudes.

A Graefenburg recording of a Shagan River explosion is shown in Figure 6. The top trace is the original broadband trace and the bottom trace is the broadband seismogram passed through a high-pass filter. The filter is a 6-pole recursive filter with a low-frequency cutoff of 0.6 Hz, which is close to that of the

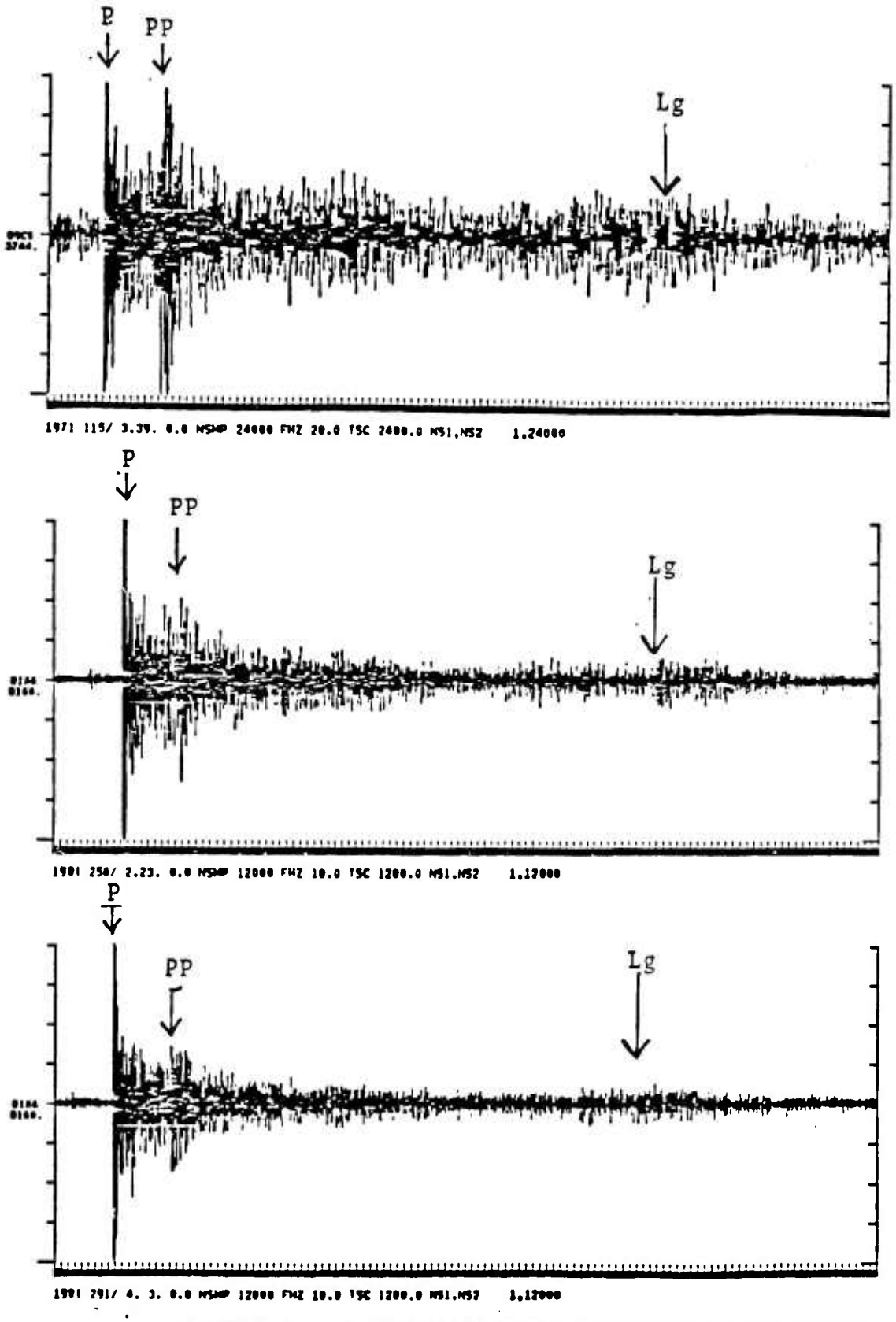

FIGURE 5 3 SEMIPALATINSK EXPLOSIONS RECORDED AT NORSAR

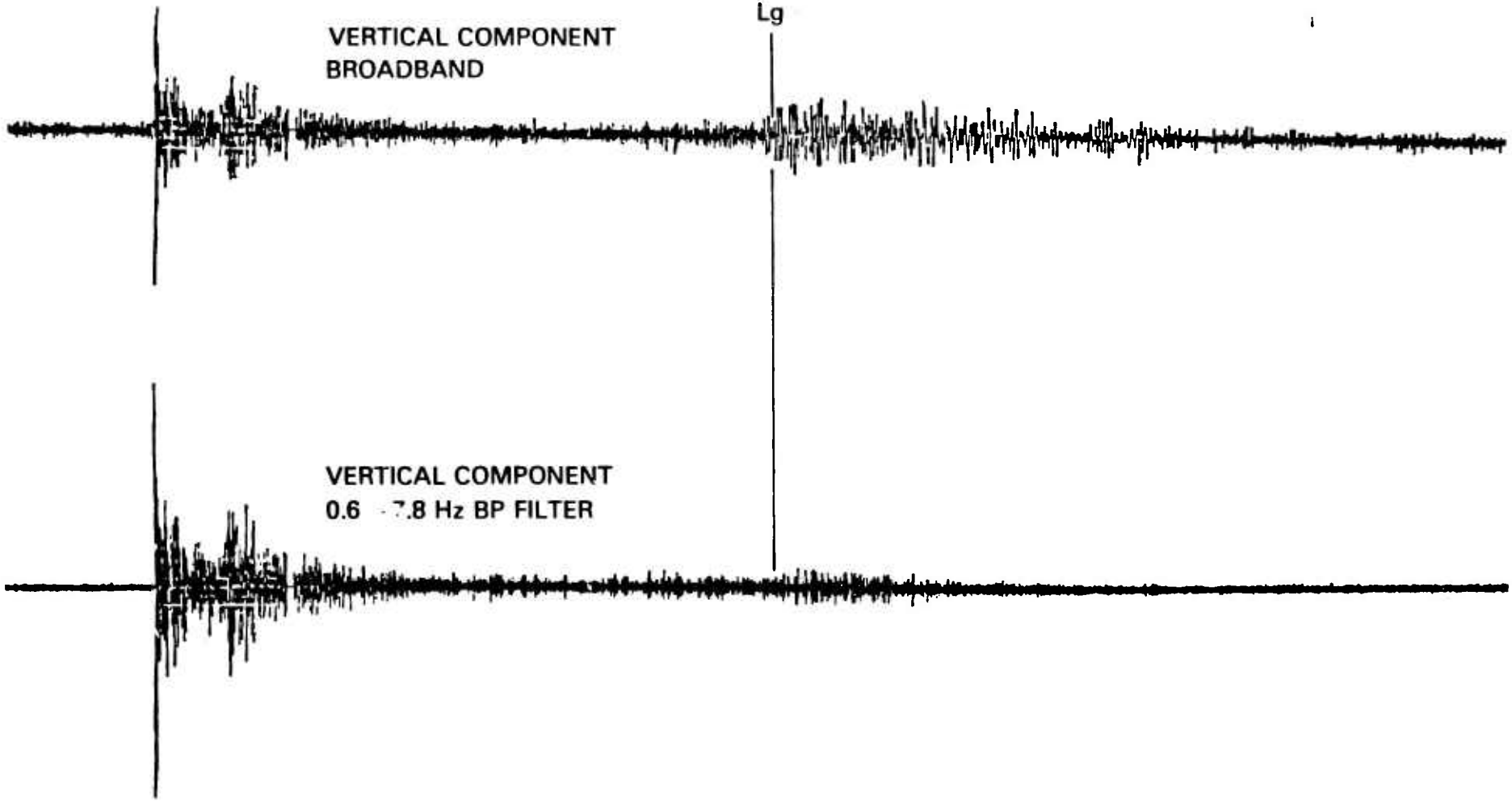

FIGURE 6 BROADBAND (TOP) AND FILTERED (BOTTOM) TRACES OF THE 4 AUGUST 1979 SHAGAN RIVER EVENT RECORDED AT THE GRAEFENBURG ARRAY

NORSAR instrument filter. Notice that the Lg wave on the broadband trace is very strong and appears to be a distinct phase as opposed to a slight increase in the coda level, as in Figure 6. However, Lg is less clear on the bottom trace which is filtered to resemble the NORSAR instrument bandpass.

Figure 7 compares seismograms written at NORSAR and Graefenburg by an explosion at Shagan River. Notice that the Lg wave is more obvious on the broadband Graefenburg trace than on the high-frequency NORSAR trace. The third trace at the bottom of Figure 7 was made by passing the broadband Graefenburg trace through the high-pass filter which simulates the high-frequency NORSAR response. In the high-frequency band at Graefenburg, the Lg phase is weaker relative to the preceding coda than in the broadband recording. Also, comparing the top and bottom traces reveals that the coda ahead of the Lg phases appears to be more intense at NORSAR than at Graefenburg. Also, note that although the Lg phase is stronger in the intermediate band than in the high-frequency band, so also is the noise level ahead of the first arrival P.

Another representation of explosion codas recorded at the NORSAR and Graefenburg arrays is given in Figure 8, where we have plotted single-channel log-rms amplitudes, computed in 5 second windows as a function of time, as discussed above (Equation 3). Each seismogram was passed through a 0.6 - 3.0 Hz filter prior to computing the rms amplitudes. The horizontal lines on each plot denote the average rms amplitude in the 50 seconds of noise background ahead of the first-arrival P. Thus, we are comparing 5 second coda levels, determined by equation 3, with the average 5 second noise level, determined by equation 2, in the 50 seconds of noise ahead of P. These plots show that the Lg amplitudes,

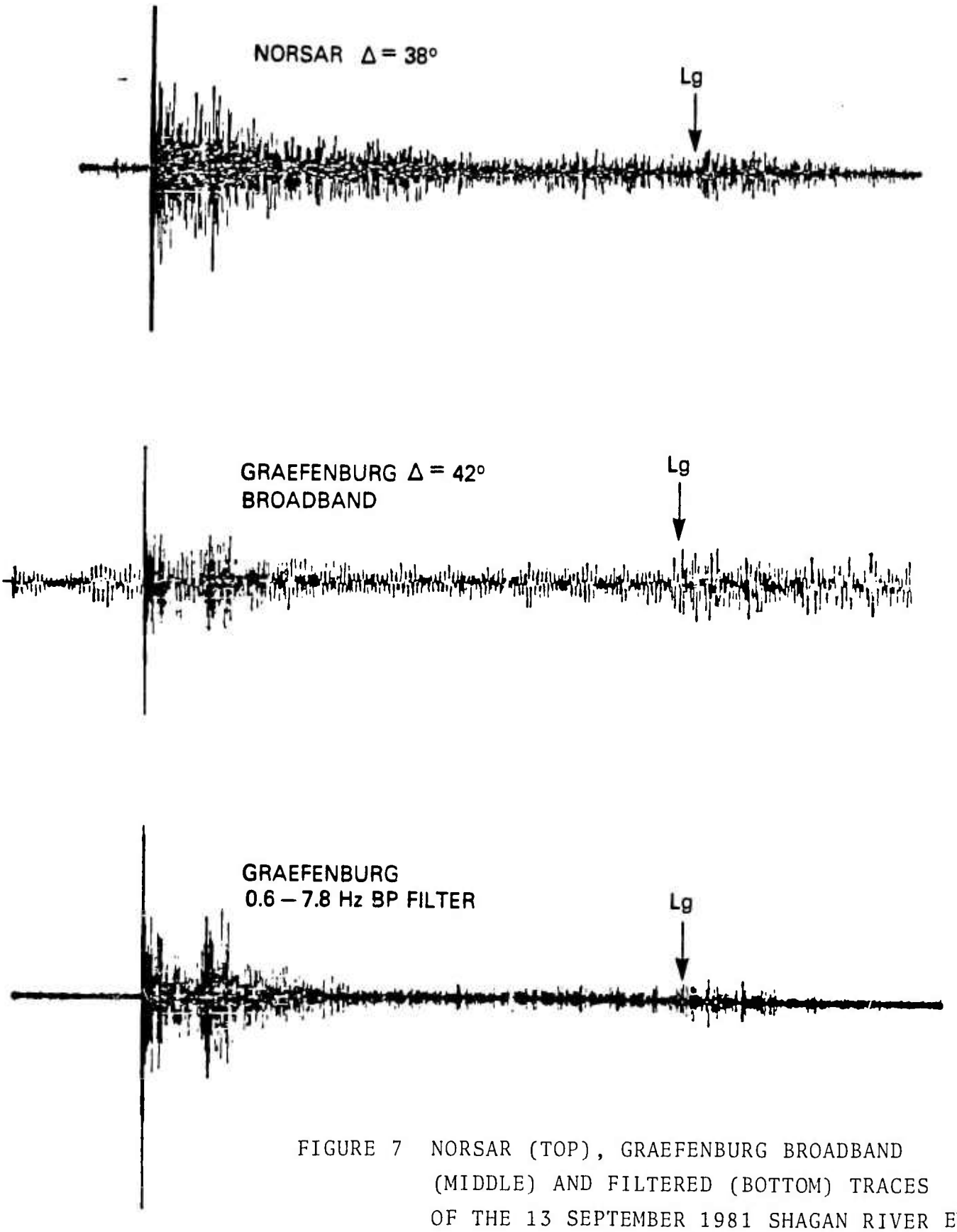

FIGURE 7 NORSAR (TOP), GRAEFENBURG BROADBAND (MIDDLE) AND FILTERED (BOTTOM) TRACES OF THE 13 SEPTEMBER 1981 SHAGAN RIVER EVENT

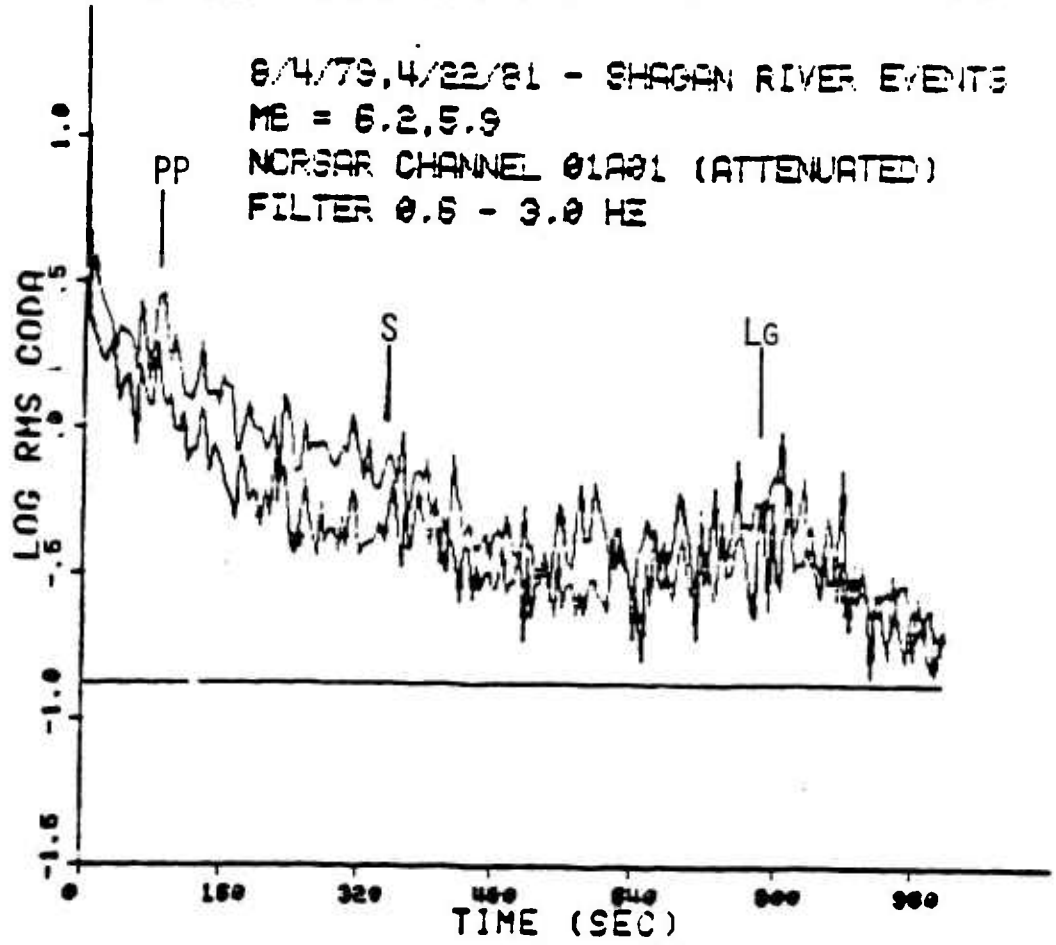

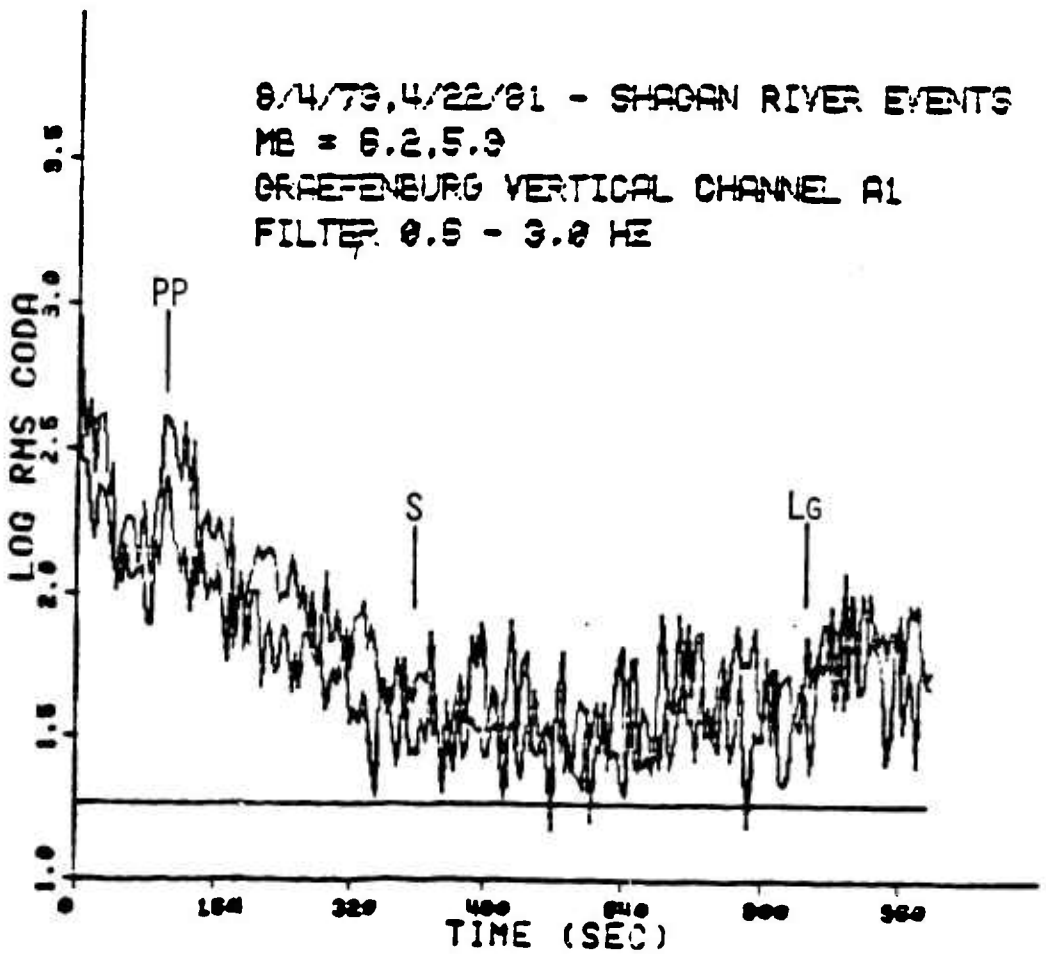

FIGURE 8 NORSAR (TOP) AND GRAEFENBURG (BOTTOM) CODA ENVELOPES OF THE 4 AUGUST 1979 AND 22 APRIL 1981 SHAGAN RIVER EVENTS

relative to the noise, are about the same at NORSAR and Graefenburg, which is consistent with the observation in Figure 7. The signal-to-noise ratios for Lg at each array are about 12 to 14 dB in the 0.6 - 3.0 Hz band. Also, note that the pre-Lg coda level appears slightly greater, relative to noise, at NORSAR than at Graefenburg.

Figure 9 shows coda plots for a Shagan River explosion recorded at Graefenburg in two frequency bands: 0.2 - 1.0 Hz at top and 0.6 - 3.0 Hz at bottom. Comparison of these two plots shows that the Lg level is clearly higher relative to the coda level in the mid-period band than in the short-period band. However, note that the noise level is also higher in the mid-period band than in the short-period band, which results in the Lg signal-to-noise ratio being about the same in the two bands.

These results illustrate the advantage and disadvantages of broadband recording of regional seismic phases. Figures 6, 7, and 8 show that Lg excitation is stronger in the mid-period range than in the high-frequency band, a fact also pointed out by (Noponen et al, 1979). However, the noise level is also higher. Thus, broadband signal-to-noise ratios are not significantly higher than those in the high-frequency band although broadband Lgs do stand out more clearly than high-frequency Lgs. Thus, Lg magnitudes may be measured more easily and reliably on broadband traces than on high-frequency traces. However, another possible problem with low-frequency Lg magnitudes is that they may be more affected by tectonic component than high-frequency Lg magnitudes. We shall consider this point again in Section 3.0.

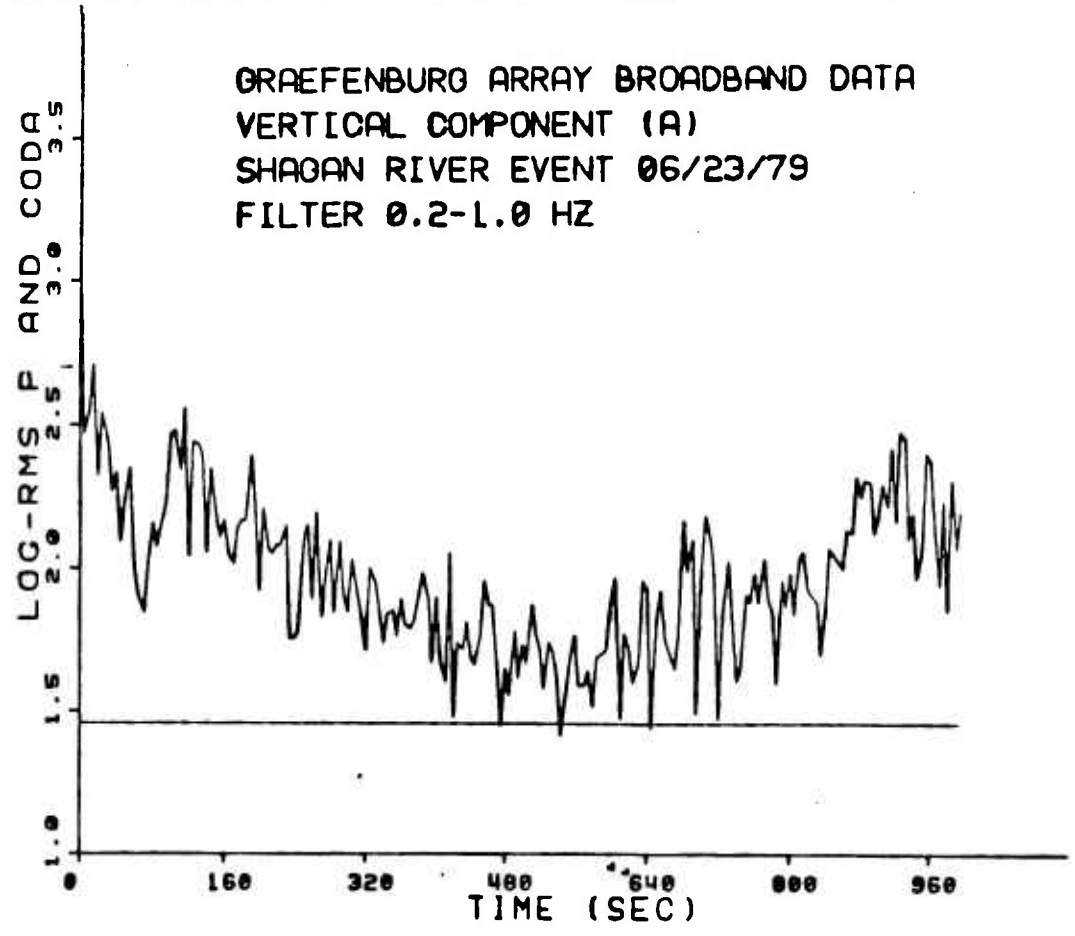

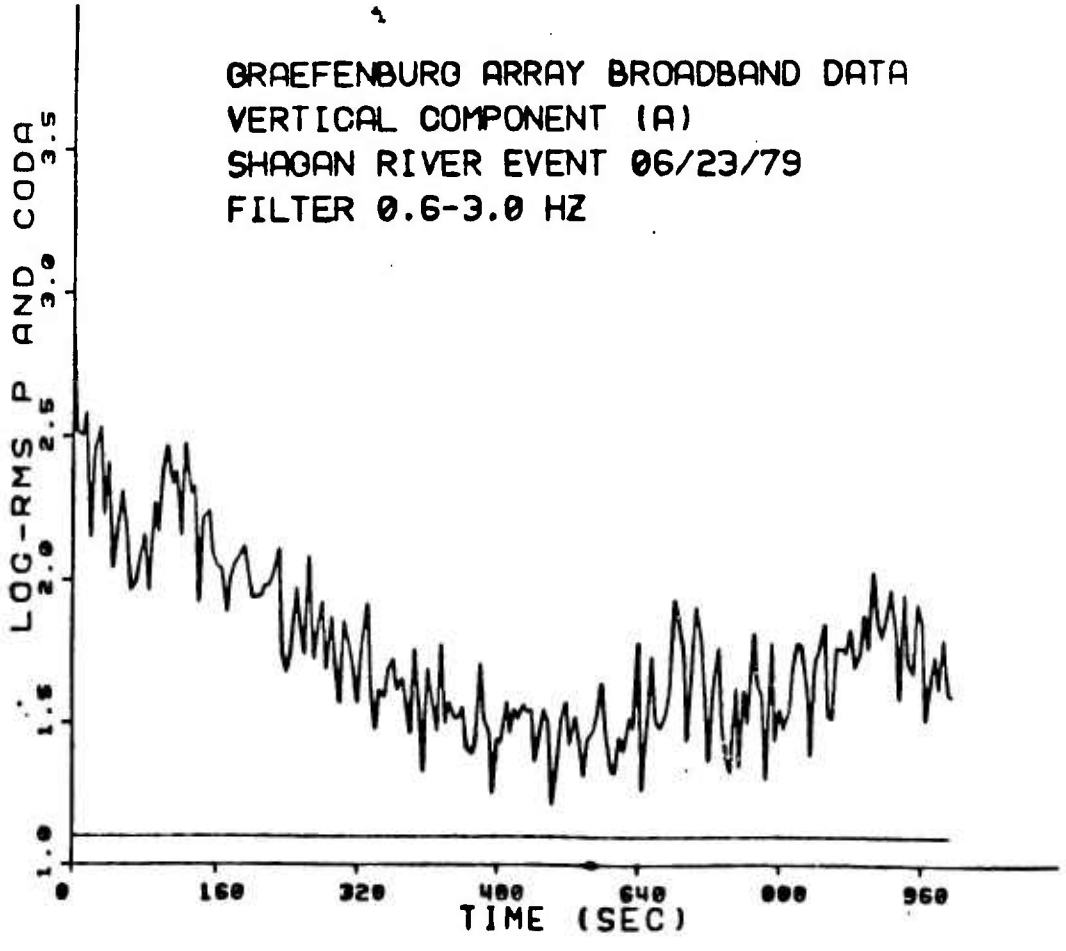

FIGURE 9 MID-BAND (TOP) AND HIGH-BAND (BOTTOM) FILTERED CODA ENVELOPES FROM 23 JUNE 1979 SHAGAN RIVER EVENT RECORDED AT GRAEFENBURG

2.4 SPATIAL VARIATION ACROSS NORSAR OF P-CODA AND Lg-WAVE AMPLITUDES

Figure 10 shows coda plots for 16 Semipalatinsk explosions recorded at the 01A01 channel at NORSAR. Clearly, the plots reveal significant scatter caused by local scattering beneath the receiver. These effects are essentially random, and the variance can be reduced by averaging the rms amplitudes across all available channels (equation 4). The result of this processing is shown in Figure 11, where the time variance has been reduced enough such that a structure can be discerned. All codas show a noticeable flattening starting at about 200 seconds and extending to about 340 seconds. A second flattening starts at about 480 seconds and extends to about the Lg time of about 745 seconds.

Figure 12 shows a plot of the standard deviations in the log-rms amplitudes across the array as a function of time (equation 5). All the codas exhibit a drop in standard deviation from about 0.2 to 0.25 for the P and PP waves to 0.05 to 0.1 in the early coda. Notice that the noise standard deviation in the log-rms levels is about 0.12. The standard deviations begin rising at about 320 seconds, peak at about 0.15 at 800 seconds, and tail off thereafter.

Figure 13 shows the log-rms amplitudes, averaged across the array, and their standard deviations plotted with time for three Shagan River events. The large standard deviations associated with the P and PP arrivals are clearly evident and are probably a result of focusing and defocusing effects from laterally heterogeneous structure beneath the array. Another phase of interest, which arrives about 60 seconds after P, is labelled P_{420} in Figure 13. This phase is very coherent across the array and

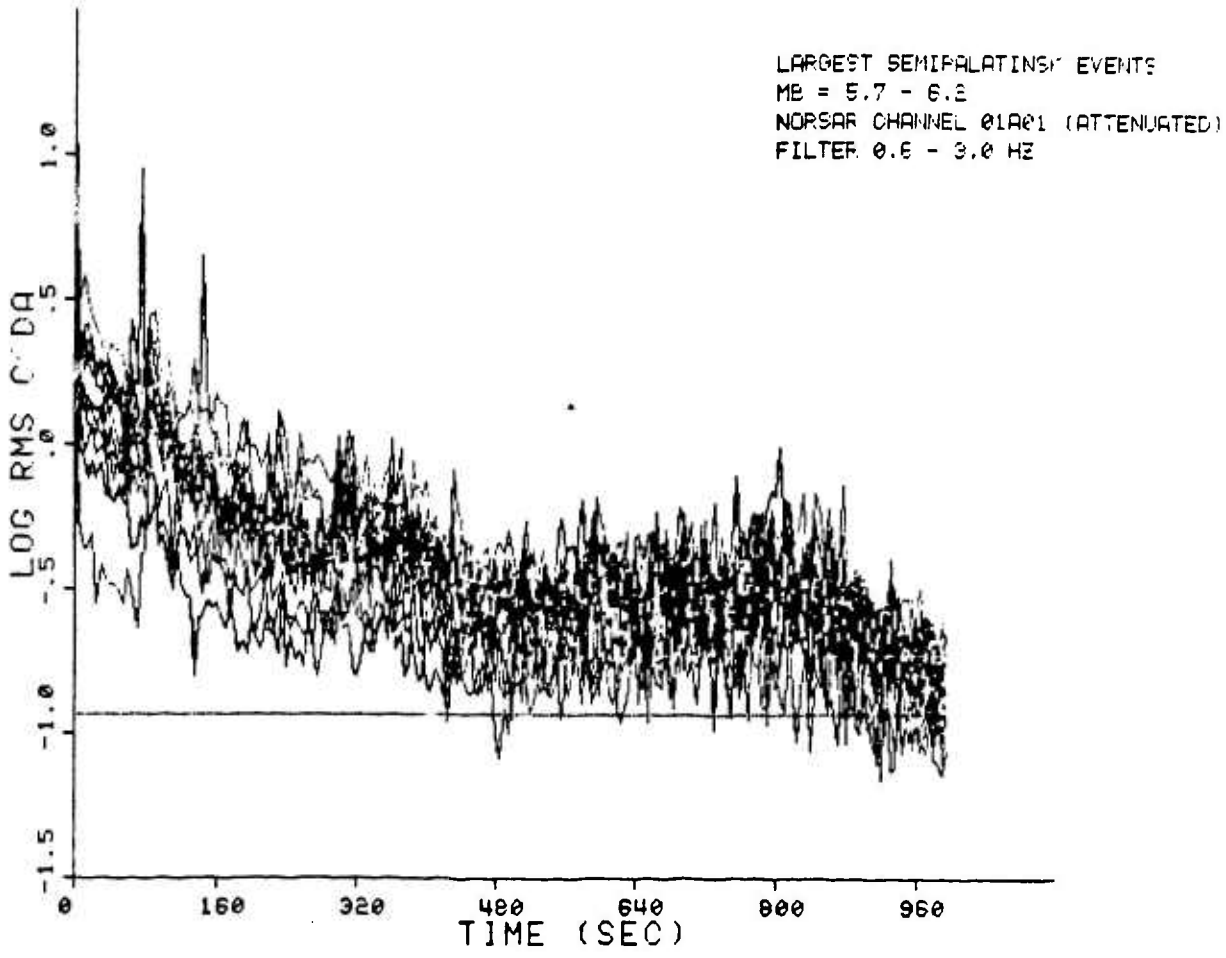

FIGURE 10 LOG-RMS P AND CODA ENVELOPES FROM 16 SEMI-PALATINSK EVENTS RECORDED AT THE 01A01 CHANNEL AT NORSAR

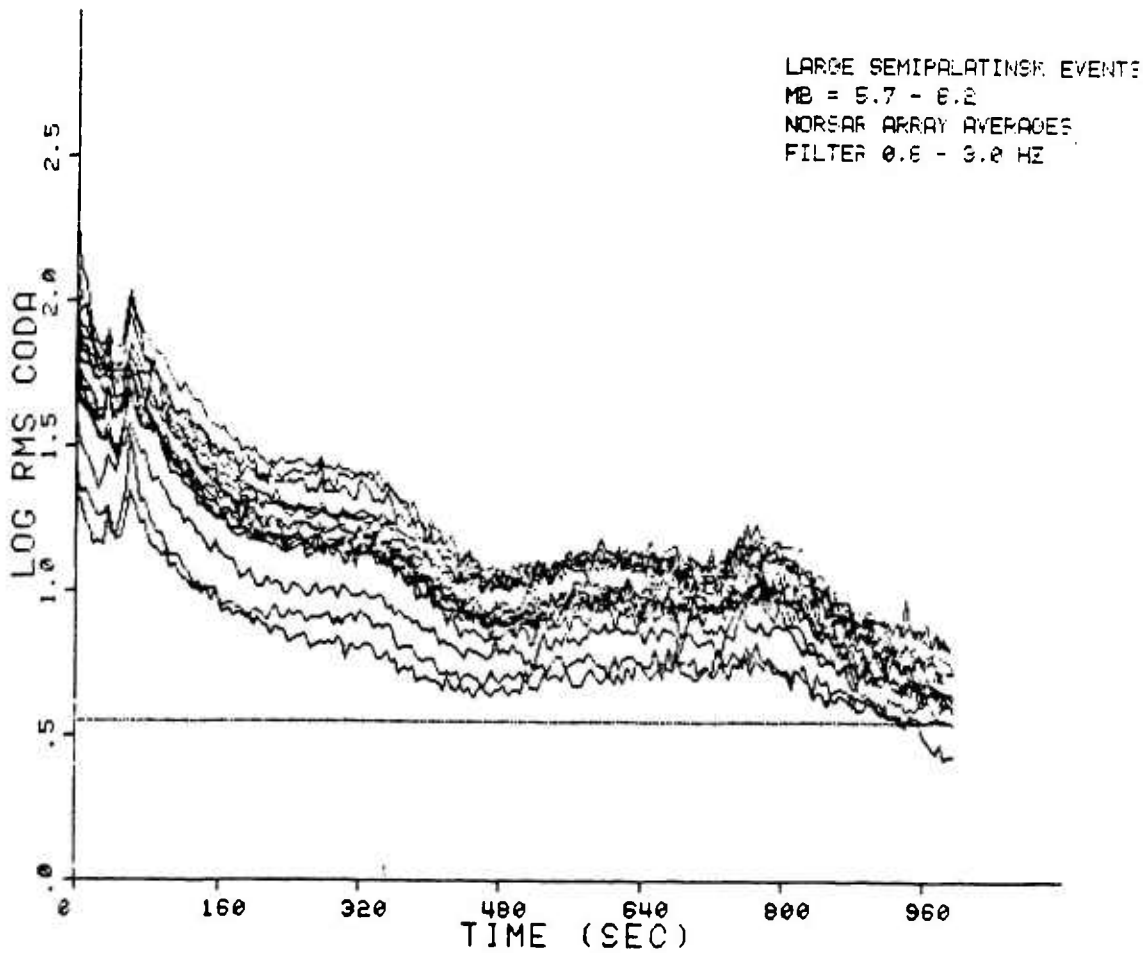

FIGURE 11 ARRAY AVERAGE LOG-RMS P AND CODA ENVELOPES FOR THE SAME EVENTS AS IN FIGURE 10

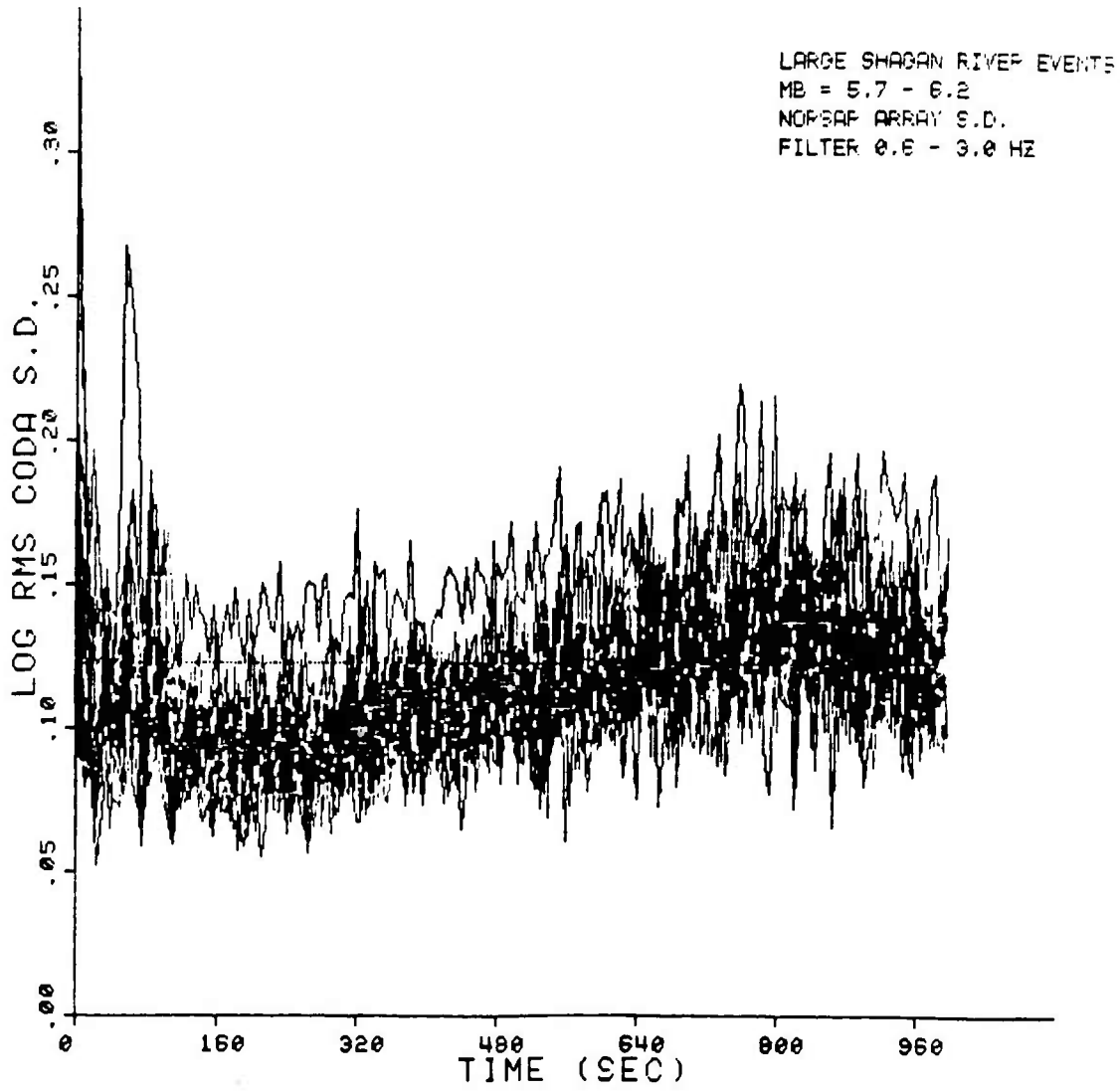

FIGURE 12 STANDARD DEVIATIONS OF LOG-RMS P AND CODA ENVELOPES FOR EVENTS IN FIGURES 10 AND 11

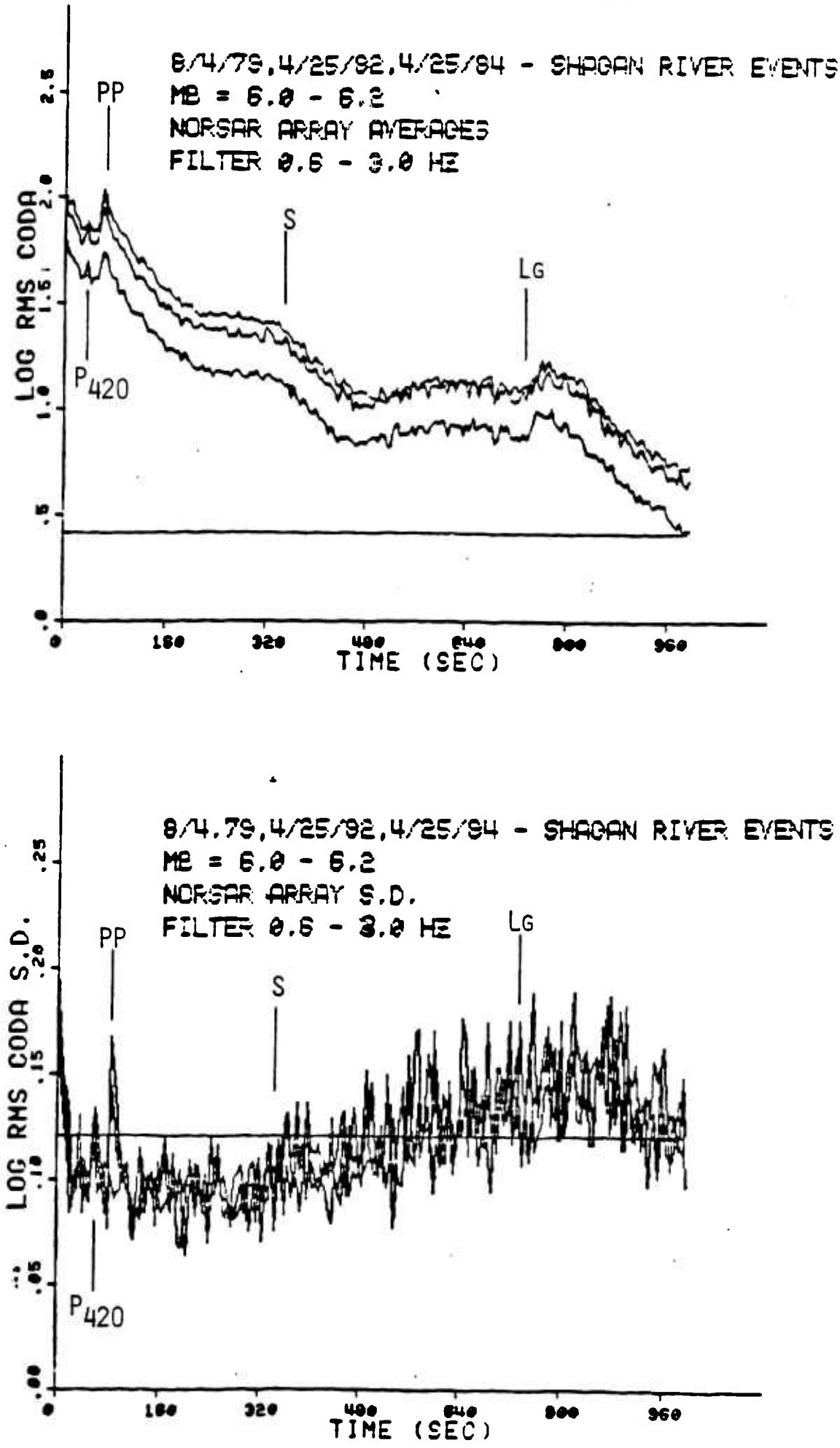

FIGURE 13 NORSAR ARRAY-AVERAGE RMS AMPLITUDES (TOP) AND STANDARD DEVIATIONS (BOTTOM) FOR 3 SHAGAN RIVER EVENTS

appears on almost all of the array-averaged coda envelopes for Semipalatinsk explosions (see Figure 11). Like P and PP, its standard deviation around the array is higher than the other coda waves.

We suggest that this phase is a wide-angle, post-critical reflected or diffracted phase from the top of the 420 kilometer discontinuity, which is the reason for our calling the phase P_{420}. King and Calcagnile's (1976) mantle model KCA for western Russia, whose travel time curve is shown in Figure 14, predicts such wide-angle reflections at distances near 38^{o}. King and Calcagnile (1976), in fact, observed wide-angle reflections out to about 32^{o}, but extrapolated the bc branch of their travel time curve out to near 38^{o}, as shown in Figure 14. Based on this extrapolation, the reflected phase at 38^{o} should arrive about 50 seconds after P and have a slowness of about 12 seconds/degree. Using the frequency-wave number method, we measure a slowness of 12.6 seconds/degree for the phase P_{420}. However, as we mentioned above, the phase arrives about 10 seconds later than predicted by the model KCA, or 60 seconds after P. Another possibility is that the phase may be associated with a group of deterministically scattered phases from the 420 discontinuity referred to by Menke and Richards (1982) as "whispering gallery phases," which may be expected to arrive later than the topside, wide-angle reflected phase.

Aside from these phases, most of the rest of the coda out to the Lg phase seems to be non-deterministically scattered phases. As has been observed in earlier studies (Nersesov et al, 1975; Baumgardt, 1983; Bullitt and Cormier, 1984; Baumgardt, 1984), high-frequency scattered waves in the P-coda have lower spatial variance than deterministic phases. In the early coda between P

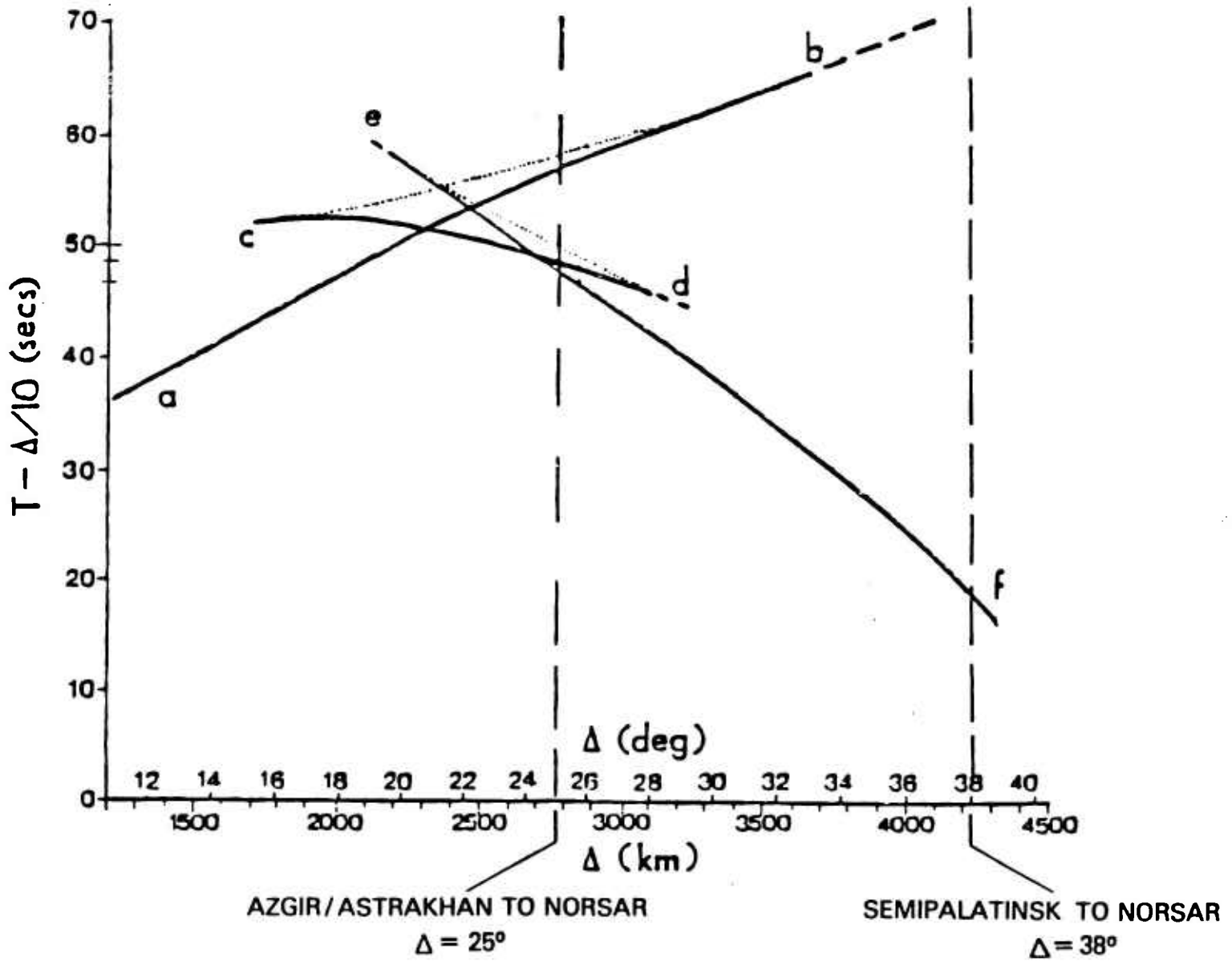

FIGURE 14 TRAVEL-TIME CURVE FOR WESTERN RUSSIA FROM KING AND CALCAGNILE (1976)

and PP and in the flat part of the coda between about 160 - 200 seconds to 340 seconds, in Figure 13, the standard deviations reach their lowest levels of about 0.08 to 0.1. Starting at about the expected arrival time of S-waves, the standard deviations begin to increase. It is interesting that there is no evidence of increased amplitudes as a result of S-wave arrivals; in fact, the coda level actually starts to decrease at that time. Thus, increased standard deviation may be the strongest indication of the arrival of shear - wave coda waves. The standard deviation peaks at about 0.15 at the Lg arrival time and then falls off again in the Lg-coda.

What is the cause of the high spatial standard deviation in the Lg-wave? Given the observed stability of Lg-wave magnitudes, it was expected that the standard deviations would be quite low. In fact, Ringdal (1983) obtained lower standard deviations (0.06 - 0.08 log-rms units) than those in Figures 12 and 13. The apparent reason for this is that Ringdal's measurements on Lg were made in 2 minute windows, whereas those in Figures 12 and 13 were made in 5 second windows. However, the fact still remains that the short-window Lg standard deviations are at least 0.05 units higher than those of the earlier P-coda and later Lg-coda.

Baumgardt (1983) suggested that the higher standard deviations of Lg may be explained by the fact that the array averages were determined after first lining up the traces on the first arrival P-waves. Thus, because Lg propagates more slowly than P (Lg apparent velocity would be 3.5 to 4.5 km/sec compared with the expected P-wave apparent velocity of about 13.21 km/sec), the Lg-waves would be misaligned on what are essentially incoherent P-wave beams in Figures 12 and 13. To check this, we compare, in Figure 15, log-rms standard deviation plots for a Semipalatinsk

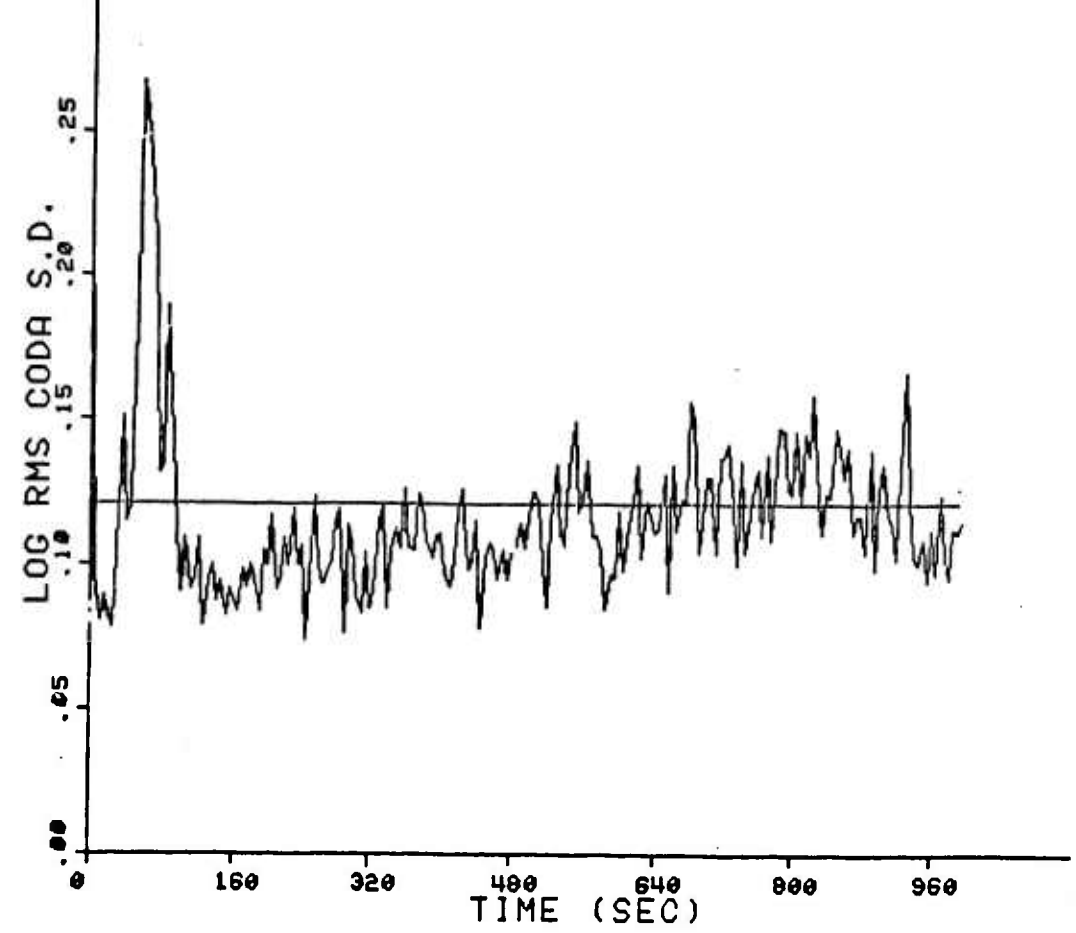

(a)

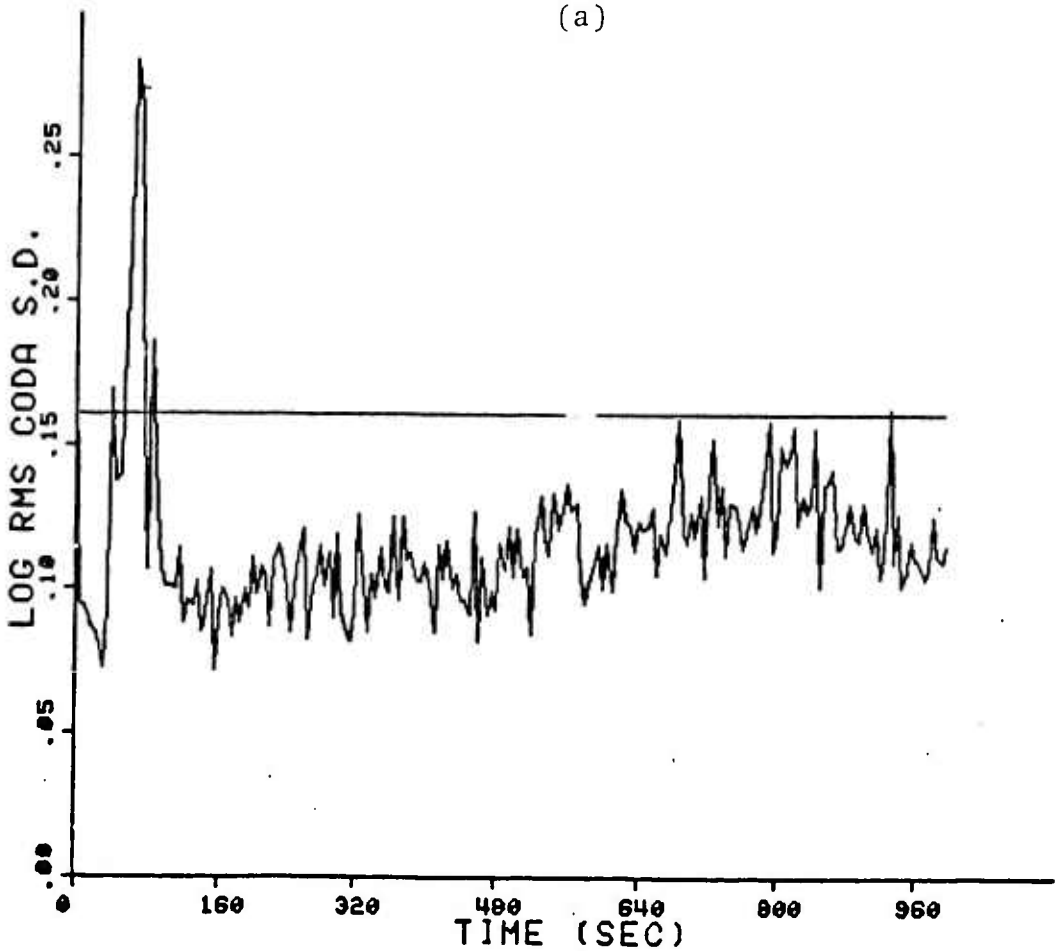

(b)

FIGURE 15 LOG-RMS CODA AMPLITUDE STANDARD DEVIATIONS FOR NORSAR RECORDINGS OF THE MARCH 25, 1971 DEGELEN MOUNTAIN EVENT FOR TRACES BEAMED TO P (TOP) AND Lg (BOTTOM)

event with the codas aligned to a P-wave (Figure 15a) and an Lg-wave (Figure 15b) velocity. The Lg velocity was assumed to be 3.5 km/sec. The comparison reveals a higher noise standard deviation for the Lg velocity average because the P wave, which is not lined up correctly, contaminates the background noise estimate. However the coda shapes for the P and Lg beams are almost identical. Even when the codas are lined up consistent with an Lg velocity, the Lg log-rms standard deviation is still 0.03 to 0.05 units higher than that of the earlier P coda.

It appears then that higher standard deviation is an intrinsic characteristic of the Lg phase and its coda. Given the low coherence of Lg-waves over intersensor separation as small as 2 to 5 km (Mrazek et al, 1980; Mykkeltveit et al, 1980; Der et al, 1984) it is probably not unsurprising that the Lg standard deviations across the entire NORSAR array, with aperture of about 50 km, do not depend strongly on the beam velocity. Also the higher standard deviations of Lg in Figures 12 and 13 last for several seconds after the 3.5 km/sec group velocity time, which is much longer than the time into the Lg coda where any spatial coherence has been observed (Der et al, 1984).

We argue that the high standard deviation in the Lg part of the coda is caused by lateral variations local structure beneath the sensors in the NORSAR array. The fact that Lg excitation is highly sensitive to geologic variations and crustal structure has been well documented (Barker et al, 1981). It is also interesting that the standard deviations in the coda begin to increase at about the expected arrival times of S waves, even though no strong S-waves are apparent in the log-rms coda envelopes in Figures 11 and 13. The coda at this time may consist of weak, incoherent shear waves produced by the source itself and/or from

mode conversion or forward scattering of other phases. Like Lg, shear waves may be more sensitive to the effects of laterally varying structure beneath the array than scattered P waves. This is because S waves have smaller wavelengths, and hence, may be more likely to be scattered by small-scale lateral heterogeneities than P waves.

2.5 Lg-TO-P FORWARD SCATTERING

The flat part of the codas, observed at NORSAR between 200 and 340 seconds after P, appears to be produced by a long burst of energy that is not associated with any known phase. We have indicated in Figure 13 the expected arrival times of major phases, and the flat-coda does not appear to be associated with any of them. The major phases, PP and PcP, arrive well ahead of the flat part, and S waves, including S_n, would be expected to arrive at NORSAR after the time indicated for S in Figure 13. A third possibility is the arrival could be Pg, although to our knowledge, there have been no observations of Pg at this great a distance ($\Delta = 38^{o}$). From close analysis of these codas we conclude that the flat part of the coda begins at about 219 seconds after P and ends at 352 seconds after P. These times correspond to group arrival times of 6.42 and 5.34 km/sec, respectively, which is within the reported range of Pg velocities of 5.2 to 6.0 km/sec. However, as pointed out by (Pomeroy et al, 1982), Pg is usually weak or unidentifiable at distances beyond 5 to 8^{o} in stable cratonic continental interiors, such as eastern United States and analogous regions in Russia.

In an earlier study (Baumgardt, 1984), we suggested that Lg forward scattering to P-waves may generate many of the pre-Lg P-coda waves. If we hypothesize that the flat part of the coda is

a burst of P-wave energy caused by Lg scattering, we can determine where the scattering occurs by timing the burst relative to Lg and use a regional travel-time curve to find the distance to the scattering point based on the P-to-Lg time. The flat part of the coda appears to begin and end roughly at 549 and 416 seconds before Lg, respectively. From the regional travel time curve of (Gupta et al, 1980), shown in Figure 16, we see that P to Lg times of 549 and 416 seconds correspond to distances of 23^{o} and 29^{o} from NORSAR respectively. In Figure 17, where the Lg propagation paths from Semipalatinsk to NORSAR and Graefenburg are shown, we see that the distance range of 23^{o} to 29^{o} from NORSAR brackets the north-south trending Ural Mountains.

The Lg-to-P forward scattering mechanism is illustrated schematically in Figure 18. The Lg wave is generally viewed as consisting of a superposition of S waves multiply reflected within the crust with near-critical incidence angles at the Moho (Campilla et al, 1984). Thus, for plane-parallel layering in the crust, there would be verly little leakage of energy into the mantle. However, if the crust-mantle or the free-surface interfaces are dipping, such as in the Ural Mountain region, the incidence angles at the Moho may become subcritical, and the S waves may leak energy into the lower mantle by mode conversion to P. The P-waves would then arrive as precursors to Lg. Also, S waves may propagate into the mantle and produce an S-wave coda at times before Lg but after the expected arrival of S from the source. Another possibility is that a mountain range like the Urals may have a number of deeply penetrating near-normal faults which, if there has been substantial vertical displacement along the faults, may produce horizontal impedance contrasts across the fault surfaces. Thus, the horizontally propagating S waves, which compose the Lg-wave packets, may impinge upon the fault

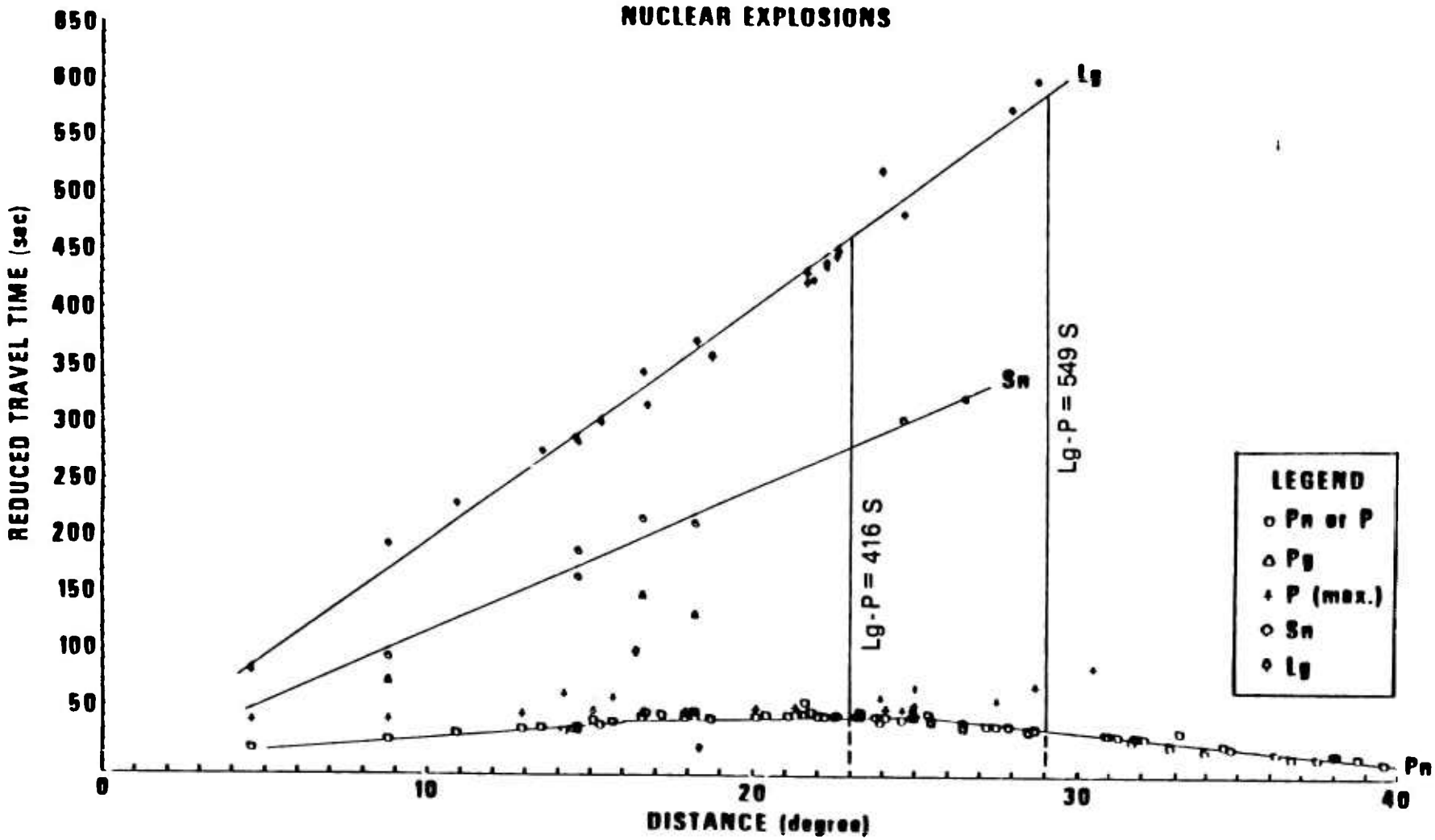

FIGURE 16 REGIONAL REDUCED TRAVEL-TIME CURVES FOR WESTERN RUSSIA (FROM GUPTA, BARKER, BURNETTI, AND DER, 1980)

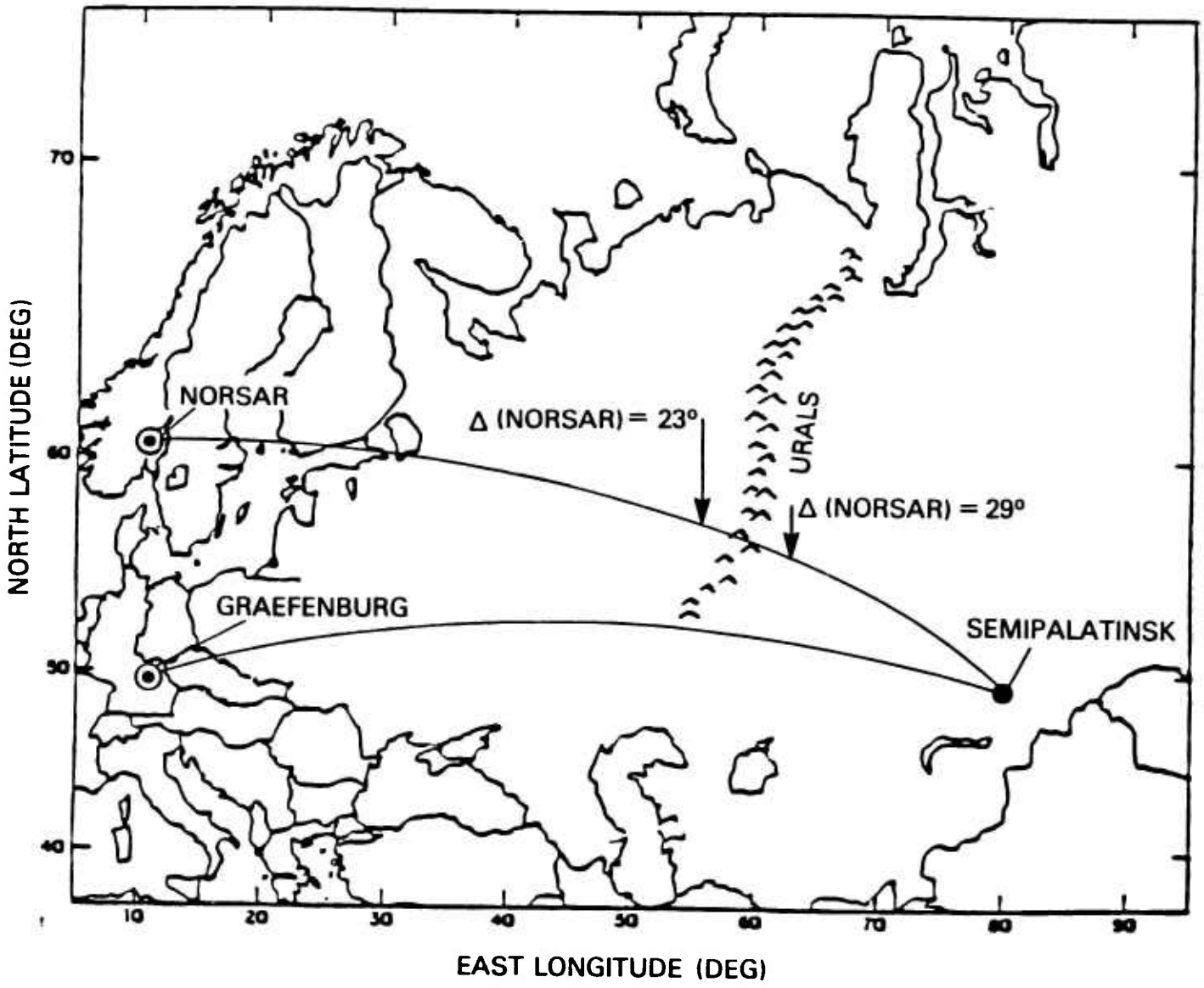

FIGURE 17 LG PROPAGATION PATHS FROM SEMIPALATINSK TO NORSAR AND GRAEFENBURG

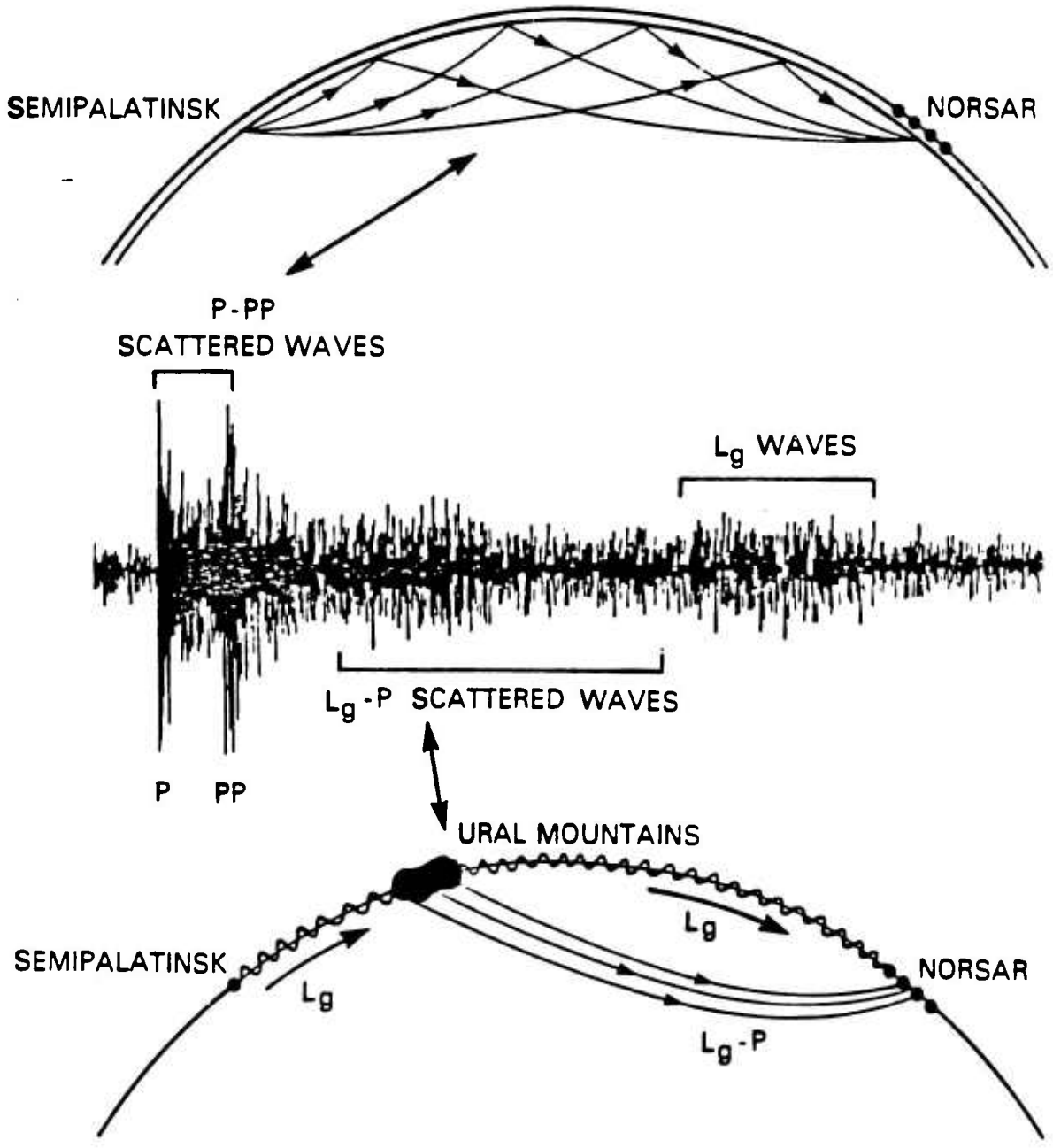

P CODA GENERATION MECHANISMS FOR SEMIPALATINSK EXPLOSIONS RECORDED AT NORSAR

FIGURE 18 SCHEMATIC ILLUSTRATION OF P AND LG SCATTERING MECHANISMS

surface and undergo mode conversion to P as a result of this impedance contrast.

As seen in Figure 17, the path from Semipalatinsk to the Graefenburg just misses the southern tip of the Urals which explains why the coda flattening is not observed in the Graefenburg coda plots (Figures 8 and 9). In contrast to the NORSAR codas, the Graefenburg codas decay monitonically with time until the possible arrival of S_n waves at about 600 seconds after P. At this point, the coda levels begin to increase and then peak after the arrival of Lg.

We conclude, therefore, that the flat envelopes from about 200 to 340 seconds after P, recorded at NORSAR for Semipalatinsk explosions, are consistent, on the basis of timing, to Lg - P forward scattering from lateral heterogeneities in the Ural Mountains. The evidence is still circumstantial, and we will be analyzing additional data for events on either side of the Urals. However, if the Lg-to-P forward scattering hypothesis holds up, it would have significant implications for Lg scattering attenuation determinations at teleseismic distances and, perhaps, at regional distances as well. Moreover, the low standard deviation of the flat part of the coda indicates that measurements of coda magnitude in this part of the coda may be more stable for yield estimation than P-wave, Lg or early P-coda measurements, which all have higher standard deviations.

3.0 RELATIVE Lg AND P-CODA MAGNITUDE ANALYSIS

3.1 INTRODUCTION

In this section, we examine the conjecture of Sykes and Cifuentes (1983) that the largest Shagan River explosions have nearly the same yield. Specifically, we focus on those explosions in Table 1 which have body-wave magnitudes, as determined by Sykes and Cifuentes (1983), in excess of 6.0. They argue that events with m_b greater than 6.0 have about the same yield and that their m_bs differ because of biasing effects caused by differing geology in the source region. Also, it is conceivable that differing amounts of non-isotropic, tectonic component for the different events may produce variation in m_b, although the extent to which short-period P-waves are affected by tectonic component is not well understood. As we discussed in the previous section, P-coda and Lg-wave measurements appear to be less sensitive to biasing effects than P-wave measurements. Thus, we expect that the P-coda and Lg amplitudes for the largest Shagan River explosions should be nearly the same if the conjecture of Sykes and Cifuentes (1983) holds true.

Log-rms amplitudes of Lg and P-coda waves recorded at NORSAR and Graefenburg were determined using equation 3 in Section 2.0. P-coda log-rms amplitudes were averaged over ten 5 second windows, or 50 seconds, starting 5 seconds after the first-arrival P time. For Lg, log-rms values in twelve 5 second windows or 120 seconds, were averaged, beginning 40 seconds ahead of the expected 3.5 km/sec group arrival time. Since we are only interested in relative magnitude estimates, no attenuation correction was made for either the Lg or P-coda measurements in order to obtain absolute magnitudes.

The Lg and P-coda measurements for NORSAR are discussed in detail in Ringdal (1983) and Baumgardt (1983), respectively. In the next section we discuss the Graefenburg measurements.

3.2 GRAEFENBURG Lg AND P-CODA MEASUREMENTS

Figure 3 shows that the Graefenburg array has three 3-component sensors, labeled A1, B1 and C1. Figure 19 shows a plot of the log-rms amplitudes of Lg on the transverse component against those on the vertical component. Transverse component traces were made by mathematically rotating the north-south and east-west horizontal components into the back azimuth of Semipalatinsk relative to Graefenburg. Measurements on the vertical and transverse components from all three sites are plotted in Figure 19. Each trace was bandpass filtered between 0.6 and 3.0 Hz prior to making measurements.

Figure 19 shows that the relative log-rms Lg amplitude measurements on the vertical and transverse components at the three sites are not perfectly consistent. The transverse Lg at the B1 site is between 0.2 to 0.4 log-rms units higher relative to the vertical Lg as compared with the A1 and C1 sites. The vertical and transverse Lg amplitudes at the A1 and C1 sites are more consistent, although the A1 amplitudes are somewhat higher on both components than the C1 amplitudes. Variations in geology between the sites probably accounts for the differences in amplification of transverse relative to vertical Lg. Gupta et al (1982) studied variations in horizontal-to-vertical Lg amplitude ratios in the eastern United States and found that the ratio is larger at soft-rock sites ($H/Z > 2$) than hard rock sites ($H/Z < 2$). The H/Z ratios at the B1 three-component site are as large as 1.6 compared with average H/Z values of 1 for the A1 and C1 sites.

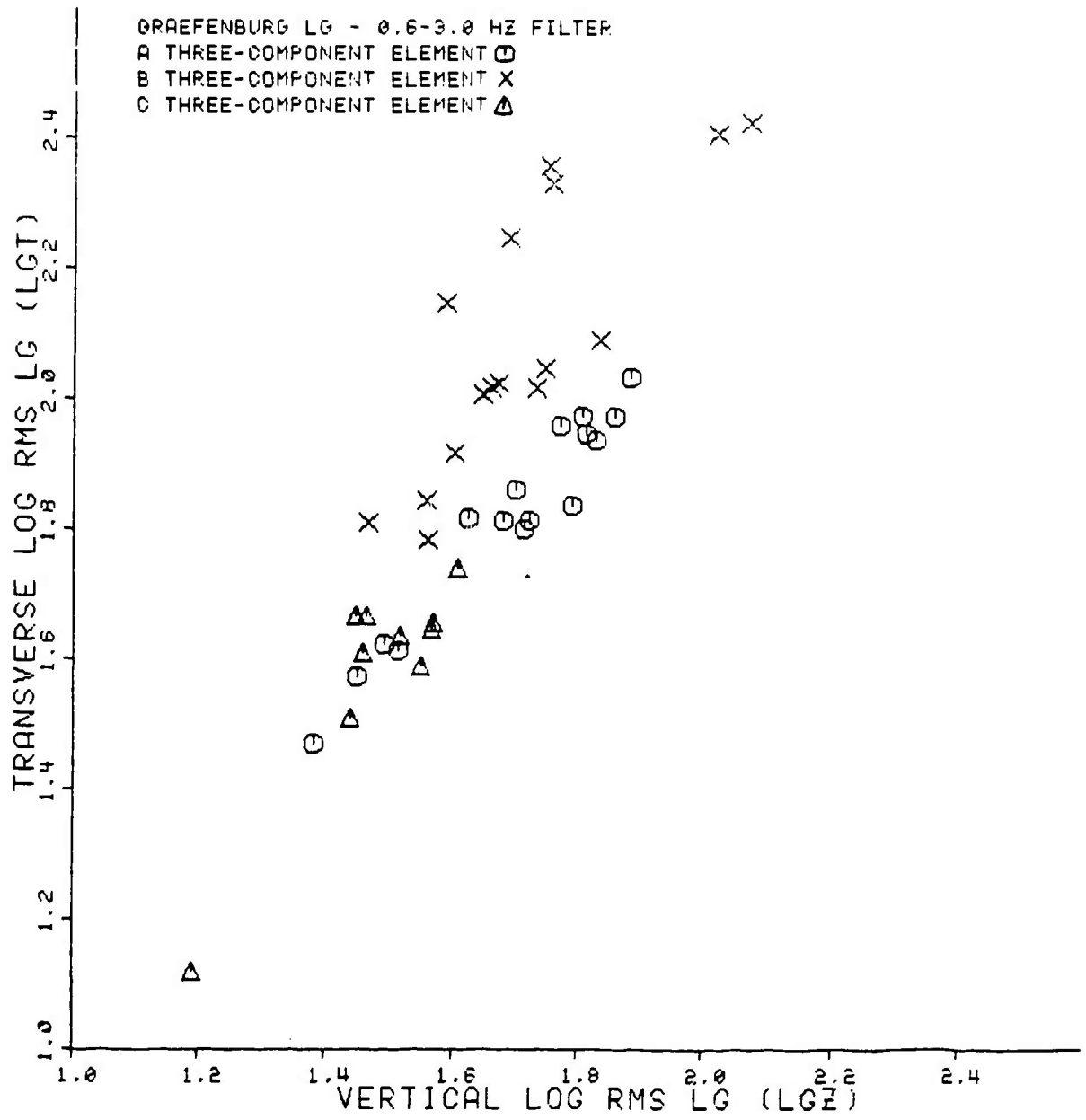

FIGURE 19 LOG-RMS AMPLITUDES OF TRANSVERSE AND VERTICAL COMPONENT LG AT GRAEFENBURG A1 SITE

We thus conclude that B1 is situated on softer rock, or underlain by more layered sediments, than A1 and C1.

We have also noticed that the noise levels on the B1 and C1 instrument are, in many cases, higher than those recorded by the A1 instrument. Because of this fact and the relatively high correlation in the vertical and transverse amplitudes at A1, we have concentrated on measurements on the A1 vertical and transverse Lg and P-coda for the relative magnitude analysis.

Because of the availability of broadband data, we determined Lg and P-coda log-rms amplitudes in two frequency bands, 0.2 to 1.0 Hz and 0.6 - 3.0 Hz. The latter covers the upper part of the mid-period band which lies between the traditional low- and high-frequency bands. Lg and P-coda measurements were made in both bands on both the vertical and transverse components. The results are tabulated in Table 2, where m^i_{lgz}, m^i_{lgt}, m^i_{cz}, and m^i_{ct} refer to vertical-Lg, transverse-Lg, vertical-P-coda and transverse-P-coda log-rms amplitude measurements, respectively. The superscript i=1 and 2 corresponds to measurements in the high-frequency (0.6 to 3.0 Hz) and mid-frequency (0.2 to 1.0 Hz) bands, respectively.

Figures 20 through 27 are scatter plots of each of the measurements in Table 2 against the m_b values of Sykes and Cifuentes (1983). Also shown on the plots are the results of two-variable-in-error regressions with $\lambda=1$ and $\lambda=0$ (Madansky, 1959). Each observation is assumed to have the same variance, and $\lambda = \sigma_x / \sigma_y$, where σ_x and σ_y are the standard deviations of the independent and dependent variables, respectively. When $\lambda=1$, we assume equal uncertainty in the Graefenburg and Sykes and Cifuentes (1983) measurements, whereas, $\lambda=0$ assumes that all the uncertainty resides in the Graefenburg measurement with no error

Table 2

LOG-RMS AMPLITUDE MEASUREMENTS OF Lg AND P-CODA AT THE GRAEFENBURG A1 SITE FOR THE LARGEST SHAGAN RIVER EXPLOSIONS

Event Number	Date	M_{lgz}^{1} (0.6-3.0Hz)	M_{lgz}^{2} (0.2-1.0Hz)	M_{lgt}^{1} (0.6-3.0Hz)	M_{lgt}^{2} (0.2-1.0Hz)	M_{cz}^{1} (0.6-3.0Hz)	M_{cz}^{2} (0.2-1.0Hz)	M_{ct}^{1} (0.6-3.0Hz)	M_{ct}^{2} (0.2-1.0Hz)
1	15 Sep 78	1.625	2.097	1.816	2.277	2.303	2.339	2.048	2.119
2	4 Nov 78	1.491	1.976	1.624	2.061	1.951	2.165	1.688	2.020
3	29 Nov 78	1.701	2.157	1.861	2.323	2.354	2.387	2.051	2.245
4	23 Jun 79	1.861	2.249	1.973	2.424	2.457	2.484	2.180	2.194
5	7 Jul 79	1.681	2.031	1.812	2.228	2.151	2.189	1.860	1.933
6	4 Aug 79	1.808	2.204	1.972	2.370	2.454	2.463	2.176	2.209
7	18 Aug 79	1.886	2.274	2.032	2.474	2.558	2.511	2.281	2.250
8	2 Dec 79	1.721	2.126	1.812	2.284	2.316	[illegible]7	2.053	2.200
9	23 Dec 79	1.831	2.233	1.938	2.379	2.515	2.481	2.240	2.265
10	29 Jun 80	1.513	1.860	1.613	2.026	2.023	2.127	1.787	1.858
11	12 Oct 80	1.773	2.212	1.960	2.372	1.503	-----	1.519	2.164
12	14 Dec 80	1.792	2.233	1.837	2.303	1.391	-----	1.511	2.282
13	22 Apr 81	1.715	2.096	1.799	2.215	2.336	2.333	1.969	2.004
14	13 Sep 81	1.813	2.193	1.945	2.360	2.558	2.592	2.137	2.239

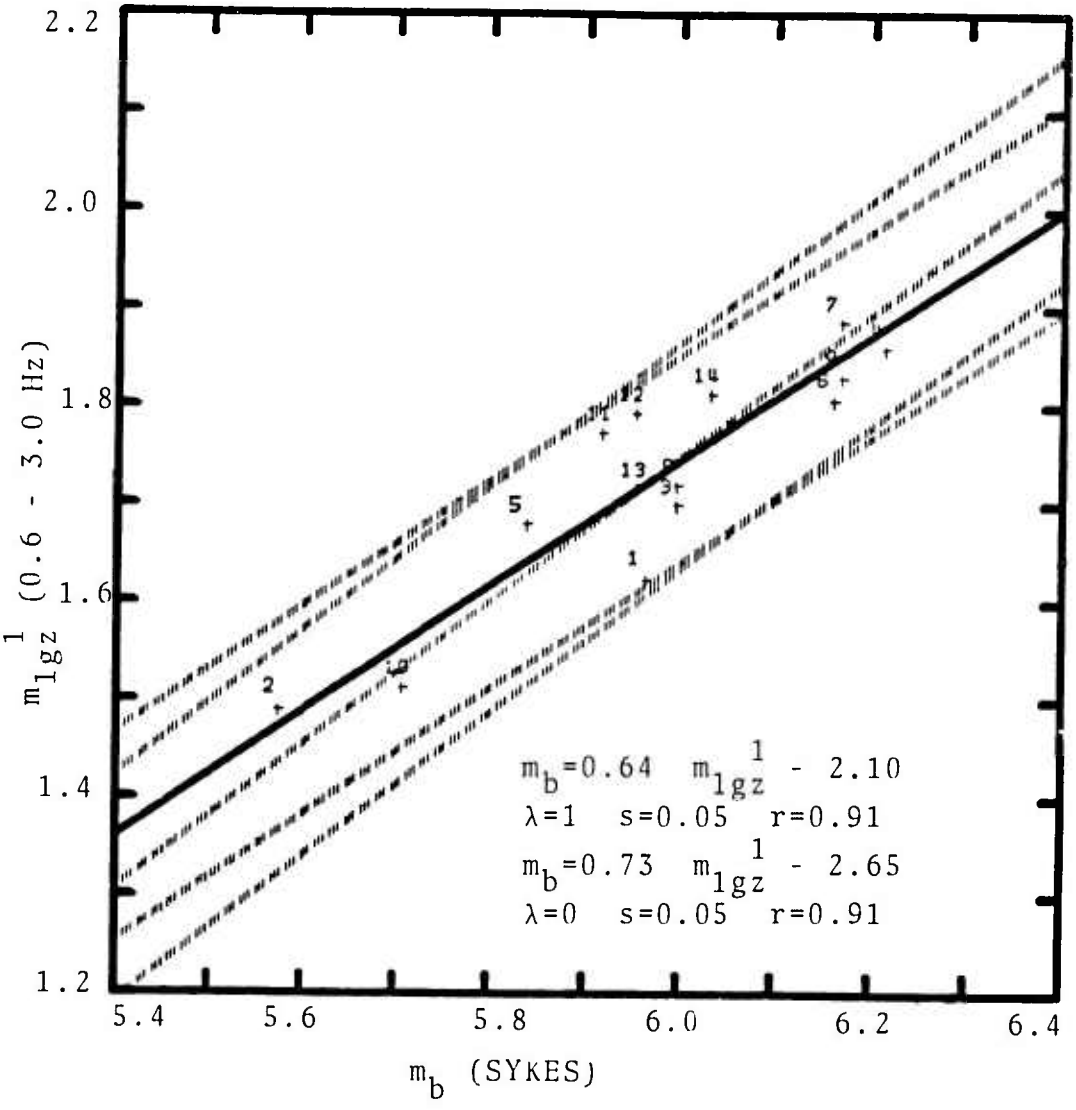

FIGURE 20 SCATTER PLOT OF VERTICAL, HIGH-FREQUENCY Lg LOG-RMS AMPLITUDES RECORDED AT GRAEFENBURG A1 VERSUS m_b

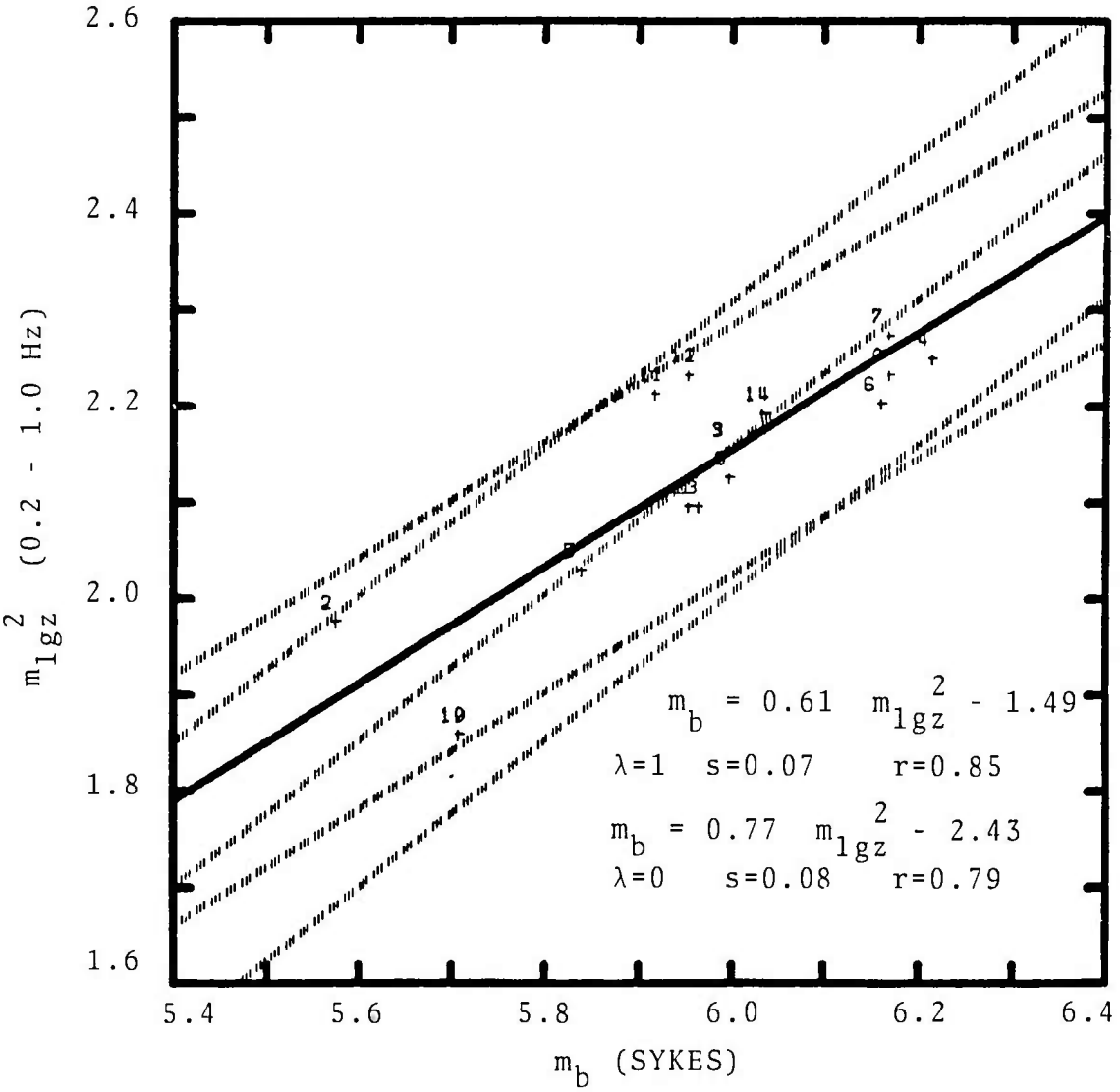

FIGURE 21 SCATTER PLOT OF VERTICAL MID-FREQUENCY Lg LOG-RMS AMPLITUDES RECORDED AT GRAEFENBURG A1 VERSUS m_b

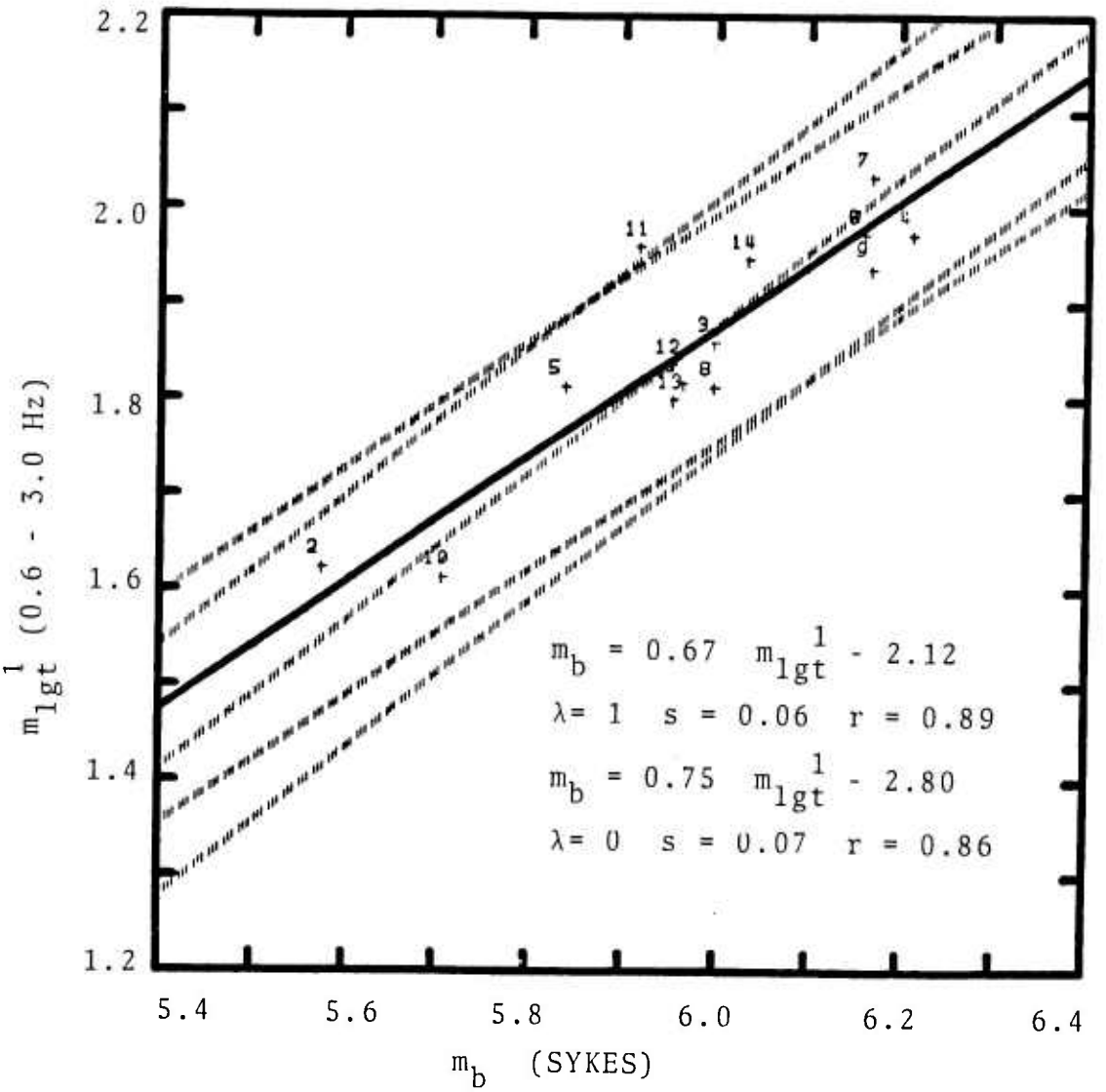

FIGURE 22 SCATTER PLOT OF TRANSVERSE HIGH-FREQUENCY Lg LOG-RMS AMPLITUDES RECORDED AT GRAEFENBURG A1 VERSUS m_b

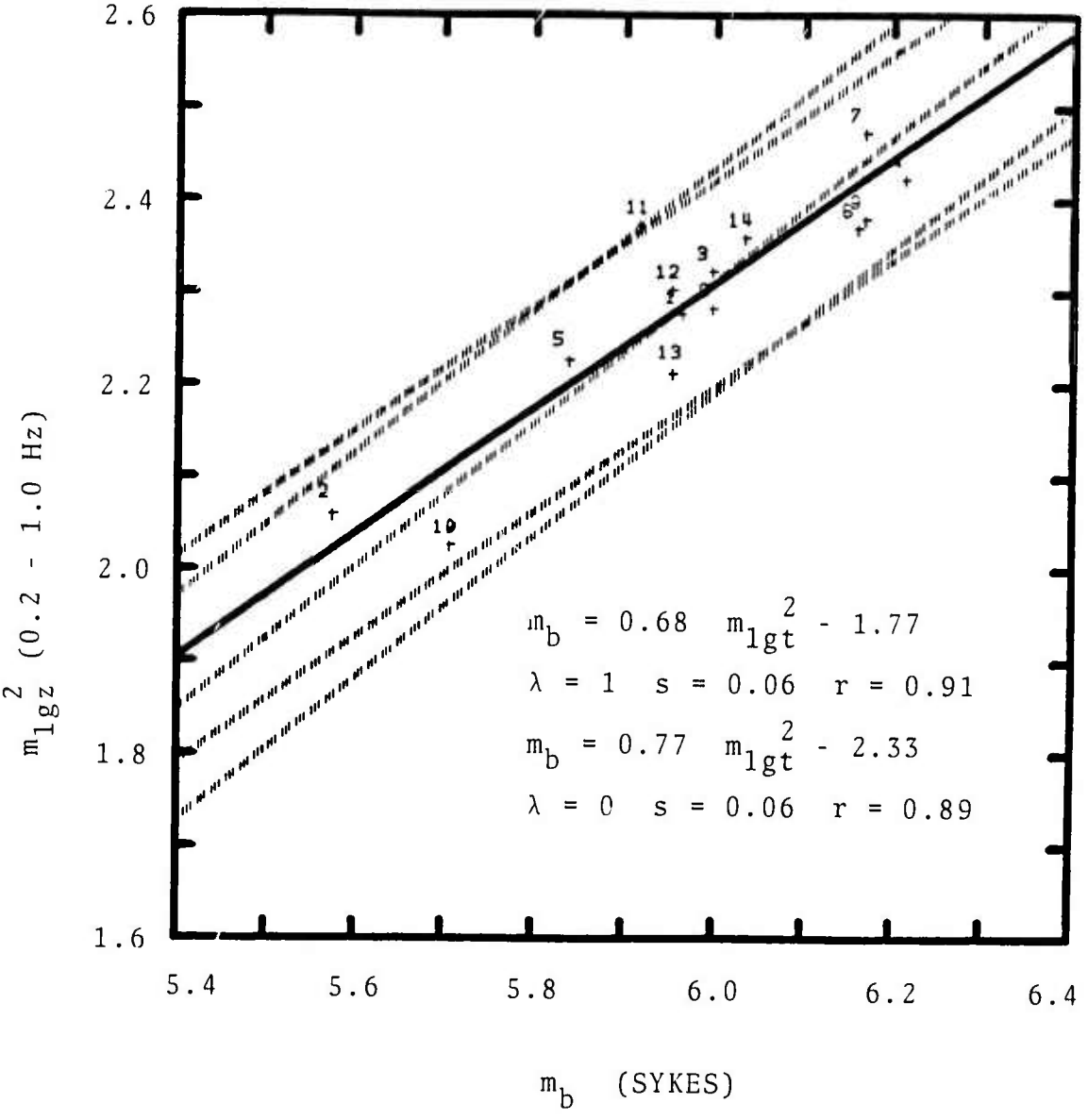

FIGURE 23 SCATTER PLOT OF MID-FREQUENCY TRANSVERSE Lg LOG-RMS AMPLITUDES RECORDED AT GRAEFENBURG A1 VERSUS m_b

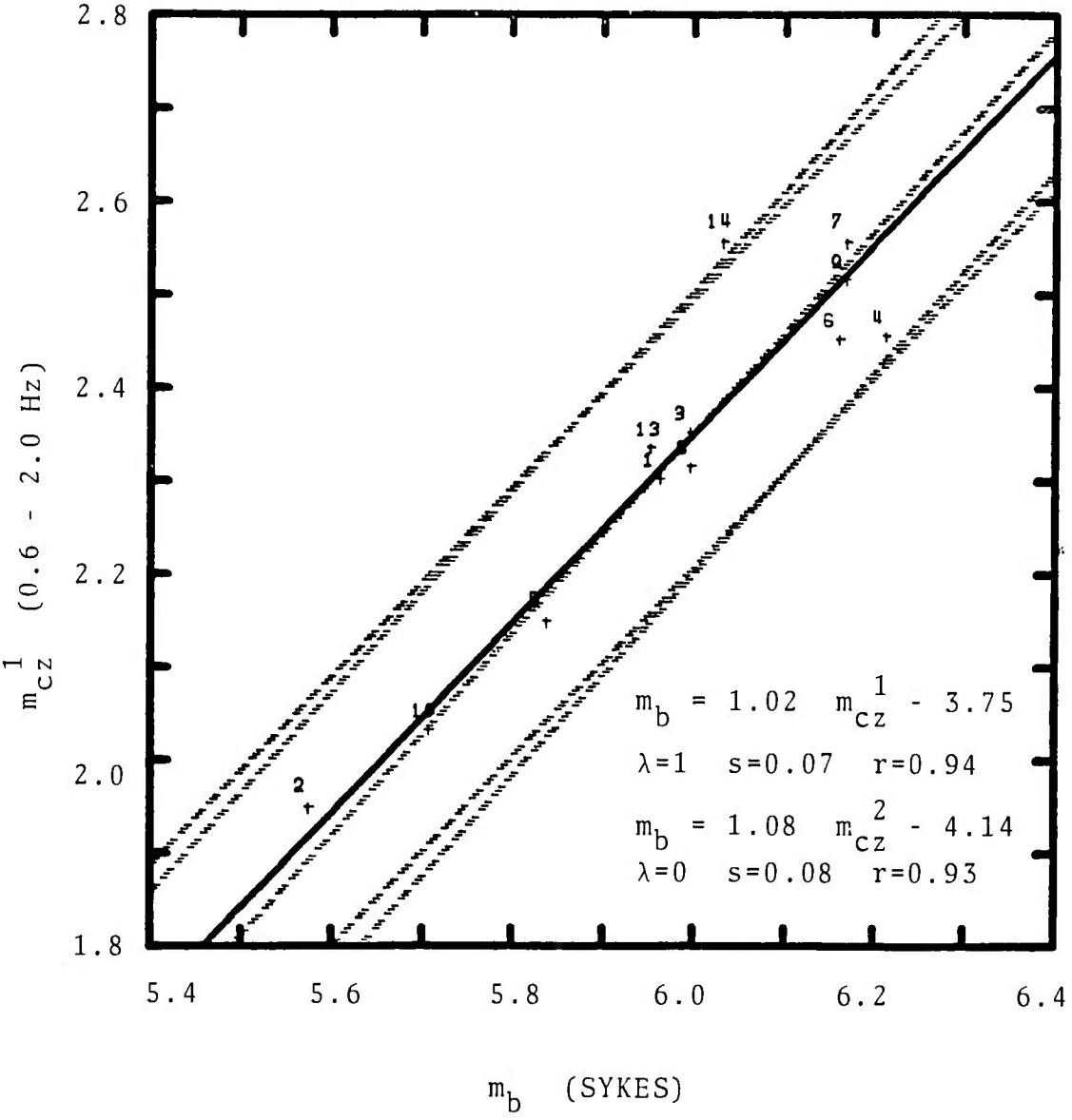

FIGURE 24 SCATTER PLOT OF HIGH-FREQUENCY, VERTICAL P-CODA LOG-RMS AMPLITUDES RECORDED AT GRAEFENBURG A1 VERSUS m_b

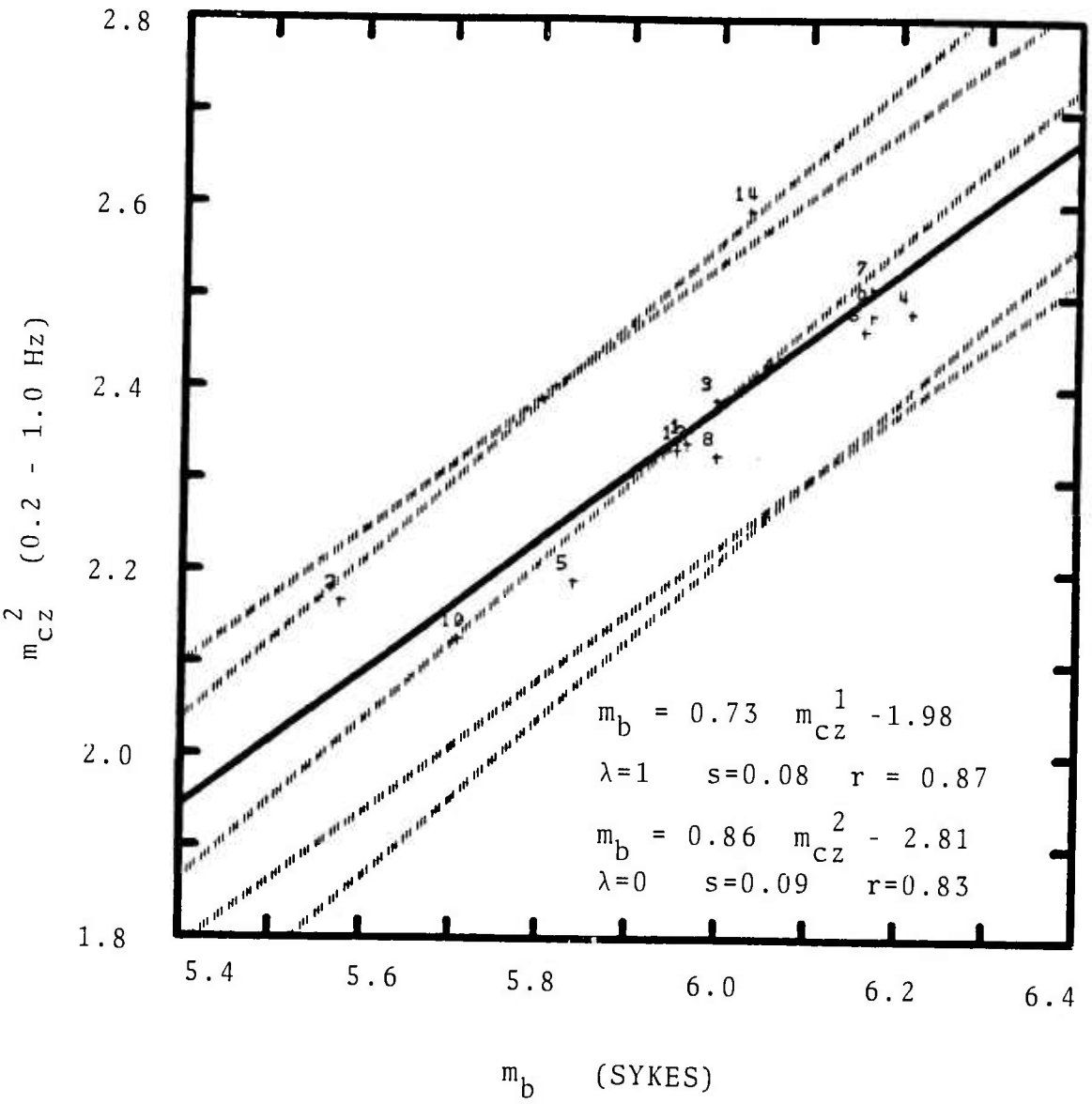

FIGURE 25 SCATTER PLOT OF MID-FREQUENCY, VERTICAL P-CODA LOG-RMS AMPLITUDES RECORDED AT GRAEFENBURG A1 VERSUS m_b

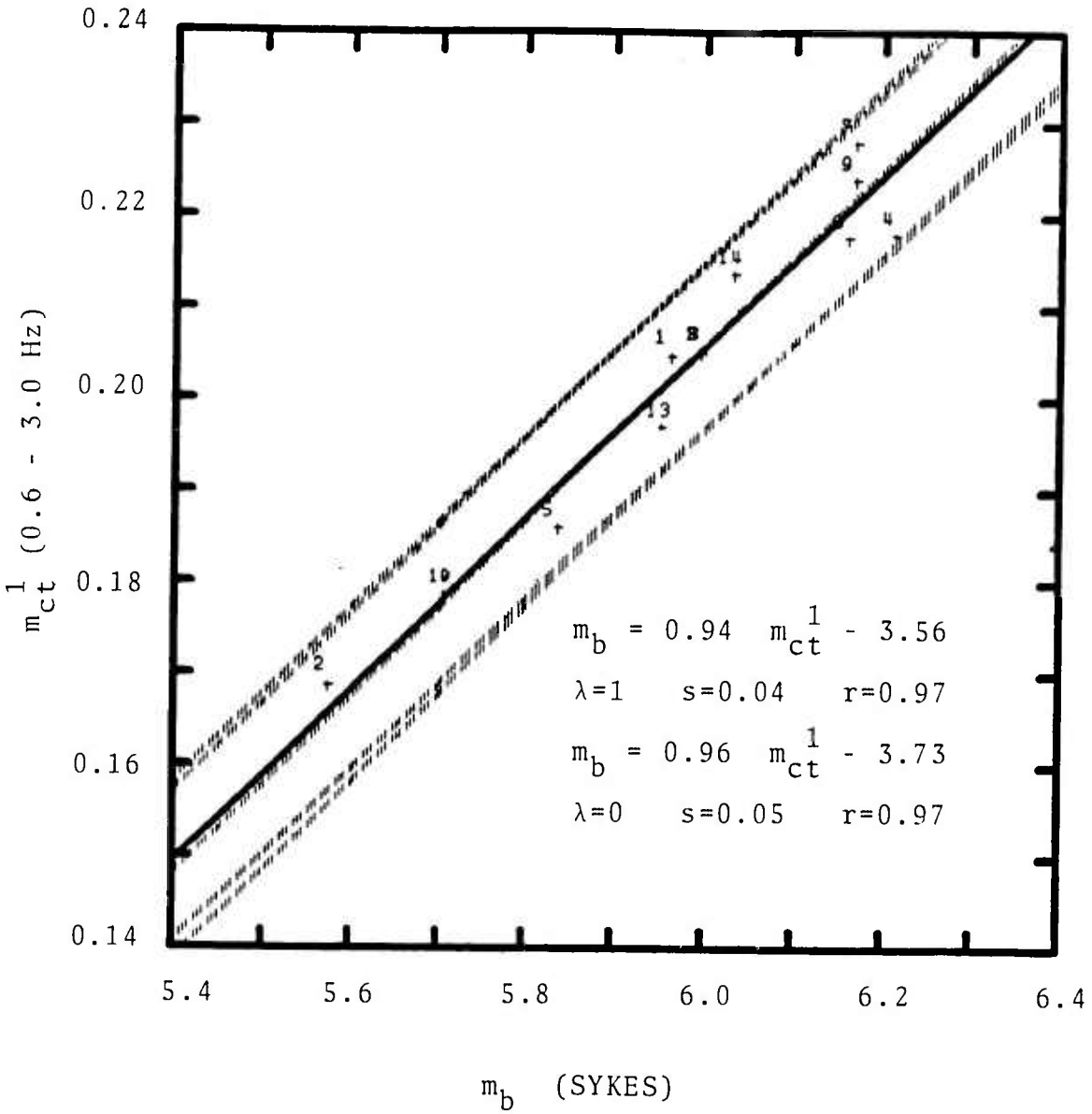

FIGURE 26 SCATTER PLOT OF HIGH-FREQUENCY, TRANSVERSE P-CODA LOG-RMS AMPLITUDES RECORDED AT GRAEFENBURG A1 VERSUS m_b

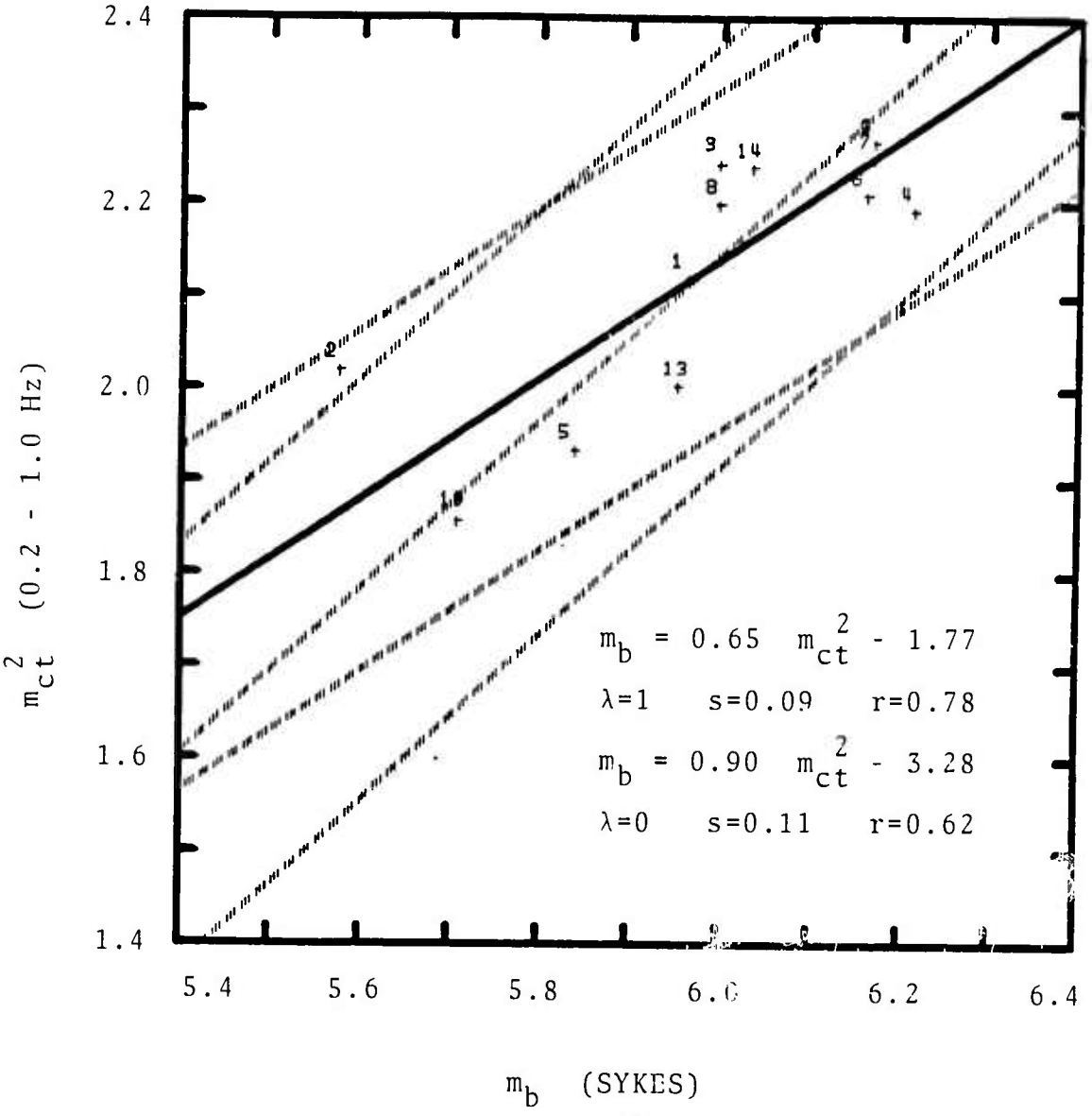

FIGURE 27 SCATTER PLOT OF MID-FREQUENCY, TRANSVERSE P-CODA LOG-RMS AMPLITUDES RECORDED AT GRAEFENBURG A1 VERSUS m_b

in m_b. The solid lines plotted in Figures 20 through 27 are the best-fitting lines for $\lambda=1$ and the dashed lines are the $\lambda=0$ lines and the 95% confidence intervals for both the $\lambda=1$ and $\lambda=0$ fits.

The Lg results in Figures 20 through 23 are reasonably consistent. The Lg amplitudes on both the vertical and transverse agree well, in general, with the network average m_bs, with standard errors ranging from 0.04 to 0.08 units. The $\lambda=1$ fits have slightly smaller standard errors and smaller slopes (by 0.1 on average) than the $\lambda=0$ fits, although these differences may not be significant.

The P-coda measurements in Figures 24 through 27 also correlate well with m_b. The best fit of all is the short-period, transverse P coda, which has a standard error of 0.04, correlation coefficient of 0.97, and a slope of greater than 0.9. The worst fits are the mid-frequency P codas, in particular the transverse component. Apparently, mid-frequency P-codas are highly contaminated by microseismic noise. On the other hand, there is no significant difference between the mid-frequency and high-frequency Lg fits. This is consistent with the results presented in Section 2.0 which showed that P-coda signal-to-noise ratios are lower in the mid-frequency band than in the high-frequency band, whereas, Lg signal-to-noise ratios are about the same in the two bands (see Figure 9).

In Table 3, the source parameters of the explosions in Table 2, including the tectonic components by Sykes and Cifuentes (1983) and Given et al (1983), are listed. As pointed out by Alexander (1984), these events have a wide range of tectonic component, with F values from 0.25 to 2.45, and yet, the low scatter in the Lg and P-coda versus m_b plots in Figures 20 through 27 indicates that mid- and high-frequency Lg and P-coda

Table 3
SOURCE PARAMETERS FOR THE LARGEST SHAGAN RIVER EXPLOSIONS

Event Number	Date	M_b*	M_s*	LQ/LR*	F'*	F**
1	15 Sep 78	5.963	3.831	0.40	0.26	0.29
2	4 Nov 78	5.576	3.582	0.60	0.79	0.82
3	29 Nov 78	5.996	-----	----	----	0.27
4	23 Jun 79	6.215	3.991	0.51	0.34	0.36
5	7 Jul 79	5.839	4.027	1.59	2.00	2.45
6	4 Aug 79	6.161	4.052	0.34	0.35	0.32
7	18 Aug 79	6.170	3.743	0.99	----	1.16
8	2 Dec 79	5.998	4.080	0.26	0.22	----
9	23 Dec 79	6.170	3.772	0.46	0.32	0.25
10	29 Jun 80	5.707	3.400	0.91	----	----
11	12 Oct 80	5.918	4.094	0.22	0.20	0.13
12	14 Dec 80	5.953	3.934	0.35	0.27	----
13	22 Apr 81	5.954	4.070	0.34	0.26	----
14	13 Sep 81	6.033	4.206	0.31	0.25	----

* Sykes and Cifuentes, 1983
** Given et al, 1983

are not strongly affected by tectonic component. Also, the scatter in the points plotted in these figures does not appear to be caused by tectonic component. For example, in Figure 20, events 11, 12, and 14 fall well off the best fitting lines, but, from Table 3, they have relatively low tectonic components. On the other hand, events 4, 5, 7, and 10, which have large tectonic components, lie closer to one or both of the best fitting lines.

Another important observation which can be drawn from these plots is that the slopes of the best fitting lines for the Lg measurements are quite small, ranging from 0.6 to 0.8. Interestingly, however, the P-coda measurements have higher slopes of 0.9 to 1.0. Baumgardt (1984) has argued that early vertical P-coda waves are produced by P-scattering beneath the source, receiver, and along the path between source and receiver. Thus, the amplitudes of P and early coda waves should be more correlated whereas P- and Lg-wave amplitudes may be more independent.

One possible cause of the low slopes is that the Lg amplitudes of the smaller events may be more contaminated by noise than those of the larger events. Although this is undoubtably a problem for events with m_bs less than 5.7 or 5.8, our sample of data only include two events in this magnitude range. While it is true that undersampling of lower magnitude events means that the slope is not well contained by the smaller events, noise contamination cannot be the principal cause of the small slopes because most of the events produce Lg amplitudes at Graefenburg which are well above the noise level.

The principal cause of the small slopes is that many of the events with different m_b have close to the same Lg and P-coda amplitude. This is particularly apparent for the largest events, with m_b greater than 6.0, where there is a noticeable flattening

of the scatter plots in Figures 20 through 27. Notice that the flattening is evident in the P-coda scatter plots, even though their slopes are larger than those for Lg. Clipping does not appear to be the cause of the flattening because the observed Lg and coda amplitudes are well within the total dynamic range of the Graefenburg recording system.

To further illustrate this observation, we have replotted the scatter diagrams in the form of histograms in Figures 28 through 35. The histograms of each Lg- and P-coda measurement are plotted on the right and the corresponding m_b histogram is plotted to the left in each figure. Examination of each m_b histogram reveals two peaks centered at about 5.95 and 6.15. Sykes and Cifuentes (1983) also pointed out these two peaks in the magnitude distributions, and suggested that all the events which cluster within the distribution centered at the higher m_b have the same yield. (Actually, their higher m_b distribution was centered on 6.2 and included events with magnitudes from 6.1 to 6.28. However, because our data sample is smaller, we have included an event with magnitude of 6.033 in the larger magnitude distribution which Sykes and Cifuentes (1983) placed in the distribution centered at about 5.98. However, we do not believe that this will invalidate the following arguments.) The arrows indicate the approximate spread of this distribution which is 0.2 m_b units. The corresponding range in Lg and P-coda log-rms amplitudes (i.e, for the same events) is denoted by the arrows on the left histograms in each of Figures 27 through 34. In most cases, the spread in the Lg or P-coda amplitudes is less than half that of the corresponding m_b values.

Thus, we conclude that the small slopes in the scatter diagrams are a result of the Lg and P-coda amplitudes clustering into distributions with tighter variances than those of the

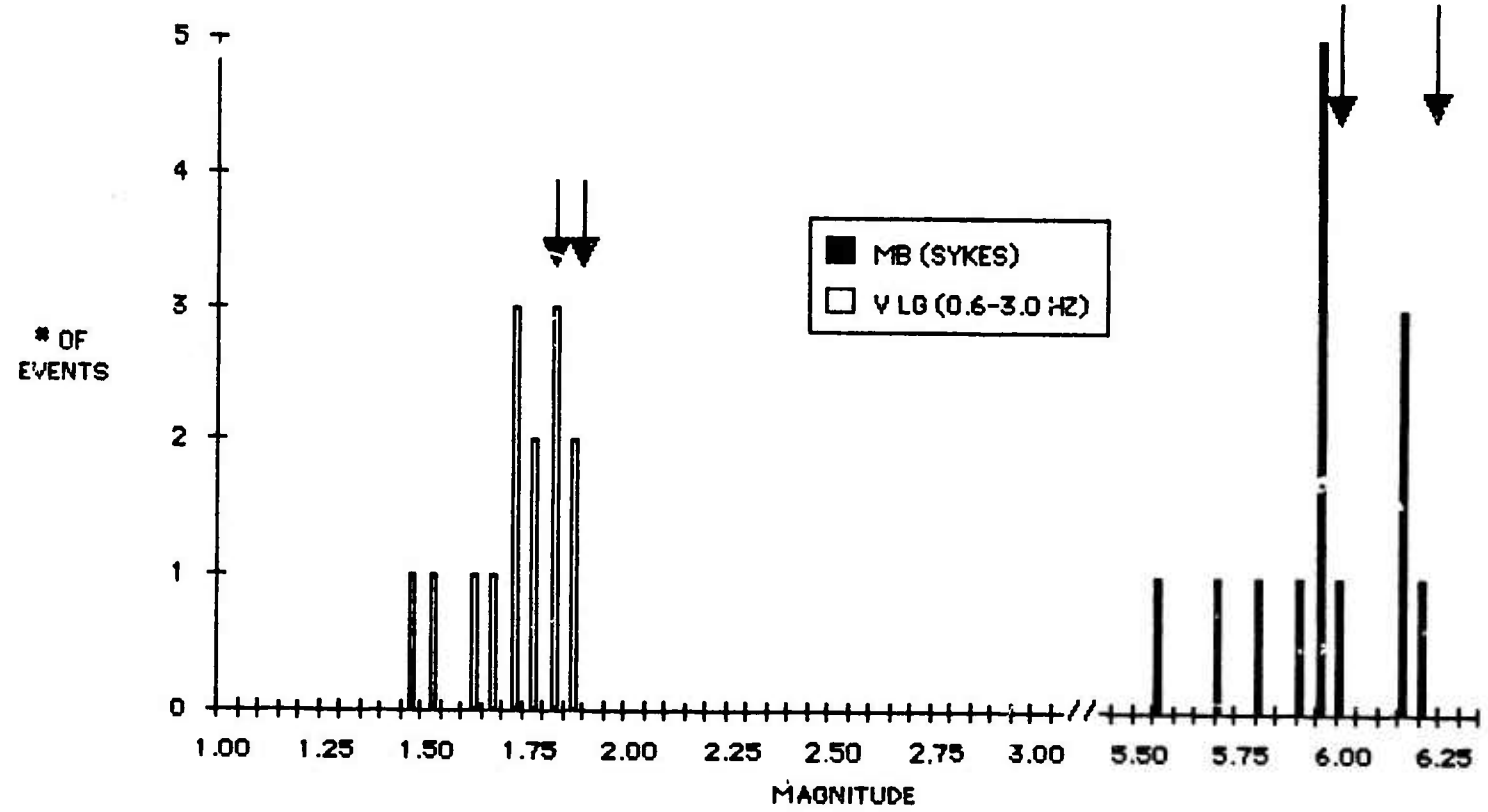

FIGURE 28 HISTOGRAMS OF VERTICAL, HIGH-FREQUENCY Lg LOG-RMS AMPLITUDES RECORDED AT GRAEFENBURG AND M_b FOR SHAGAN RIVER EVENTS

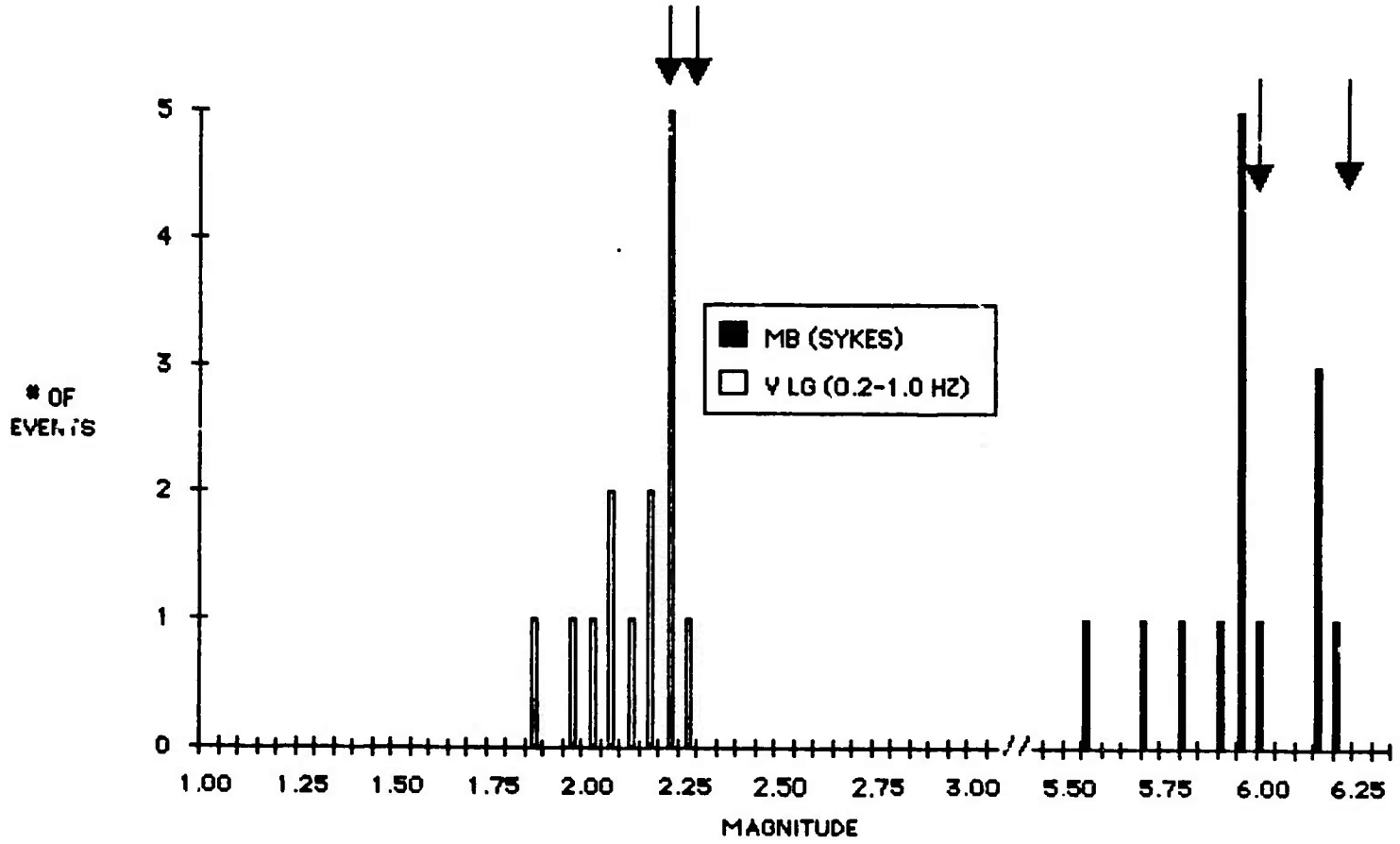

FIGURE 29 HISTOGRAMS OF VERTICAL MID-FREQUENCY Lg LOG-RMS AMPLITUDES RECORDED AT GRAEFENBURG AND m_b FOR SHACAN RIVER EVENTS

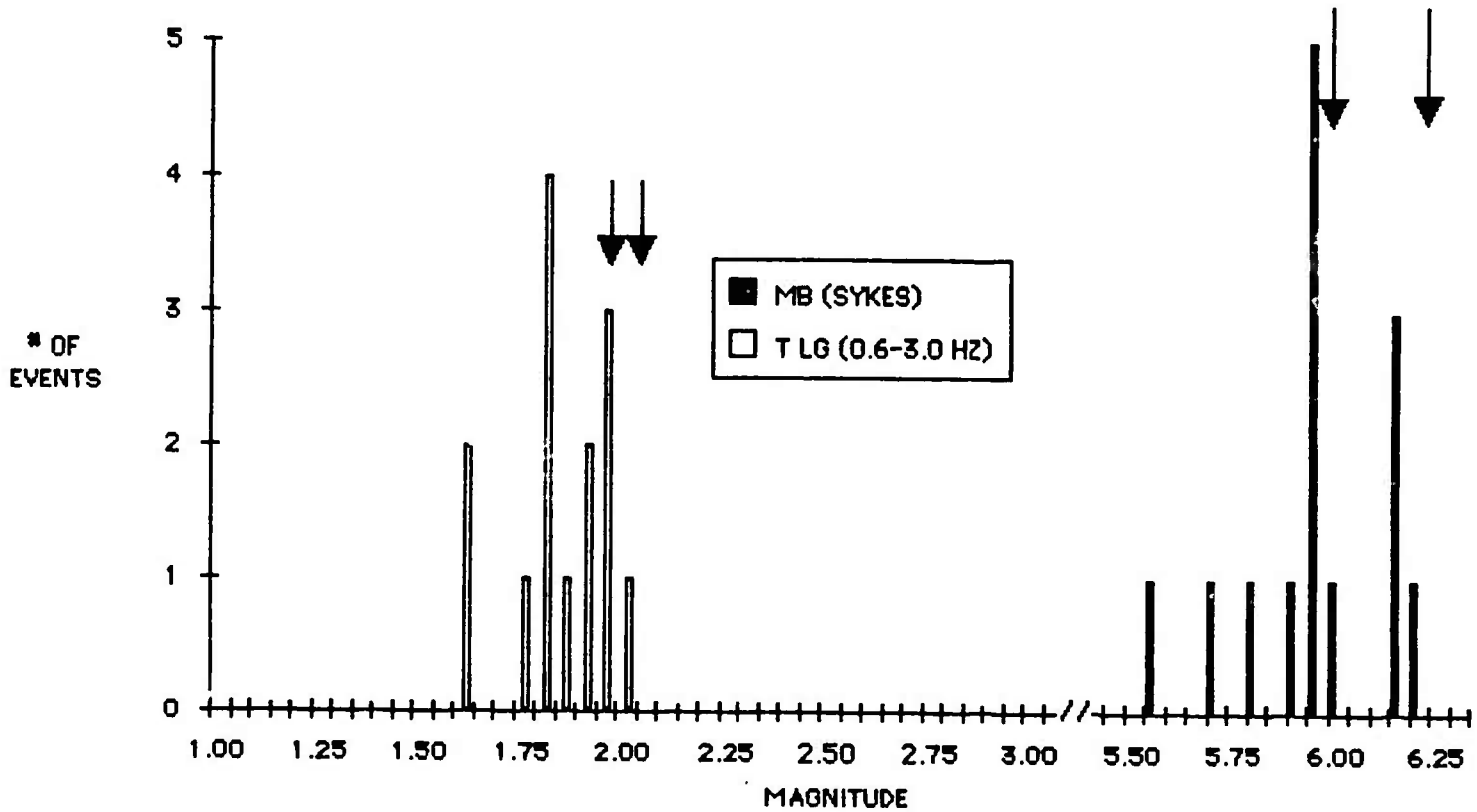

FIGURE 30 HISTOGRAMS OF TRANSVERSE, HIGH-FREQUENCY Lg LOG-RMS AMPLITUDES RECORDED AT GRAEFENBURG AND m_b FOR SHAGAN RIVER EVENTS

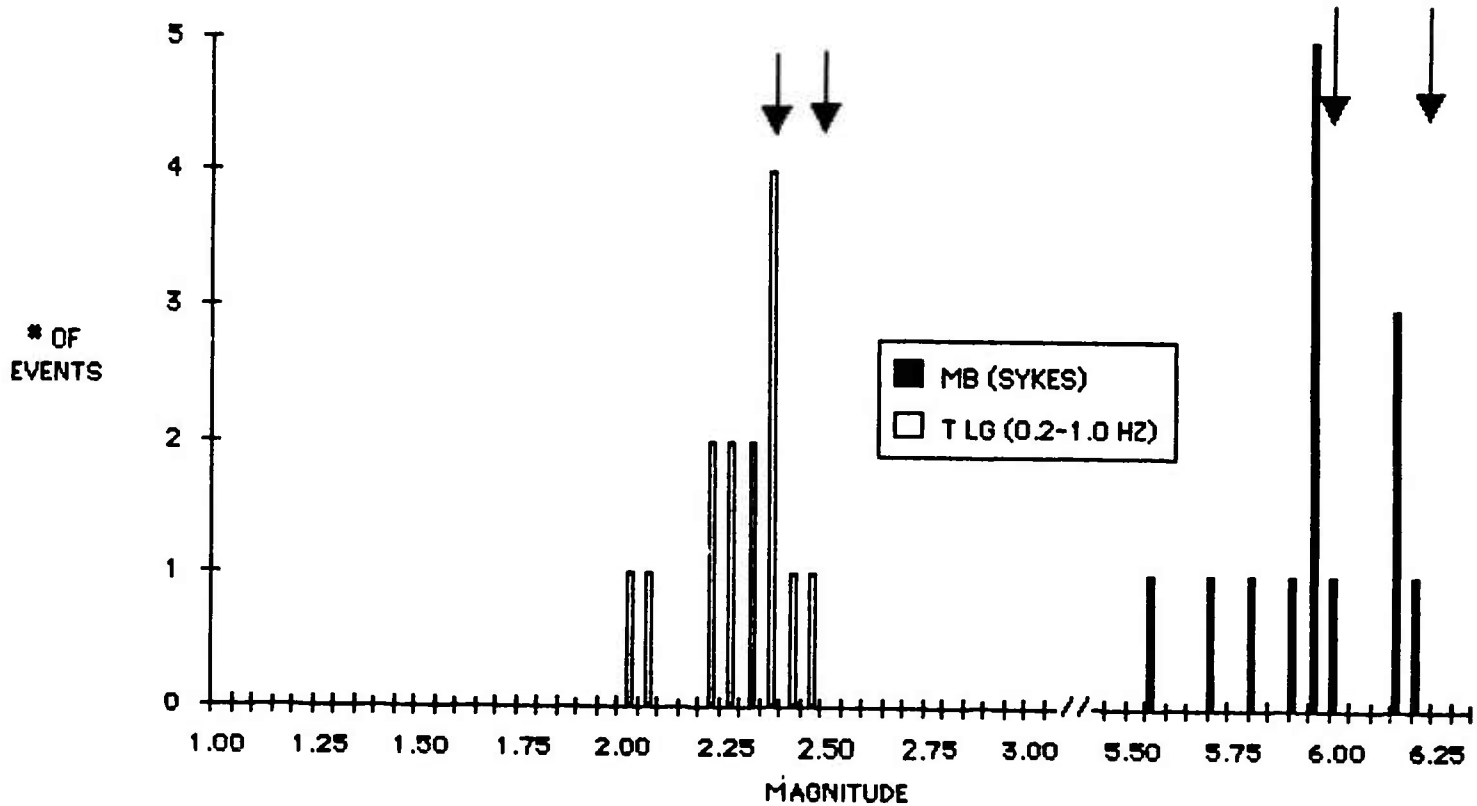

FIGURE 31 HISTOGRAMS OF TRANSVERSE, MID-FREQUENCY Lg LOG-RMS AMPLITUDES RECORDED AT GRAEFENBURG AND m_b FOR SHAGAN RIVER EVENTS

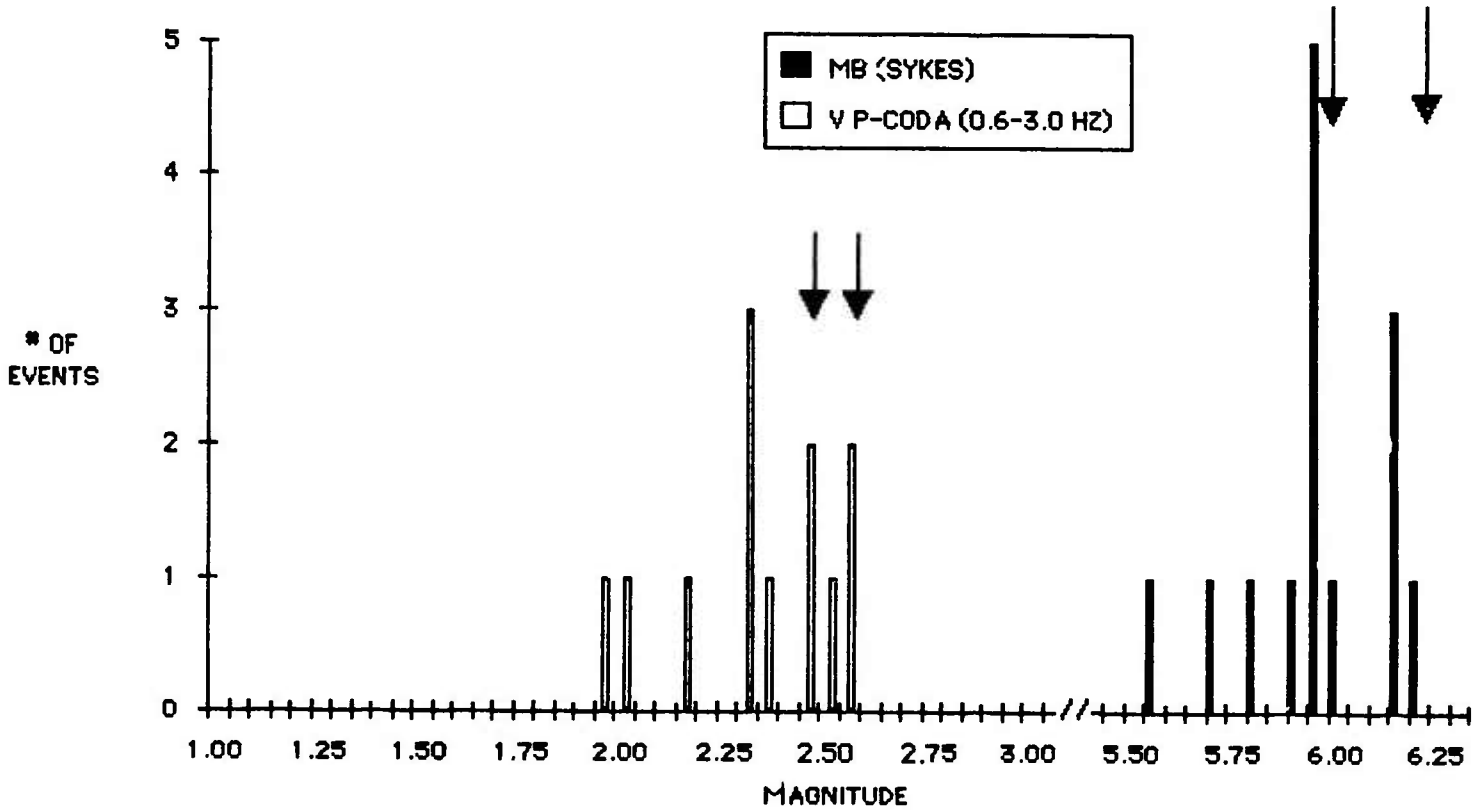

FIGURE 32 HISTOGRAMS OF VERTICAL HIGH-FREQUENCY P-CODA LOG-RMS AMPLITUDES RECORDED AT GRAEFENBURG AND m_b FOR SHAGAN RIVER EVENTS

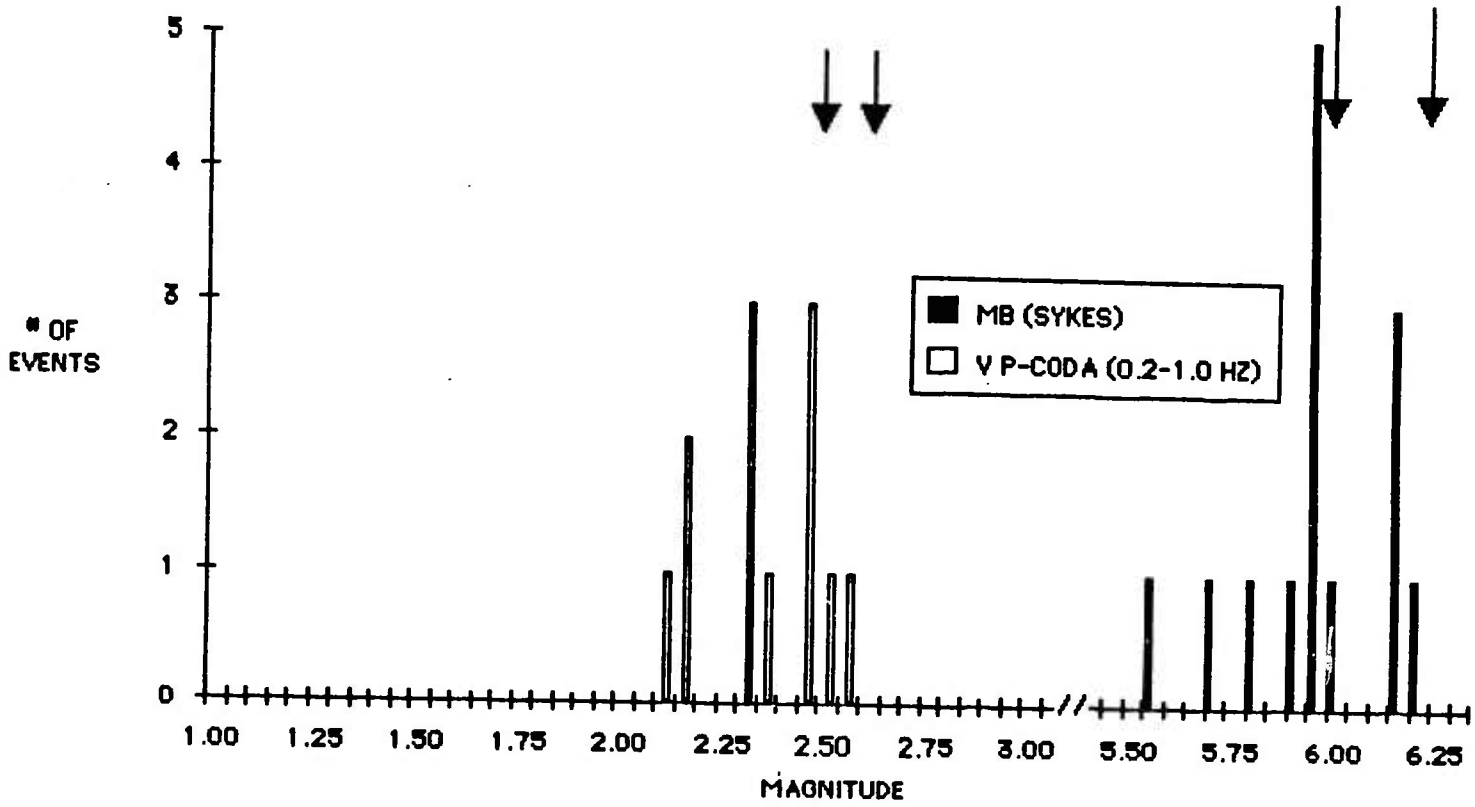

FIGURE 33 HISTOGRAMS OF VERTICAL, MID-FREQUENCY P-CODA LOG-RMS AMPLITUDES RECORDED AT GRAEFENBURG AND m_b FOR SHAGAN RIVER EVENTS

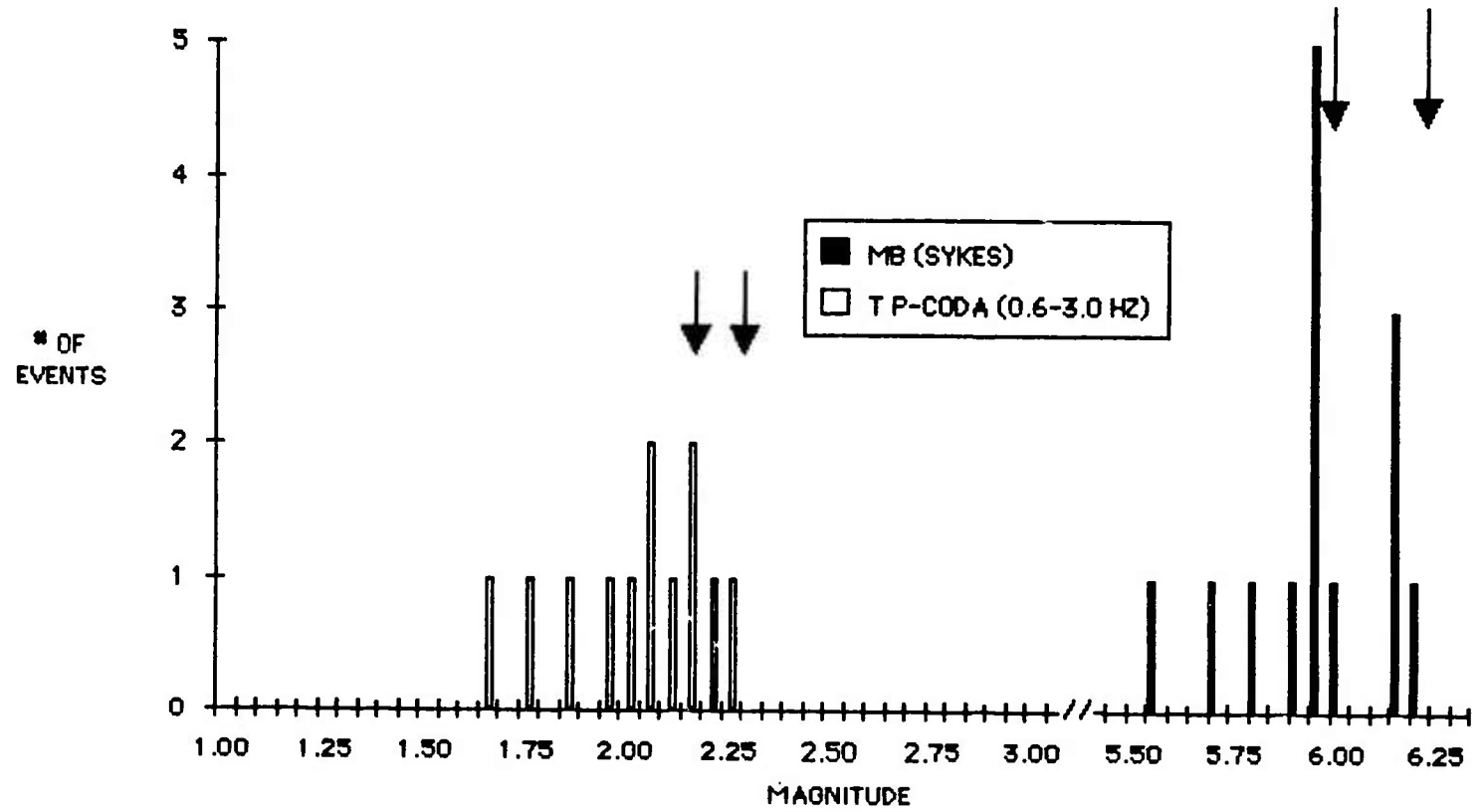

FIGURE 34 HISTOGRAMS OF TRANSVERSE, HIGH-FREQUENCY P-CODA LOG-RMS AMPLITUDES RECORDED AT GRAEFENBURG AND m_b FOR SHAGAN RIVER EVENTS

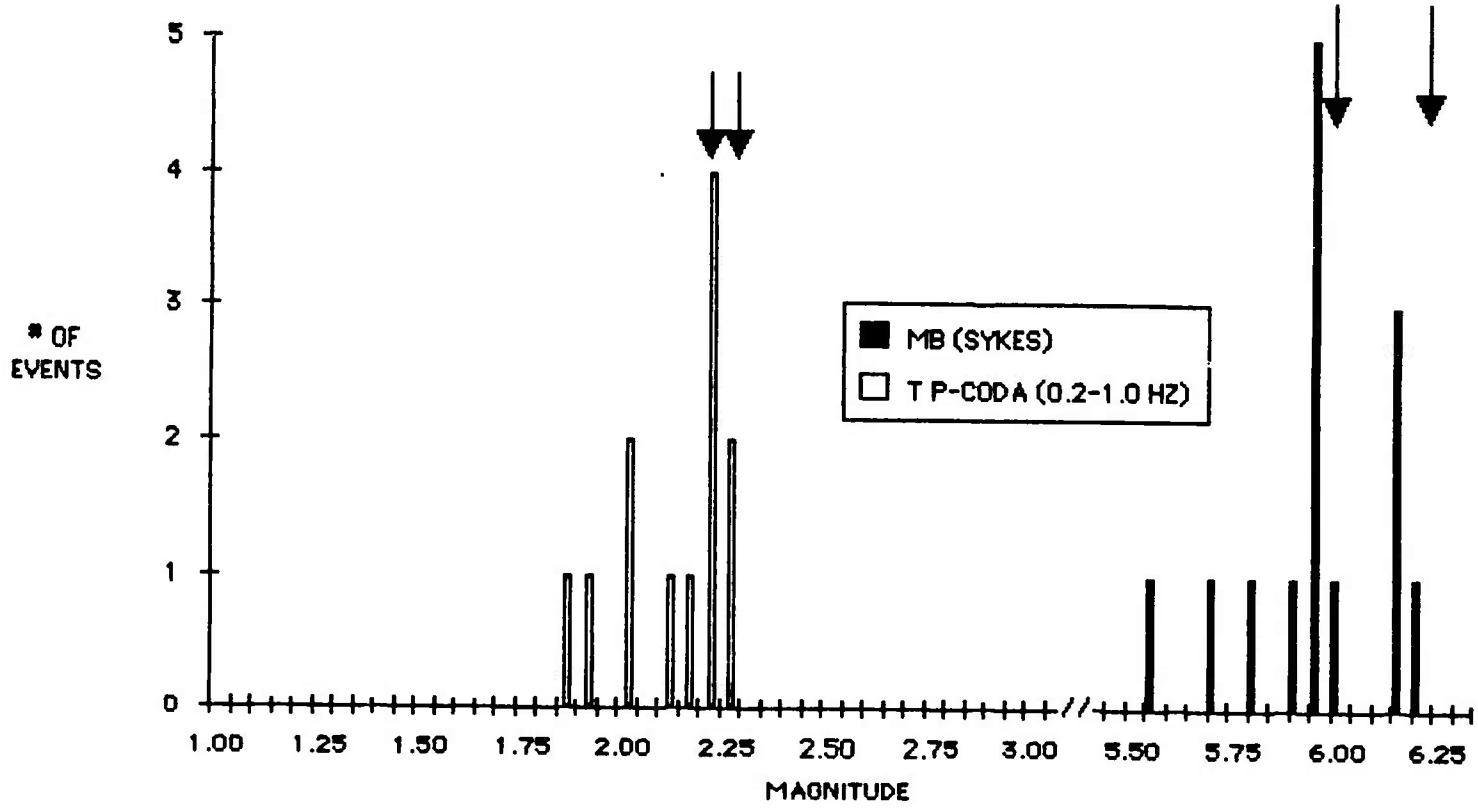

FIGURE 35 HISTOGRAMS OF TRANSVERSE, MID-FREQUENCY P-CODA LOG-RMS AMPLITUDES RECORDED AT GRAEFENBURG AND m_b FOR SHAGAN RIVER EVENTS

corresponding m_b values. This means that the Lg and P-coda amplitudes are closer together than the corresponding m_b values. We now interpret this result in terms of the relative yields of the largest Shagan River explosions.

3.3 RELATIVE MAGNITUDES AND YIELDS OF THE LARGEST SHAGAN RIVER EXPLOSIONS

In Table 4, we summarize the relative magnitude values for all Shagan River explosions with m_bs greater than 6.0. In this table we compare the relative values of several magnitude estimates, including NORSAR Lg and P-coda measurements of Ringdal (1983) and Baumgardt (1984), respectively, the Graefenburg results discussed above, the Lg magnitudes of Nuttli (1984), and the body-wave magnitudes of NEIS and Sykes and Cifuentes (1983). From this table we make the following observations.

i. The relative NORSAR Lg and P-coda magnitudes for these events vary by ± 0.04 to ± 0.05 logarithmic units as compared with ± 0.08 to ± 0.10 for P-wave magnitudes.

ii. The Graefenburg Lg and P-coda measurements vary by ± 0.03 to ± 0.05 logarithmic units as compared to ±0.07 units for the corresponding m_b values.

iii. The variation in Lg magnitudes, estimated by Nuttli (1984) is ±0.07 as compared with ±0.04 for the corresponding m_b values.

Observations (i) and (ii) indicate that the range of Lg and P-coda magnitudes for the largest explosions is half that of the m_b range. Statistical F tests reveal that these observations are significant at and above the 95% confidence level. Assuming a

TABLE 4
MEANS AND STANDARD DEVIATIONS FOR MAGNITUDE MEASUREMENTS OF LARGEST SOVIET EXPLOSIONS, 1976-1982

Method		Mean	Standard Deviation	No. of Events
1.	Single-Channel Lg NORSAR†	3.11	0.04	5
	Multi-Channel Lg NORSAR††	3.01	0.05	5
	NEIS m_b Corresponding Events	6.12	0.13	5
	Corrected m_b Corresponding Events*	6.143	0.092	5
2.	Multi-Station Lg WWSSN**	6.01	0.07	4
	NEIS m_b Corresponding Events	6.18	0.10	4
	Corrected m_b Corresponding Events*	6.167	0.036	4
3.	Single-Channel P-coda NORSAR+	1.97	0.05	6
	Multi-Channel P-coda NORSAR++	1.96	0.06	6
	NEIS m_b Corresponding Events	6.17	0.10	6
	Corrected m_b Corresponding Events*	6.160	0.082	6

TABLE 4 (cont)

Method	Mean	Standard Deviation	No. of Events
4. Vertical Lg Graefenburg Al 0.6 - 3.0 Hz	1.840	0.033	5
Vertical Lg Graefenburg Al 0.2 - 1.0 Hz	2.231	0.033	5
Transverse Lg Graefenburg Al 0.6 - 3.0 Hz	1.972	0.037	5
Transverse Lg Graefenburg Al 0.2 - 1.0 Hz	2.401	0.047	5
Vertical Coda Graefenburg Al 0.6 - 3.0 Hz	2.508	0.051	5
Vertical Coda Graefenburg Al 0.2 - 1.0 Hz	2.506	0.051	5
Transverse Coda Graefenburg Al 0.6 - 3.0 Hz	2.203	0.057	5
Transverse Coda Graefenburg Al 0.2 - 1.0 Hz	2.231	0.029	5
Corrected m_b Corresponding Events*	6.149	0.069	5

† Log-rms amplitude on channel 03C01 (Ringdal, 1983)
†† Log-rms amplitude averaged over all NORSAR channels (Ringdal, 1983)
* Station corrections derived by analysis of variance (Sykes and Cifuentes, 1983)
** Absolute m_b (Lg) magnitude estimates (Nuttli, 1983)
+ Log-rms amplitude-channel 03C01 (Baumgardt, 1984)
++ Log-rms amplitude averaged over all NORSAR channels (Baumgardt, 1984)

magnitude-yield slope of 1, the corresponding yield ranges near ±150 kt are ±17 kt for Lg and P-coda measurements as compared to ±35 kt for P-wave magnitudes.

The Nuttli (1984) network Lg results are not consistent with the single-array results in that he gets a larger magnitude range (±0.07) for Lg than for m_b (±0.04). A possible explanation for the discrepancy is that the number of stations used by Nuttli to estimate the average Lg magnitude was not the same from event to event. The number of stations used ranged from 2 to 6 stations. This large variability of the number of stations may have resulted in biased average magnitudes, particularly in the cases where the number of stations is small. A better approach would have been to apply the Least Squares Matrix Factorization (LSMF), or analysis of variance, method to estimate average magnitudes, as did Roundout Associates (1984). Also, it should be noted that Nuttli's Lg magnitudes are determined by measuring the single-point peak to trough amplitude on the maximum Lg, whereas we have measured log-rms amplitudes in long windows. Log-rms measurements may be more stable than single-point measurements.

Table 5 summarizes the results of the m_b and M_s estimates for the largest Shagan River explosions ($m_b > 6.0$) given by Sykes and Cifuentes (1983). The relative M_s values for all events with m_b greater than 6.0 and including events of high and low tectonic component have a large standard deviation (±0.15), whether or not tectonic release corrections are applied. The m_b values for the corresponding events has a standard deviation of better than half (±0.07) that for the M_s values. In the case of low tectonic release events, with or without tectonic release corrections, the

TABLE 5
SURFACE WAVE RESULTS FOR THE LARGEST SHAGAN RIVER EXPLOSIONS (SYKES AND CIFUENTES, 1983)

Method	Mean	Standard Deviation	No. of Events
1. Multi-Station M_s WWSSN All Events - Uncorrected	4.004	0.15	9
Multi-Station M_s WWSSN All Events - Corrected+	4.190	0.15	7
Corrected m_b All Events*	6.158	0.072	10
2. Multi-Station M_s WWSSN Low TR (LQ/LR 0.4) Uncorrected	4.097	0.069	5
Multi-Station M_s WWSSN Low TR (LQ/LR 0.4) Corrected+	4.246	0.072	5
Corrected m_b Corresponding Events*	6.118	0.080	5

\+ M_s corrected by Sykes and Cifuentes (1983) for pure thrust faulting.

* Station corrections derived by analysis of variance.

M_S and m_b ranges are more comparable (± 0.07 to ± 0.08) although still about double that which we obtain for Lg and P-coda measurements.

Sykes and Cifuentes (1983) based their conjecture, that the largest Shagan River events are of nearly the same yield, on the relative M_S values of only a few events of low tectonic release. They concluded that these explosions are within 10 to 20 kt of each other. Our results are consistent with a somewhat larger yield range of 30 to 35 kt, although we included events of large tectonic release ($LQ/LR > 0.4$). However, based on the Lg and P-coda measurements, we concur with the overall conclusion of Sykes and Cifuentes (1983) that the yield range of the largest Shagan River explosions is smaller, by at least a factor of two, than the yield range indicated by the m_b estimates.

4.0 CONCLUSIONS AND RECOMMENDATIONS

This study has addressed the characteristics of teleseismic Lg and P-coda waves and the precision of using measurements of the amplitude of these waves for relative yield estimation. As a result of this study we reach the following conclusions:

1. Lg waves from Shagan River explosions are well recorded at the NORSAR and Graefenburg arrays, which are at teleseismic distances (38^{o} and 42^{o} for NORSAR and Graefenburg, respectively). Our results are consistent with those of other studies which showed that the Ural Mountains do not block the propagation of Lg-waves from Semipalatinsk to NORSAR.

2. Broadband recordings of Lg at Graefenburg indicate a stronger excitation, relative to coda, in the mid-period band than in the high-frequency band. However, the noise is also higher in the mid-period band which results in Lg having about the same signal-to-noise ratios in the two bands.

3. The early P-coda at NORSAR is stronger, relative to Lg, than that at Graefenburg. Also, the coda-envelope shapes are quite different for the two arrays; the NORSAR coda flattens between about 200 to 340 seconds after P, whereas the Graefenburg coda decays monitonically from the P-wave out to the S_n and Lg arrival times.

4. The standard deviations of Lg and S-coda phases at NORSAR are higher by about 0.05 to 0.06 log-rms amplitude units than those of P-coda phases, which is probably related to differential site and propagation effects on P, S and Lg waves. The most stable part of the P coda before Lg is the flat part of the

coda, where the spatial standard deviation in log-rms amplitude in 5 second windows drops to a minimum of less than 0.1 units.

5. The flat coda envelopes from about 200 to 340 seconds after P, recorded at NORSAR for Semipalatinsk explosions, are consistent, on the basis of timing, to Lg - P forward scattering from lateral heterogeneities in the Ural Mountains. The evidence is still circumstantial, and we will be analyzing additional data for events on either side of the Urals. However, if the Lg-to-P forward scattering hypothesis holds up, it would have significant implications for Lg-scattering attenuation determinations at teleseismic distances and, perhaps, at regional distances as well.

6. Measurements on Graefenburg data of vertical and transverse log-rms amplitudes in the P-coda and Lg phase in two frequency bands were found to correlate well with network m_b. However, the slopes of the regression of Lg amplitude versus m_b were small ranging from 0.6 to 0.8. The slopes of the P-coda regressions were higher, ranging from 0.9 to over 1.0. This supports the idea that early P-coda waves are generated by P scattering.

7. Lg and P-coda log-rms amplitudes do not appear to be strongly affected by the tectonic component as revealed by surface-wave studies.

8. Relative P-coda and Lg-magnitude analysis of the largest Shagan River explosions, with $m_b > 6.0$, using NORSAR and Graefenburg data supports the conjecture of Sykes and Cifuentes (1983) that these explosions have nearly the same yield.

9. Of course, we cannot address the other contention of Sykes and Cifuentes (1983) that these explosions do not exceed the 150 kt threshold, since we did not estimate absolute Lg and P-coda magnitudes which are calibrated against the yields of events with known yield. Nuttli (1984) has done this and has obtained higher yields, some in excess of 200 kt, for the largest explosion. However, we question the precision of his estimates because the standard deviation between events of his network-averaged Lg magnitudes for the largest Shagan River explosion do not agree with our single-site estimates at both NORSAR and Graefenburg. Perhaps his magnitudes have bias because of the variable number of stations used to estimate average magnitudes and his use of single-point rather than rms amplitudes to determine Lg magnitudes.

10. Single-station Lg and P-coda measurements appear to be significantly more precise for relative yield estimation than any other method. If, in fact, the largest Shagan River explosions have about the same yield, then we can conclude that single-station P-coda and Lg magnitudes have a precision of about ±35 kt, or a factor of 1.6, for relative yield estimation compared with network m_b precision of ±60 kt or a factor of 2.3.

These conclusions are based on a very small data sample and, therefore, must still be considered preliminary. We are currently collecting more data from both arrays for more recent events which should give us a more statistically meaningful sample for relative-magnitude analysis. Also, we will be collecting data from other digital stations, such as the SRO and DWWSSN stations in Europe and Scandinavia. We plan to combine this data with the array data to investigate the precision of average Lg and P-coda magnitudes for yield estimation.

We recommend that more attention be given to broadband recordings of Lg, such as from Graefenburg, intermediate band data from DWWSSN and RSTN stations and from the newly installed NORESS broadband 3-component sensor. We find that Lg excitation is stronger in the intermediate band. However, noise is often correspondingly higher in this band as well, so methods for noise correction need to be investigated.

Finally, Lg measurements at different frequencies need to be compared to M_S measurements, with and without tectonic release corrections. Our preliminary examination of tectonic release corrections given by Sykes and Cifuentes (1983) suggest that they are not very effective for improving yield estimation precision, assuming the largest Shagan River explosions are of nearly the same yield. It should be remembered that the Sykes and Cifuentes (1983) conclusions were based almost entirely on M_S measurements for events with very low tectonic component, and they warn against using M_S for yield estimation of events whose LQ/LR ratios much exceed 0.4. More recent M_S corrections, based on moment tensor inversions, should be compared with Lg measurements.

ACKNOWLEDGEMENTS

The Graefenburg data used in this study was provided by Professor Shelton Alexander of Penn State. Dr. Frode Ringdal of NORSAR supplied the NORSAR data. Also, thanks are due to Dr. Ringdal for some useful discussions.

REFERENCES

Alewine, R. W. and T. C. Bache, Monitoring a Threshold Test Ban Treaty, abstract in E.O.S., Transactions, American Geophysical Union, 64, p. 193, 1983.

Alexander, S. S., Relationship Among Near-Field Regional, and Teleseismic Observations of Seismic Source Parameters, Draft Paper, Basic Research in the Vela Program, Vol. II, 1984.

Bakun, W. H. and A. G. Lindh, Local Magnitudes, Seismic Moments, and Coda Durations for Earthquakes Near Oroville, California, Bull. Seism. Soc. Am., 67, p. 615, 1977.

Barker, B. W., Z. A. Der and C. P. Mrazek, the Effect of Crustal Structure on the Regional Phases Pg and Lg at the Nevada Test Site, J. Geophys. Res., 86, pp. 1686-1700, 1981.

Baumgardt, D. R., Teleseismic P-coda Stability and Coda Magnitude Yield Estimation, Semi-annual Technical Report, SAS-TR-83-01, ENSCO, Inc., Springfield, VA, 1983.

Baumgardt, D. R., Analysis of Short-Period P-coda Measurements for Presumed Underground Nuclear Explosions in Eurasia, Final Report, SAS-TR-84-01, ENSCO, Inc., Springfield, VA, 1984.

Bullitt, J. T. and V. F. Cormier, The Relative Performance of m_b and Alternative Measures of Elastic Energy in Estimating Source Size and Explosion Yield, Bull. Seism. Soc. Am., 74, pp. 1863-1882, 1984.

Campillo, M., M. Bouchon and B. Massinon, Theoretical Study of the Excitation, Spectral Characteristics, and Geometrical Attenuation of Regional Seismic Phases, Bull. Seism. Soc. Am., 74, pp. 79-90, 1984.

Der, Z., M. E. Marshall, A. O'Donnell and T. W. McElfresh, Spatial Coherence Structure and Attentuation of the Lg Phase, Site Effects, and Interpretation of the Lg Coda, Bull. Seism. Soc. Am., 74, pp. 1125-1148, 1984.

Given, J. W., D. S. Cavit, G. R. Mellman, and D. M. Hadley, Application of the Moment Tensor Inversion Method to Surface Waves from Shagan River Events, SGI-R-83-102, Sierra Geophysics, Inc., Redmond, WA, 1983 (S).

Given, J. W. and G. R. Mellman, Correction to Surface Wave Amplitude Measurements from Shagan River Events Based on Moment Tensor Inversion Method, SGI-R-84-104, Sierra Geophysics, Inc., Redmond, WA, 1984 (S).

Given, J. W. and D. V. Helmberger, Upper Mantle Structure of Northwestern Eurasia, J. Geophys. Res., 85, pp. 7183-7194, 1980.

Gupta, I. N., B. W. Barker, J. A. Burnetti and Z. A. Der, A Study of Regional Phases from Earthquakes and Explosions in Western Russia, Bull. Seism. Soc. Am., 70, pp. 851-872, 1980.

Gupta, I. N., R. R. Blandford, R. A. Wagner, J. A. Burnetti and T. W. McElfresh, Use of P-coda for Explosion Medium and Improved Yield Determination, TGAL-TR-83-7a, Teledyne Geotech, Alexandria, VA, 1984.

Gupta, I. N., D. H. von Seggern and R. A. Wagner, A Study of Variations in the Horizontal to Vertical Lg Amplitude Ratio in the Eastern United States, Bull. Seism. Soc. Am., 72, pp. 2081-2088, 1982.

Harjes, H. P. and D. Seidl, Digital Recording and Analysis of Broadband Seismic Data at Graefenburg (GRF) Array, J. Geophys. Res., 44, pp. 511-523, 1978.

Herrmann, R. B., The Use of Duration as a Measure of Seismic Moment and Magnitude, Bull. Seism. Soc. Am., 68, pp. 899-913, 1975.

Herrmann, R. B., Q Estimates Using the Coda of Local Earthquakes, Bull. Seism. Soc. Am., 70, pp. 447-468, 1980.

Herrmann, R. B. and C. Wang, Lg Wave Excitation and Propagation with Application to Nuclear Field Determination, Semi-annual Report, 30 November 1983.

King, D. W. and G. Calcagnile, P-wave Velocities in the Upper Mantle Beneath Fennoscandia and Western Russia, Geophys. J. R. Astr. Soc., 46, pp. 407-432, 1976.

Madansky, A., The Fitting of Straight Lines When Variables Are Subject to Error, J. Am. Stat. Assoc., 54, 00. 173-205, 1959.

Menke, W. H. and P. G. Richards, Crust-Mantle Whispering Gallery Phases: A Deterministic Model of Teleseismic P_n Wave Propagation, J. Geophys. Res., 85, pp. 5416-5422, 1980.

Mrazek, C. P., Z. A. Der, B. W. Barker and A. O'Donnell, Seismic Array Design for Regional Phases in Studies of Seismic Wave Characteristics at Regional Distances, AL80-1, Teledyne Geotech, Alexandria, VA, 1980.

Mykkeltveit, S., F. Ringdal and H. Bungum, An Experimental Small Array Subarray within the NORSAR Array: Crustal Phase Velocities and Azimuths from Local and Regional Events, AFTAC-TR-80-37, 1980.

Nersesov, I. L., Y. F. Kopnichev and G. A. Vostrikov, Calibration of Earthquakes in Terms of Magnitude Based on Coda Waves at Distances as Great as 3000 km., Translation from Doklady Akademii Nauk, SSSR, 222, pp. 76-78, 1975

Noponen, I. T., E. B. McCoy and H. S. Sproules, Evaluation of National Seismic Station, SDAC-TR-79-9, Teledyne Geotech, Alexandria, VA, 1979.

North, R. G., Propagation of the Lg Phase Across the Urals and the Baltic, Semi-annual Technical Summary, Seismic Discrimination, Lincoln Laboratory, Massachusetts Institutes of Technology, Cambridge, Massachusetts, 31 March 1978

Nuttli, O. W., Seismic Wave Attenuation and Magnitude Relations for Eastern North America, J. Geophys. Res., 78, pp. 876-885, 1973.

Nuttli, O. W., On the Attenuation of Lg-Waves in Western and Central Asia and Their Use as a Discriminant between Earthquakes and Explosions, Bull. Seism. Soc. Am., 71, pp. 249-261, 1981.

Nuttli, O. W., Methodology of Using Lg Waves for Estimating Explosion Yield and Body-Wave Magnitude Bias Between Test Sites, Final Report, 1 Oct 1982 - 30 Sep 1984, 27 November 1984

Pomeroy, P. W., W. J. Best and T. V. McEvilly, Test Ban Treaty Verification with Regional Data - A Review, Bull Seism. Soc. Am., 72, S89 - S130, 1982.

Ringdal, F., Magnitudes from P-coda and Lg Using NORSAR Data, NORSAR Semi-annual Technical Summary, 1 October 1982 - 31 March 1983, 1983.

Rondout Associates, The Use of Regional Seismic Waves for Yield Determination, Semi-Annual Technical Report, No. 1, Rondout Associates, Stone Ridge, New York, 1984.

Shapira, A., Regional Coda Magnitudes of Underground Nuclear Explosions, Phys, Earth Planet Int., 26, pp. 188-197, 1981.

Singh, S. and R. B. Herrmann, Regionalization of Crustal Coda Q in the Continental United States, J. Geophys. Res., pp. 527-538, 1983

Suteau, A. M. and J. H. Whitcomb, A Local Earthquake Coda Magnitude and Its Relation to Duration, Moment M_o, and Local Richter Magnitude M_l, Bull. Seism. Soc. Am., 69, pp. 353-368, 1979.

Sykes, L. R. and I. L. Cifuentes, Yields of Soviet Underground Nuclear Explosions from Seismic Surface Waves: Compliance with the Threshold Test Ban Treaty, Proc. Nat'l Acad. Sci. USA, 81, pp. 1922-1925, 1984.